University of Washington

Department of Orthopaedics and Sports Medicine
2007 Research Report

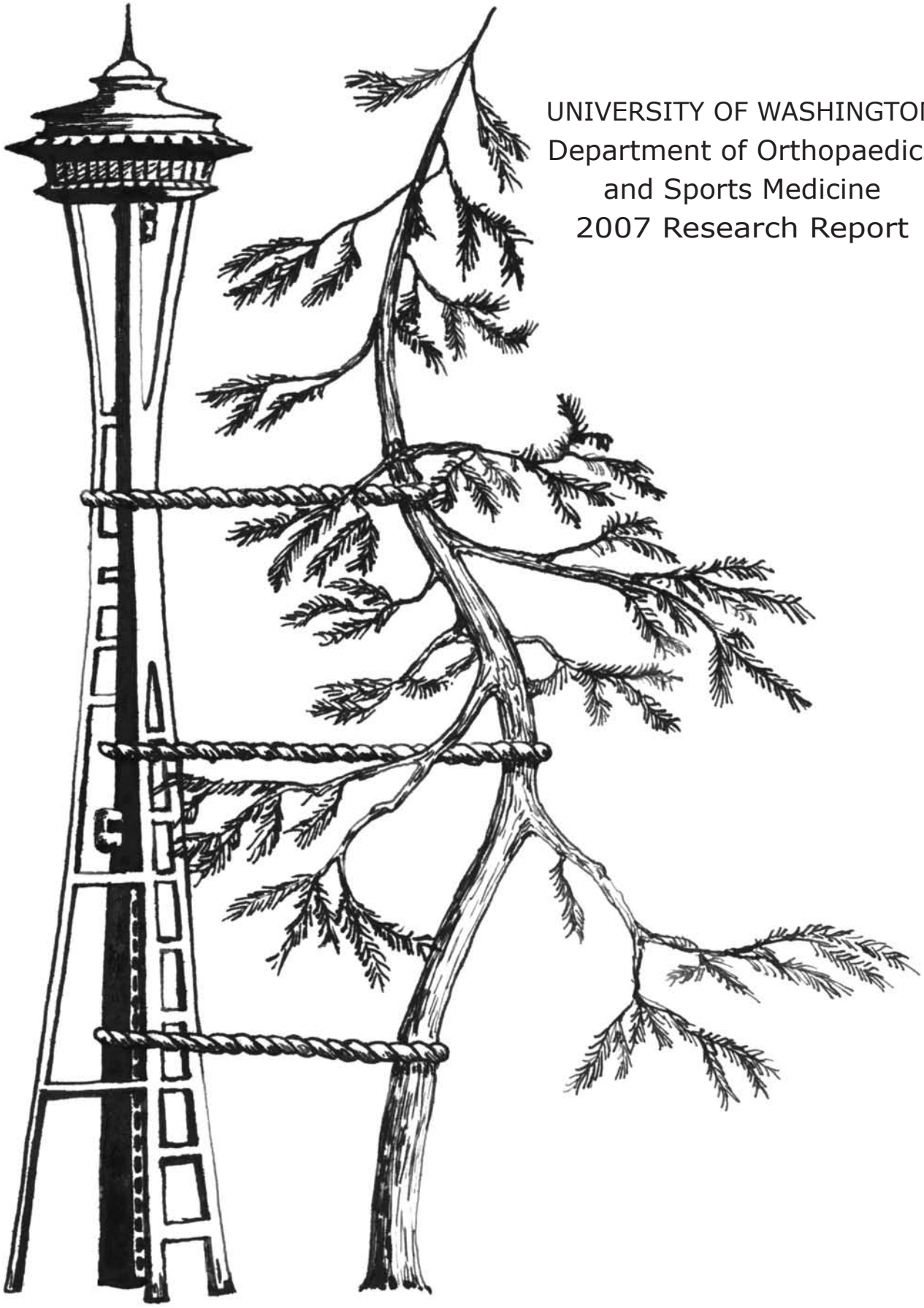

UNIVERSITY OF WASHINGTON

Department of Orthopaedics and Sports Medicine 2007 Research Report

UW Medicine
SCHOOL OF MEDICINE

Department of Orthopaedics and Sports Medicine
University of Washington
Seattle, WA 98195

Editor:
Frederick A. Matsen III, M.D.
Fred Westerberg

Design & Layout:
Fred Westerberg

Cover Illustration: "Red Tree, Yellow Sky"
by Georgia O'Keefe, 1952.
Museum of Fine Arts, Boston, MA, USA
Photograph©2007 Museum of Fine Arts, Boston

Contents

Foreword

This year's research report cover is graced with Georgia O'Keeffe's Red Tree, Yellow Sky (1952) that hangs in the American Moderns Gallery of the Museum of Fine Arts in Boston (465 Huntington Avenue). O'Keeffe (1887-1986) is one of the best known American artists, presenting, as in this painting, crisply painted organic objects against an environmental background. Her art first won recognition in 1908 when the 21-year-old artist presented Dead Rabbit with Copper Pot, which earned her a scholarship to attend the outdoor summer school of the Art Student's League. In 1924, she married famed photographer Alfred Stieglitz, who featured his wife in many, often revealing, photographs. In 1929 she moved to New Mexico eventually settling in Abiquiu near Ghost Ranch, which inspired many of her best known paintings, including Ram's Head White Hollyhock and Little Hills. In 1946 she became the first woman to be featured in a solo retrospective at the Museum of Modern Art in New York. I like her art, because like those of us in Orthopaedics, she seeks to bring her subject into sharp focus, but also understands that the subject exists in a context that plays a major role in defining the treatment.

As I was meeting with our resident applicants this year, I was often asked about the challenges we face in orthopaedic education. I found myself describing the challenge in terms of tree shape. Thirty years ago Orthopaedics was like a Joshua Tree - a long trunk of common diagnostic and therapeutic tools with minimal diversity at the top, making the teaching of fundamentals straightforward and enabling the concept of 'general orthopaedics'. Now, Orthopaedics is better represented by the tree on our cover, showing a very short trunk with dramatically diverging branches, such as gene expression, molecular biology, biological mechanics, arthroscopy, image guided spinal instrumentation, minimally invasive joint replacement, and advanced management of fractures. Our challenge as educators is now to pack the elements of specialty orthopaedics into the best possible five year, 80 hour per week educational experience for the terrific orthopaedic residents who come to the University of Washington.

This diversity is well demonstrated by the articles in this research report. On turning these pages, you will see how wonderfully broad our faculty and residents are in their pursuit of new ways to benefit patients with musculoskeletal and sports medicine conditions. Yet this is only a small sample of the work of our prodigiously productive academic team; to get a more complete picture, please see the 2006-2007 bibliography on page 75. This productivity is even more remarkable when we realize that this same team offers our patients over 10,600 surgical repairs and reconstructions each year.

From the forgoing, you may be able to sense the direction of Orthopaedics and Sports Medicine. Specifically, our vision is to become the best possible resource for research, education and clinical care for individuals whose lives have been compromised by problems related to their bones, joints and spine. Our foundation in sports medicine teaches us that each patient has an athlete within them. Inspiring that athlete to participate actively in their rehabilitation program is essential to a rapid and full recovery. Our foundation in science teaches us that we can always improve on the current understanding, evaluation and treatment of musculoskeletal disorders. Having chaired this Department for 20 years now, I am thrilled with the relentless efforts of the faculty to continually raise the standard of care and with the profound effect these efforts have had on the practice of our specialty. Our foundation as educators enables us to share these advances in knowledge with our residents, fellows and practicing physicians so that the benefit is shared with patients throughout the world. Finally, our foundation as physicians and surgeons commits us to the expert management to individuals with bone and joint problems. Because our field is growing so rapidly and because many of these advances are in specialized surgical care, we continue to recruit to our faculty highly trained specialists each year. This year we are proud to welcome Mike Lee to the spine team and Winston Warme to the shoulder and elbow team. Each year our teams become broader, deeper and stronger.

The academic activity of our Department is supported in part by grant funding, but also in large part by the generosity of private individuals who wish to enhance our ability to continue our pursuit of the best possible ways to restore comfort and function to our patients. If you would like to learn more about what we are doing or how you might support our efforts, just drop me a letter or an email.

Best wishes for the best in health,

Frederick A. Matsen III, M.D.
University of Washington
Department of Orthopaedics and Sports Medicine
1959 NE Pacific Street, Box 356500
Seattle, WA 98195
Office Phone (206) 543-3690
matsen@u.washington.edu
www.orthop.washington.edu

Department of Orthopaedics and Sports Medicine Faculty

Frederick A. Matsen III, M.D.
Professor and Chair
University of Washington Medical Center
Shoulder and Elbow
matsen@u.washington.edu

Howard A. Chansky, M.D.
Professor
VA Puget Sound Health Care System
Tumor Service
chansky@u.washington.edu

Christopher H. Allan, M.D.
Associate Professor
Harborview Medical Center
Hand and Wrist
callan@u.washington.edu

Jens R. Chapman, M.D.
Professor
Harborview Medical Center
Spine
jenschap@u.washington.edu

David P. Barei, M.D.
Assistant Professor
Harborview Medical Center
Trauma
barei@u.washington.edu

Ernest U. Conrad III, M.D.
Professor
Children's Hospital and Regional Medical Center
Tumor Service
chappie.conrad@seattlechildrens.org

Carlo Bellabarba, M.D.
Associate Professor
Harborview Medical Center
Spine and Trauma
cbella@u.washington.edu

Robert P. Dunbar, M.D.
Assistant Professor
Harborview Medical Center
Trauma
dunbar@u.washington.edu

Daphne M. Beingessner, M.D.
Assistant Professor
Harborview Medical Center
Trauma
daphneb@u.washington.edu

David R. Eyre, Ph.D.
Professor
University of Washington Medical Center
Research
deyre@u.washington.edu

Stephen K. Benirschke, M.D.
Professor
Harborview Medical Center
Foot and Ankle
beniskb@u.washington.edu

Russell J. Fernandes, Ph.D.
Research Assistant Professor
University of Washington Medical Center
Research
rjf@u.washington.edu

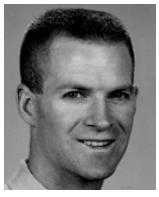

Richard J. Bransford, M.D.
Assistant Professor
Harborview Medical Center
Spine
rbransfo@u.washington.edu

John R. Green III, M.D.
Associate Professor
University of Washington Medical Center
Sports Medicine
jgreen3@u.washington.edu

Department of Orthopaedics and Sports Medicine Faculty

Ted S. Gross, Ph.D.
Associate Professor
Harborview Medical Center
Research
tgross@u.washington.edu

Seth S. Leopold, M.D.
Associate Professor
University of Washington Medical Center
Hip and Knee
leopold@u.washington.edu

Douglas P. Hanel, M.D.
Professor
Harborview Medical Center
Hand and Wrist
dhanel@u.washington.edu

Paul Manner, M.D.
Assistant Professor
University of Washington Medical Center
Hip and Knee
pmanner@u.washington.edu

Sigvard T. Hansen, Jr., M.D.
Professor
Harborview Medical Center
Foot and Ankle
hansetmd@u.washington.edu

Sohail K. Mirza, M.D.
Professor
Harborview Medical Center
Spine
mirza@u.washington.edu

M. Bradford Henley, M.D.
Professor
Harborview Medical Center
Trauma
bhenley@u.washington.edu

Vincent S. Mosca, M.D.
Associate Professor
Children's Hospital and Regional Medical Center
Pediatric Orthopaedics
vincent.mosca@seattlechildrens.org

Nancy J. Kadel, M.D.
Associate Professor
University of Washington Medical Center
Foot and Ankle
kadel@u.washington.edu

Sean E. Nork, M.D.
Associate Professor
Harborview Medical Center
Trauma
nork@u.washington.edu

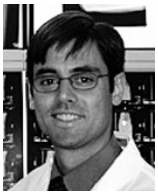

Leonid I. Katolik, M.D.
Assistant Professor
University of Washington Medical Center
Hand and Wrist
lkatolik@u.washington.edu

John W. O'Kane, M.D.
Associate Professor
University of Washington Medical Center
Sports Medicine
jokane@u.washington.edu

Roger V. Larson, M.D.
Associate Professor
University of Washington Medical Center
Sports Medicine
drlarson@u.washington.edu

Milton L. Routt, Jr., M.D.
Professor
Harborview Medical Center
Trauma
mlroutt@u.washington.edu

Department of Orthopaedics and Sports Medicine Faculty

Bruce J. Sangeorzan, M.D.
Professor
Harborview Medical Center
Foot and Ankle
bsangeor@u.washington.edu

Carol C. Teitz, M.D.
Professor
University of Washington Medical Center
Sports Medicine
teitz@u.washington.edu

Gregory A. Schmale, M.D.
Assistant Professor
Children's Hospital and Regional Medical Center
Pediatric Orthopaedics
Gregory.Schmale@seattlechildrens.org

Allan F. Tencer, Ph.D.
Professor
Harborview Medical Center
Research
atencer@u.washington.edu

John A. Sidles, Ph.D.
Professor
University of Washington Medical Center
Research
sidles@u.washington.edu

Thomas E. Trumble, M.D.
Professor
University of Washington Medical Center
Hand and Wrist
trumble@u.washington.edu

Douglas G. Smith, M.D.
Professor
Harborview Medical Center
Foot and Ankle
dgsmith@u.washington.edu

Theodore Wagner, M.D.
Clinical Professor
University of Washington Medical Center
Spine
wagner@u.washington.edu

Kit M. Song, M.D.
Associate Professor
Children's Hospital and Regional Medical Center
Pediatric Orthopaedics
Kit.Song@seattlechildrens.org

Christopher J. Wahl, M.D.
Assistant Professor
University of Washington Medical Center
Sports Medicine
wahlc@u.washington.edu

Sundar Srinivasan, Ph.D.
Research Assistant Professor
Harborview Medical Center
Research
sundars@u.washington.edu

Jason S. Weisstein, M.D., M.P.H.
Assistant Professor
University of Washington Medical Center
Tumor Service
weisstei@u.washington.edu

Lisa A. Taitsman, M.D., M.P.H.
Assistant Professor
Harborview Medical Center
Trauma
taitsman@u.washington.edu

Klane K. White, M.D., M.Sc.
Assistant Professor
Children's Hospital and Regional Medical Center
Pediatric Orthopaedics
klane.white@seattlechildrens.org

Department of Orthopaedics and Sports Medicine Faculty

Jiann-Jiu Wu, Ph.D.
Research Associate Professor
University of Washington Medical Center
Research
wujj@u.washington.edu

Emeritus Faculty

Stanley J. Bigos, M.D.
Professor Emeritus

Theodore K. Greenlee, Jr., M.D.
Associate Professor Emeritus

Lynn T. Staheli, M.D.
Professor Emeritus

Adjunct Faculty

Basia R. Belza, R.N., Ph.D.
Associate Professor, Physiological Nursing

Jack W. Berryman, Ph.D.
Professor, Medical History & Ethics

Charles H. Chesnut, M.D.
Professor, Nuclear Medicine

Randal P. Ching, Ph.D.
Associate Professor, Mechanical Engineering

Richard A. Deyo, M.D.
Professor, Medicine

Gregory C. Gardner, M.D.
Professor, Rheumatology

Thurman Gillespy III, M.D.
Associate Professor, Radiology

Daniel O. Graney, Ph.D.
Professor, Biological Structure

Frederick A. Mann, M.D.
Professor, Radiology

Susan M. Ott, M.D.
Associate Professor, Division of Metabolism

Wendy Raskind, M.D., Ph.D.
Professor, General Internal Medicine

Michael L. Richardson, M.D.
Professor, Radiology

Peter A. Simkin, M.D.
Professor, Medicine

Tony J. Wilson, M.D.
Professor, Radiology

Miqin Zhang, Ph.D.
Associate Professor, Materials Science and Engineering

Joint Faculty

Michael M. Avellino, M.D.
Associate Professor, Neurological Surgery

Randy M. Chestnut, M.D.
Associate Professor, Neurological Surgery

Janet F. Eary, M.D.
Professor, Radiology

Mark A. Harrast, M.D.
Clinical Assistant Professor, Rehabilitation Medicine

John E. Olerud, M.D.
Professor, Division of Dermatology

Nathan J. Smith, M.D.
Professor Emeritus, Pediatrics

Michael D. Strong, Ph.D.
Research Professor, Surgery

Nicholas B. Vedder, M.D.
Professor, Plastic Surgery

Clinical Faculty

Sarah E. Jackins, R.P.T.
Assistant Professor, Rehabilitation Medicine

Visiting Lecturers

Ken Yamaguchi, M.D.
2007 LeCocq Lecturer

This year at our annual LeCocq lecture on January 18th and 19th, we were honored to have Dr. Ken Yamaguchi as our 2007 LeCocq Lecturer. Dr. Yamaguchi is the Sam and Marilyn Fox Distinguished Professor of Orthopaedic Surgery, and currently Chief of the Shoulder and Elbow Service in the Department of Orthopaedic Surgery at Barnes-Jewish Hospital, Washington University School of Medicine.

Dr. Yamaguchi received his medical degree from George Washington School of Medicine in Washington, D.C. He completed his residency at George Washington Hospital and a fellowship in shoulder and elbow surgery at the Columbia-Presbyterian Medical Center in New York. His clinical interests include arthroscopic treatment of rotator cuff disorders, shoulder and elbow total joint replacement and arthroscopy for elbow arthritis. Dr. Yamaguchi has been listed in "America's Top Doctors" as well as "The Best Doctors in America" publications.

Dr. Yamaguchi is involved in several professional societies. He is currently on the executive committee of the American Shoulder and Elbow Surgeons and was recently elected to the American Academy of Orthopaedic Surgeon's Board of Directors.

Dr. Yamaguchi is an author of more than 100 total publications, and has given numerous scientific presentations nationally and internationally. He also is a former Associate Editor of the Journal of Bone and Joint Surgery and Deputy Editor for the Journal of the American Academy of Orthopaedic Surgeons' section on upper extremity, shoulder and elbow. Additionally, he was also recently appointed to become the Deputy Editor for Shoulder at the Journal of Bone and Joint Surgery.

The recipient of various awards and honors throughout his career, Yamaguchi was selected to complete the American Orthopaedic Association's prestigious John J. Fahey Memorial North American Traveling Fellowship, was recognized with the Thomas M. Coffman Career Development Award from the Orthopedic Research and Education Foundation and received the Palma Chironis Teaching Award from the Washington University Department of Orthopaedic Surgery.

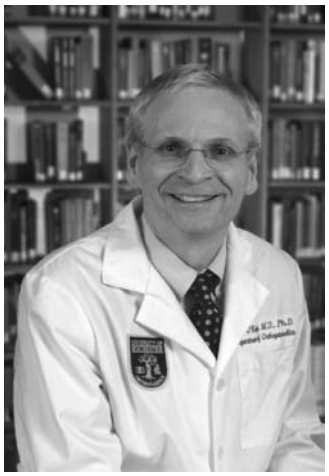

Regis J. O'Keefe, M.D., Ph.D.
2007 OREF Hark Lecturer, Residents' Research Days

This year at our annual Resident Research Days on June 28-29, we were honored to have Dr. Regis O'Keefe as our OREF Hark Lecturer. Dr. O'Keefe is the Chairman of the Department of Orthopaedics and Rehabilitation and the Director of the Center for Musculoskeletal Research at the University of Rochester School of Medicine and Dentistry in Rochester, New York. He also has faculty appointments in Departments of Pathology, Biochemistry and Biophysics, and Biomedical Genetics.

Dr. O'Keefe earned his BA in philosophy and religious studies and graduated magna cum laude at Yale University in New Haven, Connecticut. After earning his medical degree from Harvard Medical School in Boston, Massachusetts, he completed a Ph.D. in biochemistry and biophysics from the University of Rochester School of Medicine and Dentistry. Dr. O'Keefe served his internship in surgery at New England Deaconess Hospital in Boston, his residency in orthopaedics at the University of Rochester Medical Center and completed an oncology fellowship at the Massachusetts General Hospital. In 1993 he joined the faculty at the University of Rochester.

Dr. O'Keefe has authored or coauthored over 160 articles, more than 300 abstracts, 14 book chapters and reviews concerning bone repair and development, cancer, inflammatory diseases of bone, genetics, and related topics. He is on the editorial board of the Journal of Bone and Mineral Research and the Journal of Bone and Joint Surgery. Dr. O'Keefe is a member of the American Academy of Orthopaedic Surgeons (AAOS) and is the Secretary of the Orthopaedic Research and Education Foundation. He is a Past President of the United States Bone and Joint Decade, a coalition of over 100 organizations advancing the cause of the Bone and Joint Decade. He was Treasurer of the Orthopaedic Research Society and is currently a 3-year member of the program committee.

Dr. O'Keefe has received a variety of teaching and scientific awards including the prestigious ABC Traveling Fellowship from the American Orthopaedic Association and the Kappa Delta Award, recognizing excellence in orthopaedic research.

Dr. O'Keefe has worked diligently to promote and advance the basic understanding of musculoskeletal diseases and to translate these discoveries into therapies designed to improve the care of orthopaedic patients.

Msx-1 and Ki67 Expression in Human Fetal Digits After Tip Amputation

Brendan Inouye, Abby L. Navratil, B.S., Marcia L. Usui, B.S., Robert Underwood, B.F.A., Philip Fleckman, M.D., Rima Kulikauskas, B.S., and Christopher Allan, M.D.

Limb regeneration, although commonplace for organisms such as salamanders, is not successful in adult humans who have undergone a severe limb injury. However, if a successful regenerative response can be stimulated, quality of life for injured individuals could be significantly improved. Recent studies in our lab and others have identified a population of cells that express Msx-1, a transcription repressor, along the amputation plane following a distal tip amputation of the digit in both mice and young humans. The present study focused on a single mechanism for the arrival of the Msx-1 expressing cells, namely, the activation of proliferation of Msx-1 expressing cells following amputation. Through immunohistochemistry, mutually exclusive expressional patterns for Msx-1 and the proliferation marker Ki67 have suggested that on site proliferation is not the mechanism by which the Msx-1 expressing cells arise at the amputation site.

Introduction

Currently, surgical success in completely restoring lost limbs following injury is an uncommon occurrence. However, if a regenerative response could be elicited in humans, the amputee could not only regain the lost limb, but limb function as well. Limb regeneration has become an ultimate goal for regenerative medicine. In adult humans, successful regenerative responses are not generally observed, and instead the wound healing process concludes with the creation of a scar. One notable exception is the regrowth of fingertips in children.

Successful whole-limb regeneration is observed in some lower level vertebrates, most commonly the newt and salamander, and early-stage xenopus (frog). Studies have also shown mice can successfully regenerate lost digit tips following distal tip amputations. A distal tip amputation as described here refers to a loss of the tissues and bone of the digit from a cut through the nailbed. Most recently studies have shown that successful digit tip regeneration has also been observed in fetal human tissues, and is linked to the expression of a transcription repressor called Msx-1. Msx-1 is thought to maintain a population of cells in a stemlike state which then allows for the differentiation of these cells into many different tissue types following injury. In humans Msx-1 expression has been shown to be localized under the developing nailbed.

Following a distal tip amputation it has been observed that a population of Msx-1 expressing cells arises along the leading edge of the amputation plane. The primary focus of this study is to test the hypothesis that the Msx-1 expressing cell population arises in correspondence with a localized increase in proliferating cells. To accomplish this, our study used both immunoperoxidase and immunofluorescent techniques to first characterize proliferation throughout a human fetal developmental series, and then characterize the Msx-1 and proliferation characterization patterns following distal tip amputation and organ culture.

Materials and Methods

Tissue Preparation

Human fetal digits of estimated gestational age (EGA) between 53 and 110 days were collected in compliance with the University of Washington's Internal Review Board. A total of 10 digits of EGAs 53, 59, 63, 72, 76, 85, 87, 92, 105, and 110 days were frozen in O.C.T. (Finetek, Sakura Inc., Torrance, CA) and stored at -70°C. A cryostat (Leica) was used to dissect six micron sagittal sections of each digit. Sections were taken until a mid-digit location was obtained. Developmental structures such as the developing nailfold and phalanges were used to identify and confirm orientation and location within each digit. Sections were then desiccated overnight for staining.

Developmental Series

Standard immunoperoxidase immunohistochemistry techniques were used to determine the expressional pattern of Ki67, a marker for proliferation, within developing fetal digits. Digits of EGAs 59, 63, 72, 76, 85, 92, 105, and 110 days were used. Tissue samples were fixed in cold acetone for 5-10 minutes prior to staining. Mouse anti-human antibody (Novocostra) was used in a 1:200 dilution as the primary antibody. Goat anti-mouse antibody (Vector, Burlingame, CA), was used in a 1:200 dilution as the secondary antibody. The Vector Elite Kit (Vector, Burlingame, CA) was used for streptavidin and diaminobenzidene was used as a chromogen. Counterstaining in hematoxylin was done to further highlight developmental structures. Experimental protocols were performed at room temperature with washes done with Tris Buffered Saline solution.

Organ Culture

Human fetal digits of EGA 53 and 87 days were both tip amputated (one hand) and left intact (opposite hand), and cultured for 1,2 and 4 days using standard tissue culture protocol as described by Zeltinger et al. Standard immunofluorescence immunohistochemistry techniques were used to determine expressional patterns of both Msx1 and Ki67 in tissue cultured and non-cultured digits. Primary antibodies used were a rabbit pan-keratin, goat anti-human Msx-1, and mouse anti-human Ki67 which stained for keratin, Msx-1 expressing cells, and proliferation respectively. Secondary antibodies used which contained fluorescent tags were Cy5, FITC, and Texas Red. These secondary antibodies were anti-rabbit, anti-goat, and anti-mouse respectively. A DAPI counterstain was also used to better identify cellular components within each section.

Imaging

Tissue samples from both the developmental series and organ culture

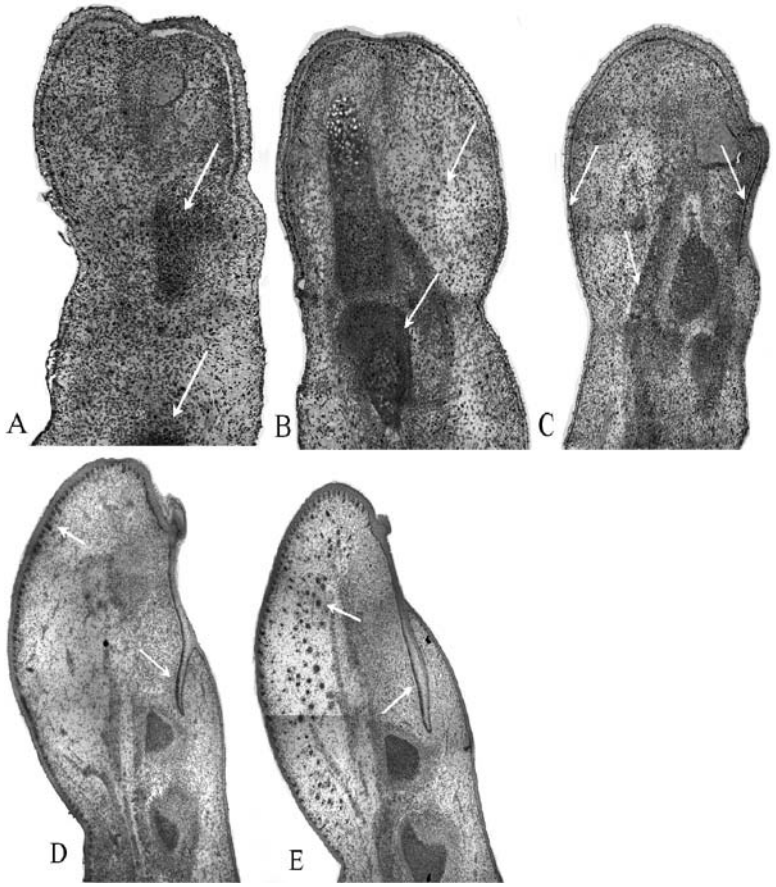

Figure 1: Ki67 expressional pattern in developmental series of human fetal digits of 57(A), 63(B), 72(C), 92(D), and 110(E) day EGA. The white arrows indicate a high concentration of proliferating cells.

experiments were imaged using a Nikon Microphot-SA microscope, outfitted with a Photometrics Sensys digital camera. Images were then montaged, adjusted, and analyzed using Adobe Photoshop.

Results

Developmental Series

From the immunoperoxidase results the developmental expression for Ki67 in fetal digits is initially distributed throughout the entire digit, but becomes more isolated to specific structures within the digit as EGA increases. Younger digits (EGA < 72 days) (Figure 1 A and B) were shown to have cellular expression of Ki67 throughout the entire digit with higher localized concentrations of proliferating cells within the developing phalangeal structures. As age increased to 72 days EGA (Figure 1C) the expression pattern of Ki67 became more isolated to the developing nailfold, nailbed, and basement membrane. As EGA continued to increase proliferating cell populations became more dorsally and distally isolated to structures such as the developing nailbed, nailfold, and the developing sweat glands. This can be seen in Figure 1 D and E.

Immunofluorescence

From the triple labeled cultured and non-cultured and tip-amputated and control digits the expression patterns of Ki67 and Msx-1 appear to be mutually exclusive. Within the control digits Msx-1 expression was localized to within the developing nailfold and under the developing nailbed, while Ki67 was localized to the more proximal dermal tissues (results not shown). In tip-amputated cultured digits the expressive pattern for Msx-1 was localized to cells along the leading edge of the amputation sight. This can be seen in Figures 2 and 3, which are 53 day EGA and 87 day EGA digits respectively. The expressional pattern for Ki67 in tip-amputated digits was localized to the more proximal dermal tissues as seen in Figures 2 and 3, structure C. Similar mutually expressional patterns for Msx-1 and Ki67 were observed for digits culture for 2 and 4 days (results not shown).

Discussion

From the immunoperoxidase results it can be concluded that the expression pattern of Ki67, which is initially evenly distributed throughout the digit, becomes more isolated and localized to the developing sweat glands, nailfold, and nailbed as EGA increases. From the immunofluorescence results it can be concluded that the expression patterns of cells for Msx-1 and Ki67 is mutually exclusive and that during response to tip amputation Msx-1 expressing cells are not actively proliferating. This suggests that the increase in Msx-1 expression noted along the leading edge of the amputation site is not due to an increase in proliferation of local Msx-1-expressing cells. Among other mechanisms we can hypothesize two intriguing possibilities: first, migration from a nearby stem cell niche (for example the Msx-1-rich region beneath the nail field), or second, an upregulation of Msx-1 expression in local cells associated with dedifferentiation in response to tip amputation. We are pursuing further studies to explore these possibilities.

Acknowledgements

The lead author would like to thank the University of Washington Engineered Biomaterials (UWEB) program as well as the National Science Foundation for providing the funding for the research. He would also like to thank the Dermatology Research Center and his mentor Dr. Christopher Allan.

Recommended Reading

Allan CH, Fleckman, P, Fernandes, RJ, Hager, B, James J, Wisecarver Z, Satterstrom FK, Guitierrez A, Norman A, Pirrone A, Underwood RA, Rubin BP, Zhang M, Ramay HR, Clark JM. Tissue response and Msx1 expression after human fetal digit tip amputation in vitro. Wound Repair and Regeneration 2006; 14:398-404.

Brockes JP, Kumar A. Appendage Regeneration in Adult Vertebrates and implications for Regenerative Medicine. Science 2005; 310:1919-1923.

Gardiner DM, Carlson MRJ, Roy S.

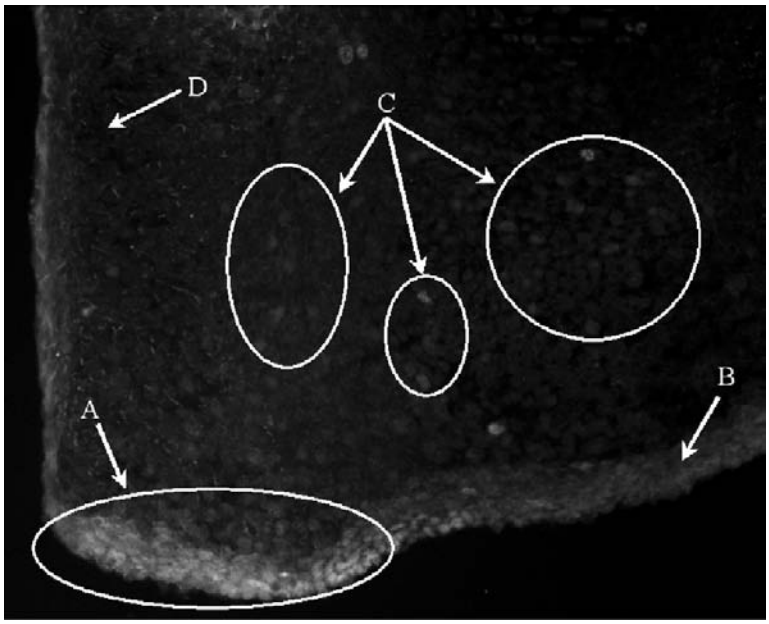

Figure 2: 53 day EGA tip-amputated digit after 1 day in culture (cut tip toward bottom of image). Msx-1 expressing cells (A) are located along long the dorsal edge of the amputation plane (D). Proliferating cells or Ki67 expressing cells (C) are located in the deeper proximal tissues near the developing nailbed (D).

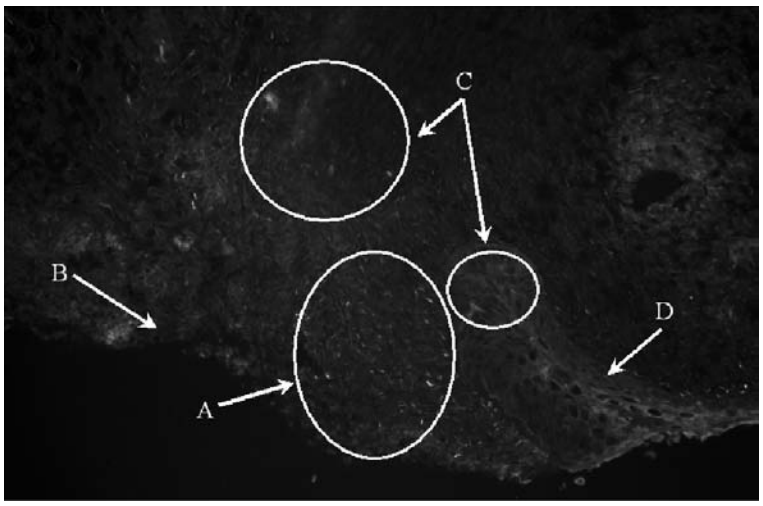

Figure 3: 87 day EGA tip-amputated digit after 1 day in culture (cut tip toward bottom of image). The population of Msx-1 expressing cells (A) is located along the dorsal edge of the amputation plane (B). Cells expressing Ki67 (proliferating cells) (C) are located in the deeper proximal tissues as well as in the developing nailfold (D).

Towards a functional analysis of limb regeneration. Cell and Developmental Biology 1999; 10:385-393.

Han M, Yang X, Farrington J, Muneoka K. Digit regeneration is regulated by Msx1 and BMP4 in fetal mice. Development 2003; 130:5123-5132.

Han M, Yang X, Taylor G, Burdsal C, Anderson R, Muneoka K. Limb Regeneration in Higher Vertebrates: Developing a Roadmap. The Anatomical Record 2005; 287B:14-24.

Muller T, Ngo-Muller V, Reginelli A, Taylor G, Anderson R, Muneoka K. Regeneration in higher vertebrates: Limb buds and digit tips. Cell and Developmental Biology 1999; 10:405-413.

Reginelli A, Wang Y, Sassoon D, Muneoka K. Digit tip regeneration correlates with regions of Msx1 (Hox7 7) expression in fetal and newborn mice. Development 1995; 121:1065-1076.

Zachary S, Peimer C. Salvaging the "Unsalvageable" Digit. Hand Clinics 1997; 2:239-249.

Zeltinger J, Holbrook K. A model system for long-term serum-free suspension organ culture of human fetal tissues: experiments on digits and skin from multiple body regions. Cell and Tissue Research 1997; 290:51-60.

A Gene-Therapy Approach to Suppressing EWS/FLI-1 Leads to Cellular Senescence Through Rb Family Dependent and Independent Pathways

Hsien-Ming Hu, Ph.D., Anna Zielinska-Kwiatkowska, M.S., Daniel Wu, M.D., Ph.D., Liu Yang, Ph.D., and Howard Chansky, M.D.

The defining cytogenetic abnormality of Ewing's sarcoma is a balanced t(11;22) translocation expressing the EWS/FLI-1 chimeric fusion protein. We have generated an adenovirus system to efficiently deliver short interfering RNA (siRNA) targeting the EWS/FLI-1 transcript into several Ewing's cell lines. A sustained and near-complete knockdown of EWS/FLI-1 is achieved. More importantly, after EWS/FLI-1 knockdown the cells assume a senescence-like phenotype with G1 growth arrest, flattened and enlarged cell morphology, and expression of senescence marker SA-β-galactosidase. These findings have led to the hypothesis that the EWS/FLI-1 fusion protein blocks cellular senescence and promotes uncontrolled cell proliferation in Ewing's sarcoma.

To identify pathways leading to the senescence phenotype, we investigated expression of the Rb family members (including Rb, p130 and p107) that are known tumor suppressor genes and regulate the G1/S checkpoint. We found that both pRb and p130 are activated after EWS/FLI-1 knockdown. We next investigated whether inactivating the G1/S checkpoint can prevent cellular senescence (i.e. restore the malignant phenotype) induced by EWS/FLI-1 knockdown. We generated Ewing's sarcoma cells that stably express the human papillomavirus E7 protein that interferes with the Rb family G1 checkpoint. Preliminary results indicate that Ewing's cells with an inactive G1 checkpoint also undergo growth arrest when EWS/FLI-1 is knocked down. Together, these results suggest that EWS/FLI-1 bypasses cellular senescence through both Rb family-dependent and –independent mechanisms.

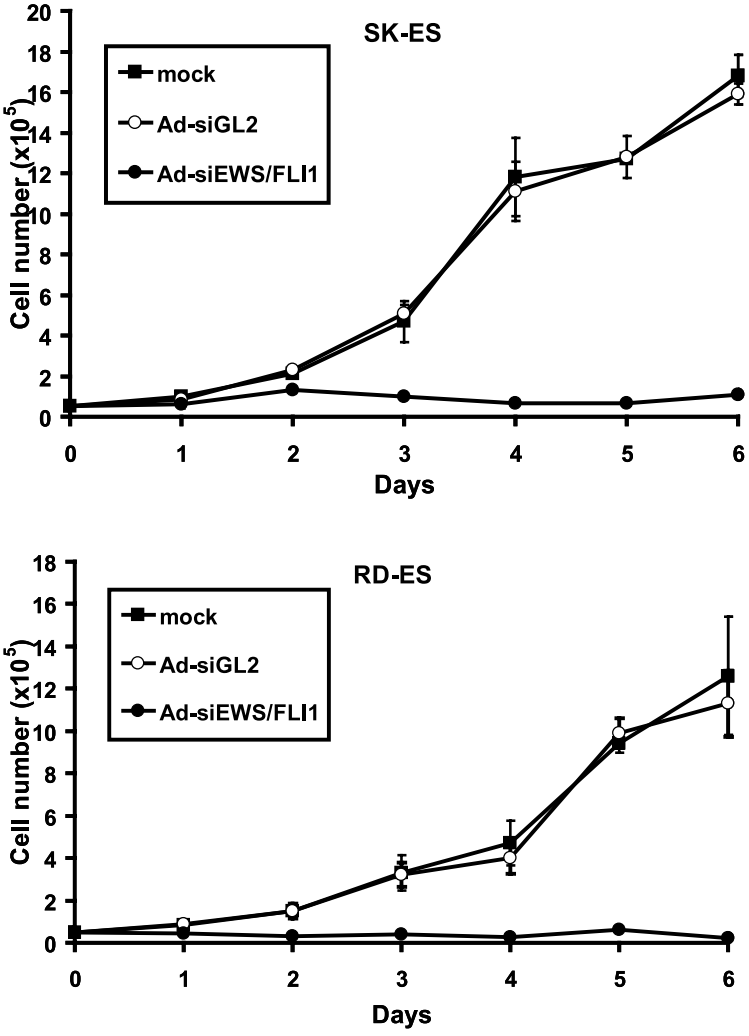

Figure 1: Growth curves of adenovirus-treated Ewing's cells. SK-ES and RD-ES cells were infected for 6 hours. 50,000 cells were seeded on 6-cm plates and cell numbers were counted at day 1 through day 6 by trypan blue exclusion.

Materials and Methods

SK-ES and RD-ES, both Ewing's sarcoma cell lines carrying the t(11;22) translocation, were infected with adenovirus encoding siRNA targeting EWS/FLI1, or GL2 luciferase as a negative control. Whole cell lysates were prepared at different time points after infection. Western blotting analysis was performed with antibodies against pRB, p130, p107, cyclin A and β- actin.

SK-ES and RD-ES cells with stable expression HPV-V16 E7 protein or empty vector control were generated by infecting the cells with retrovirus containing LXSN-E7 or LXSN followed by G418 selection.

Results

Adenovirus-mediated RNA interference effectively suppressed the expression of EWS/FLI-1 in SK-ES and RD-ES Ewing's sarcoma cell lines

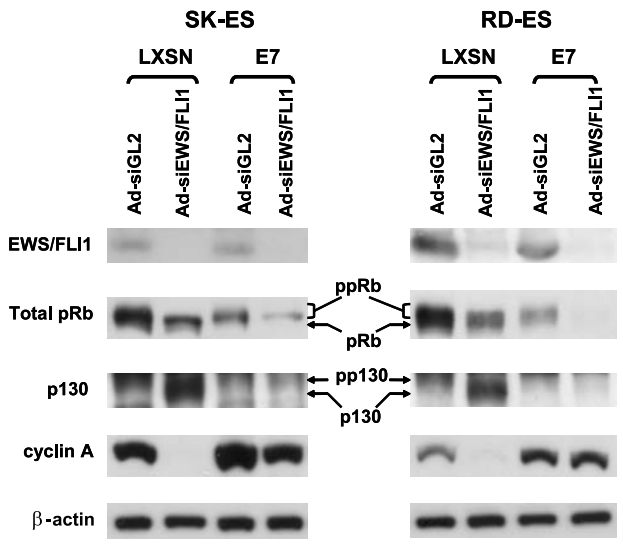

Figure 2: Functional inactivation of the Rb family tumor suppressors by ectopic expression of HPV16 E7. Immunoblotting analysis of SK-ES and RD-ES cells stably expressing E7, or empty vector (LXSN) after infection with adenovirus containing the siRNA targeting EWS/FLI1. Cell lysates were examined for levels of EWS/FLI1, Rb, p130 and cyclin A. Beta actin serves as a loading control.

for at least 6 days and for as long as 10 days. Tumor cells in which EWS/FLI1 was knocked down underwent growth arrest (Figure 1) and the majority of the cells were blocked at the G1 phase of the cell cycle. The cells assumed a uniformly enlarged and flat morphology with cytoplasmic inclusions, a feature of senescence. To investigate if the Rb family members play a role in inducing the G1 growth arrest, we examined these proteins by Western blotting (data not shown) for their expression levels and phosphorylation status in cells that underwent EWS/FLI1 knockdown. Rb shifts to the predominantly hypo- or non-phosphorylated forms at 48 hours, coinciding with the onset of growth arrest. In addition, the level of Rb family member p130 was sharply increased and accompanied by a similar down shift in phosphorylation. The third member p107 does not seem to play a role since the level was reduced in senescent cells. The diminished expression level of cyclin A, a downstream target of Rb family members that is essential for transition to S-phase is further evidence of activation of the Rb family tumor suppressor proteins.

To determine if bypass of the G1/S block by Rb family members is sufficient to avert cellular senescence induced by EWS/FLI-1 knockdown, we generated Ewing's cells stably expressing human papillomavirus E7 (HPV E7). HPV E7 inactivates the Rb family proteins. When the cells expressing HPV E7 were infected with adenovirus expressing siRNA targeting EWS/FLI-1, the cells remained growth arrested despite expression of S-phase proteins such as cyclin A. This result strongly suggests the existence of a second block, perhaps involving a different tumor suppressor protein that is activated in the absence of EWS/FLI1.

Discussion

Our data show that the G1 growth arrest induced by EWS/FLI-1 knockdown can be in part attributed to activation of the Rb family tumor suppressor proteins, pRb and p130. Failure to maintain expression of cyclin A is further evidence that the cells were stalled at the G1/S transition and essentially are blocked from the replicative pathway after knockdown of EWS/FLI1. In an initial attempt to evaluate the relative contribution of the G1/S block to cellular senescence, we tested the effect of EWS/FLI-1 knockdown in Ewing's cells in which HPV E7 inactivated the Rb-dependent G1/S checkpoint (in effect, HPV E7 prevents Rb from blocking the progression of the cells into the replicative phase of the cell cycle). We again used western blotting to analyze expression of the pRb family proteins (pRb and p130) as well as cyclin A. As can be seen if Figure 2, HPV prevents the shift to hypophosphorylated (active) forms of pRb and p130 and in addition blocks the down-regulation of the pro-proliferative factor, cyclin A. These cells still assumed a senescent phenotype thus indicating that a secondary block, unrelated to the Rb pathway, exists post-knockdown Ewing cells. The nature of this block is being investigated.

Recommended Reading

Chansky, HA; Barahmand-Pour, F; Mei, Q; et. al. (2004): Targeting of EWS/FLI-1 by RNA interference attenuates the tumor phenotype of Ewing's sarcoma cells in vitro. J Orthop Res. Jul;22(4):910-7

Rachel S. Roberson, Steven J. Kussick, Eric Vallieres, Szu-Yu J. Chen and Daniel Y. Wu. (2005): Escape from Therapy-Induced Accelerated Cellular Senescence in p53-Null Lung Cancer Cells and in Human Lung Cancers. Cancer Res. Apr 1;65(7):2795-803.

Inhibitor of DNA Binding Protein Id2 Negatively Regulates Chondrogenic Differentiation of ATDC5 Cells

Liu Yang, Ph.D., Xiaoyun Ma, Ph.D., Anna Zielinska-Kwiatkowska, M.D., and Howard A. Chansky, M.D.

The process of chondrogenesis can be mimicked in vitro by insulin treatment of mouse ATDC5 chondroprogenitor cells. To identify novel factors that are involved in the control of chondrogenesis, we carried out a large-scale screening through retroviral insertion mutagenesis and isolated a fast-growing ATDC5 clone incapable of chondrogenic differentiation. Inverse-PCR analysis of this clone revealed that the retroviral DNA was inserted into the promoter region of mouse Id2 gene. This retroviral insertion increased Id2 protein level to twice as much as that in normal ATDC5 cells. To investigate whether an elevated level of Id2 protein was responsible for inhibition of chondrogenic differentiation, ATDC5 cells were infected with a retrovirus to stably express Id2. Cells expressing ectopic Id2 exhibited an advantage in proliferation and a blockage of differentiation, and insulin failed to induce expression of type II collagen (COL2) in these cells.

Endochondral bone formation involves condensation of mesenchymal cells and their subsequent differentiation into mature chondrocytes that express type II collagen (COL2). In the center of this rudimentary bone, mature chondrocytes can further differentiate into hypertrophic chondrocytes. These hypertrophic cells express type X collagen and mineralize the surrounding matrix before undergoing apoptosis. The cartilage matrix left behind then provides a scaffold for growth of osteoblasts/osteoclasts along with other cells that comprise mature bone. In the past decade, much progress has been made by characterizing transcription factors and signaling molecules involved in chondrogenesis.

The process of chondrocyte differentiation can be mimicked in vitro by insulin treatment of the mouse ATDC5 chondroprogenitor cells. Following insulin stimulation, these cells condense to form nodules and synthesize cartilage-like extracellular matrix that stains positive with Alcian blue. After prolonged culture in insulin medium, these cells initiate the synthesis of type X collagen and eventually die through apoptosis.

To identify novel factors that are involved in the control of chondrogenesis, we carried out a large-scale screening through random retroviral integration into the genome of ATDC5 cells. If these random insertions disrupted genes critical in the control of chondrogenesis, the end result could be spontaneous chondrogenic differentiation of ATDC5 cells in the absence of insulin on one hand, or blockage of chondrogenic differentiation of ATDC5 cells in the presence of insulin on the other hand.

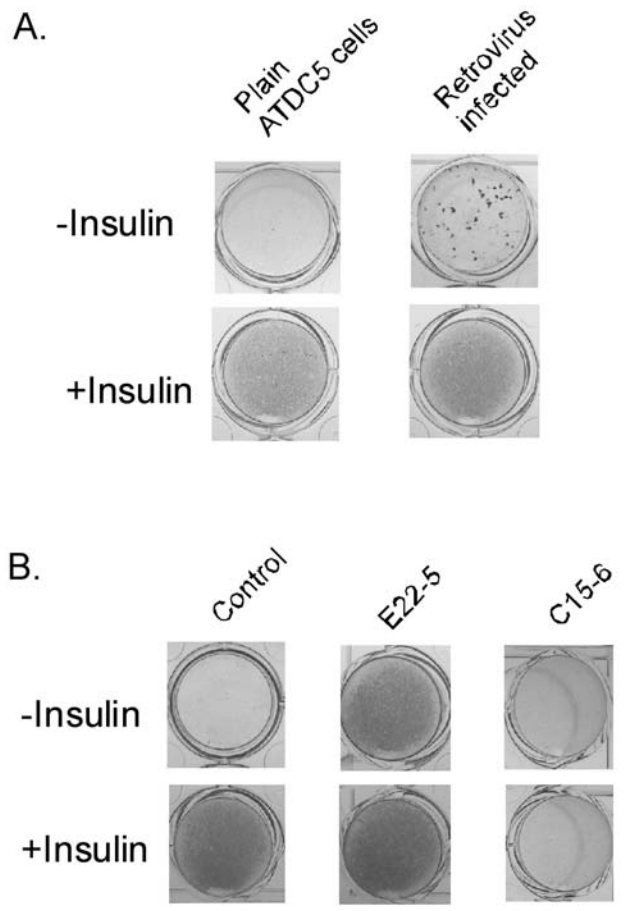

Figure 1: Screening for mutant ATDC5 clones after retroviral insertion. (A) Plain ATDC5 cells were seeded into two wells on a 24-well plate, cultured in medium with or without insulin for 21 days, then stained with 0.2% Alcian blue (left panels). The same ATDC5 cells were also infected with a retrovirus. The infected cells were first selected with G418, then pooled and cultured with or without insulin for 21 days. Note the few colonies that stained positive with Alcian blue in the absence of insulin treatment (top right panel). (B) Individual retrovirus-infected ATDC5 clones were isolated after G418 selection. Normal clone E22-4 (lane 1), mutant clone E22-5 that underwent spontaneous differentiation (lane 2), and mutant clone C15-6 that was unable to differentiate (lane 3) were expanded and cultured in medium with or without insulin for 21 days, then stained with Alcian blue. C15-16 is the clone that was used in this report.

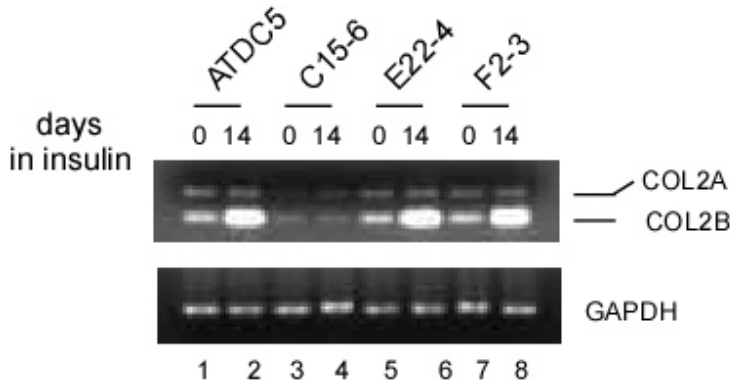

Figure 2: Repression of endogenous COL2 gene by Id2 protein. Expression of COL2 gene was analyzed by RT-PCR using total RNAs from plain ATDC5 cells (lanes 1-2), Id2 over-expressing clone C15-6 (lanes 3-4), normal clones E22-4 and F2-3 (lanes 5-8). Induction of COL2 expression was achieved by treatment with insulin for 14 days. Two splicing isoforms of COL2 transcripts are indicated. RT-PCR analysis of GAPDH mRNA was performed to show similar amounts of total RNAs were used in the analysis.

As these mutant ATDC5 clones can be isolated via Alcian blue staining, identification of the corresponding retroviral integration sites (and the likely affected genes) within the ATDC5 genome will add to our understanding of the complex network that regulates chondrogenesis.

Discussion

The growth of mouse ATDC5 chondroprogenitor cells normally will slow down upon reaching confluence. However, when cultured in medium containing insulin, confluent ATDC5 cells will form nodules and start to undergo chondrogenic differentiation. This eventually leads to the production of a cartilage-like matrix that can be stained by Alcian blue (Figure 1A, left panel). We noticed that when ATDC5 cells were infected with a retrovirus and then cultured for 21 days, a few the retrovirus-infected cells could form colonies that also stained positive with Alcian blue even in the absence of insulin (Figure 1A, right panel). As it is known that a retrovirus can randomly integrate into the genome of the host cells, we speculated that a small number of the retroviral integrations would integrate within genes critical to insulin-dependent chondrogenic differentiation of ATDC5 cells. Activation or silencing of these critical genes could result in spontaneous chondrogenic differentiation of ATDC5 cells, resulting in a phenotype of positive staining with Alcian blue stain even in the absence of insulin. On the other hand, activation or silencing of these critical genes could also interfere with chondrogenic differentiation, resulting in a phenotype of negative Alcian blue staining even in the presence of insulin. Individual colonies with stable retroviral integration were selected by G418 and screened in duplicate 98-well plates for their response to insulin by Alcian blue staining. Out of 10 x 103 colonies examined, the vast majority showed no change in phenotype (Figure 1B, left panel). A few of the colonies such as E22-5 showed spontaneous differentiation in the absence of insulin (Figure 1B, middle panel). One clone, designated C15-6, did not stain with Alcian blue even when cultured in insulin for 21 days (Figure 1B, right panel). Therefore, a small number of the retroviral insertions resulted in deregulation of genes that are important for chondrogenic differentiation of ATDC5 cells. The feasibility of this strategy was confirmed by our identification of Id2 as a negative regulator of chondrocyte differentiation. To confirm our hunch that Id2 was in fact responsible for the phenotypic changes in the ATDC5 cells, we performed additional experiments and demonstrated that ectopic expression of Id2 (to create excess or supraphysiologic intracellular levels of Id2) promoted proliferation and blocked differentiation in ATDC5 cells.

To analyze changes in type II collagen expression (COL2), we isolated total RNA from plain ATDC5 cells, from clone C15-6 (which had an elevated level of endogenous Id2 protein) as well as from unaffected clones E22-4 and F2-3. Alternative splicing of the COL2 pre-mRNA transcripts usually generates splicing isoforms COL2A and COL2B that change their ratio during the differentiation of chondrocytes. In plain ATDC5 cells and normal clones E22-4 and F2-3 cultured with insulin, expression of the COL2 gene was upregulated with a concomitant COL2A→2B switch (Figure 2, lanes 1-2 and 5-8). In contrast, insulin failed to induce COL2 expression in clone C15-6 (Figure 2, lanes 3-4).

Id2 belongs to a subfamily of proteins that function as Inhibitors of Differentiation. As Id2 inhibition of ATDC5 chondrogenic differentiation is manifested by repression of collagen genes such COL2 and COL11A2, it will be interesting to examine whether Id2 suppresses expression of collagen genes by dimerizing with basic helix-loop-helix proteins or by interacting with other collagen gene regulators such as Sox9. In ATDC5 cells, Id2 may also globally decrease expression of differentiation-specific genes by diverting cells into S-phase and the cell cycle. We are currently working to decipher the mechanism by which ID2 can profoundly affect chondrogenesis.

Id2 may be necessary for normal maintenance of chondroprogenitor cells since the existence of a basal level of Id2 protein in ATDC5 cells does not negatively impact chondrogenic differentiation following insulin treatment. However, a modest increase in Id2 protein is able to completely block insulin-induced differentiation of these chondrogenic cells. As expression of Id2 can be either up- or down-regulated in response to growth factors in most cell types, our results raise the possibility that the Id2 gene could be a critical down-stream target of multiple signaling pathways to achieve a fine balance between growth and differentiation in chondrocytes.

Acknowledgement

This work is supported by NIH grant RO1 AR051455 to L.Y.

Recommended Reading

Kronenberg, H. M. (2003) Nature 423(6937), 332-336.

Atsumi, T., Miwa, Y., Kimata, K., and Ikawa, Y. (1990) Cell Differ Dev 30(2), 109-116.

Post-Translational Overmodification of Collagen Expressed by SAOS-2 Osteoblast-Like Cells

Russell J. Fernandes Ph.D., Michael A. Harkey Ph.D., and David R. Eyre Ph.D.

Bone type I collagen can be distinguished from type I collagen of other tissues by a characteristic post-translational chemistry. In particular, it has a distinctive profile of cross-linking amino acids that reflects the degree of lysine hydroxylation of telopeptide and helical cross-linking sites in the component α1(I) and α2(I) chains. Hydroxylysyl pyridinoline (HP) cross-links are formed between two telopeptide hydroxylysine residues and a specific triple helical hydroxylysine residue. Lysyl pyridinoline (LP) cross-links are a post-translational variant found prominently in bone type I collagen that form from two telopeptide hydroxylysines and a lysine at the triple helical site. The overall content of hydroxylysine in bone collagen has been shown to vary with stage of bone maturity and to be higher in osteosarcoma bone, osteoporotic cancellous bone and woven repair bone than in normal mature bone. The functional significance and mechanism of regulation of these differences are not understood. We have investigated the relationship between collagen post-translational quality and lysyl hydroxylase (LH) expression in the SAOS-2 osteosarcoma cell line.

Materials And Methods

Cell culture

The SAOS-2 cell line (ATCC # HTB 85) was maintained in monolayer culture in McCoys media containing 10% FBS and 50mg/ml ascorbate.

Collagen extraction

After one month in culture, collagen was extracted from the cell layer, first by neutral 1M NaCl and then pepsin digestion. Harvested medium was saved for collagen analysis. Hydroxyproline was assayed colorimetrically after acid hydrolysis as a measure of collagen content.

SDS-PAGE

Collagen types were identified by electrophoresis of the pepsin digested protein. Gels were scanned densitometrically to determine approximate ratios of collagen types in the extracts.

Collagen cross-link analysis

Cell layers were hydrolysed in 6M HCl at 108°C for 24h. Hydroxylysyl pyridinoline (HP) and lysyl pyridinoline (LP) were resolved and quantified by RP-HPLC.

Lysyl hydroxylase expression

RNA was extracted using TriZol (BRL). A co-RT-PCR assay was developed that yielded 748, 879, 434 and 378 bp products specific for LH1, LH2, G3PDH and COL1A1 respectively in a single reaction. The assay was applied to mRNA extracted from SAOS-2 cells, fetal human bone, various other fetal human tissues, CH1 human chondrosarcoma cells, (a gift from Dr. Linda Sandell) and human foreskin fibroblasts. Products were separated on polyacrylamide gels and quantified by densitometry.

Comparative genome analysis

Regions of the LH1 and Type X collagen genes were amplified by multiplex-PCR, using 300 ng genomic DNA from human fetal liver or SAOS-2 cells. After electrophoresis, products were quantified by densitometry.

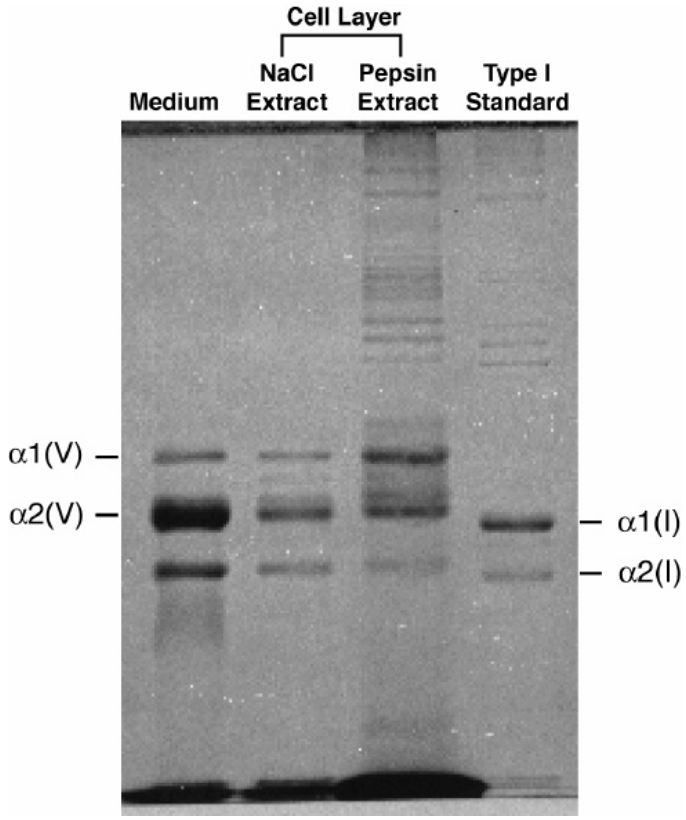

Figure 1: Collagen types synthesized by the SAOS-2 cell line in culture.

Results

The medium and cell layer on pepsin digestions showed types I and V collagen a-chains on SDS-PAGE. The α1(I) and α2(I) chains ran slightly slower than pepsin extracted control preparations from human bone, suggesting post-translational over-modification (Figure 1).

Of the total collagen synthesized, 65% was present in the medium, 2% in the 1M NaCl extract and 33% in the pepsin extract of the cell layer. The insolubility of the cell-layer collagen without pepsin digestion indicated extensive covalent cross-linking.

Type I collagen is the major collagen

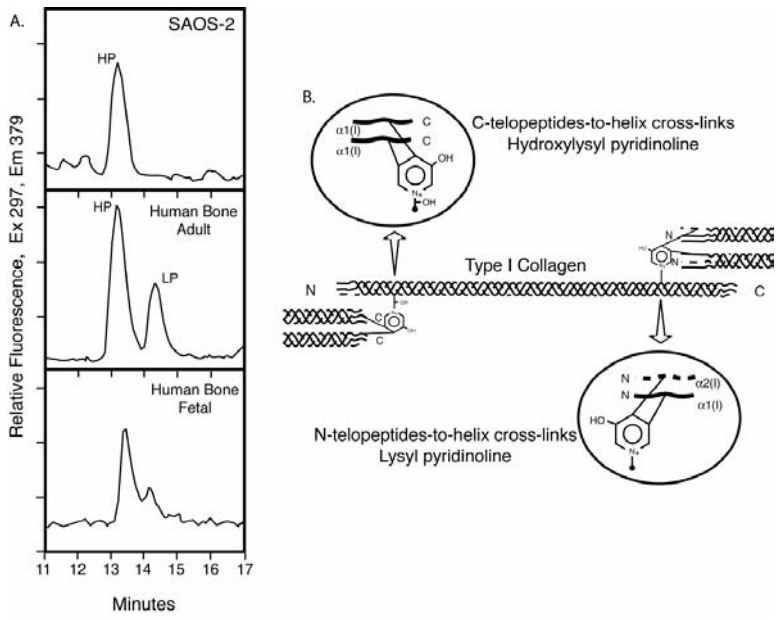

Figure 2: (A) Pyridinoline cross-links in SAOS-2 cell layer collagen compared with human bone. (B) Diagram showing the location of pyridinoline cross-links in bone type I collagen molecule.

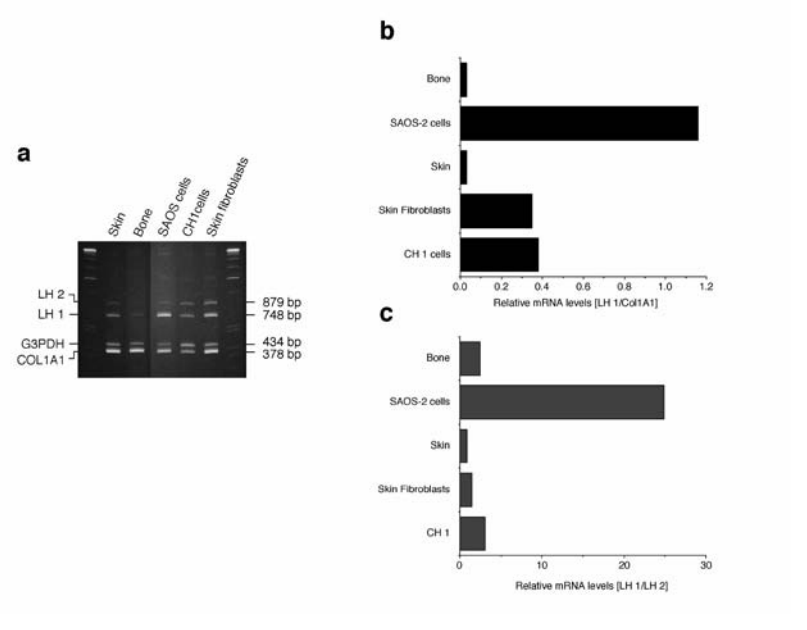

Figure 3: Expression of lysyl hydroxylase mRNA.

synthesized by the cell line accounting for 80% of the total collagen in the culture. Most of the type I collagen was in the medium. About equal amounts of types I and V collagens were recovered in the pepsin extract of the cell layer, indicating a preferential deposition of type V collagen in cross-linked extracellular fibrils.

RP-HPLC analysis of pyridinoline cross-links in the cell layer collagen showed HP alone in contrast with the ratio of about 2:1 for HP/LP typical of human bone (Figure 2A). This result indicates that the triple-helical domain cross-linking lysines were fully hydroxylated in the SAOS-2 collagen, whereas in bone collagen they are only partially hydroxylated. The total pyridinoline (HP+LP) concentration in the SAOS-2 collagen (0.28 mol/mol of collagen) was similar to that of human bone (0.24 mol/mol collagen). On further analysis, the pyridinolines were shown to be present primarily in type I collagen.

Expression of two human lysyl hydroxylase genes LH1 and LH2 were analyzed.

6% polyacrylamide gels showing the ethidium bromide stained RT-PCR products of LH1, LH2, G3PDH and COL1A1 from human skin, human bone, SAOS-2 cells, cultured human chondrosarcoma cells (CH1) and cultured skin fibroblasts are seen in Figure 3A.

A similar RT-PCR experiment was performed after labeling with $dCT^{32}P$ to assess relative levels of LH1 message. For each tissue or cell culture, RNA was amplified and resolved on a 6% gel. Autoradiograghs were scanned to compare bands quantitatively. As shown in the bar graphs (Figure 3 B, C), regardless of the RNA chosen as reference (COL1A1 or LH2), LH1 mRNA was much higher (10 to 30 fold) in SAOS-2 cells than in bone, skin and cultured cells.

A 6% polyacrylamide gel showing multiplex-PCR products of the LH1 gene and type X collagen gene is seen in Figure 4. To address the possibility that the elevated LH1 expression could be due to either karyotype abnormalities or to tandem duplication of the gene, a multiplex-PCR assay was run, which compared the abundance of the LH1 sequence in genomic DNA to that of a reference gene, type X collagen.

The relative abundance of LH1 and type X collagen PCR products was similar in SAOS-2 DNA and in normal fetal liver DNA, indicating a normal LH1 copy number in SAOS-2 cells. Thus, the high levels of LH1 mRNA are due to elevated expression and/or stability of these products in SAOS-2 cells.

Discussion

The human osteosarcoma-derived cell line SAOS-2, exhibits many of the phenotypic characteristics of osteoblasts including the deposition of types I and V collagens in an extracellular matrix. Lesser amounts of collagen XI chains were also detected. The cell layer collagen contains hydroxylysyl pyridinoline cross-links but without the accompanying lysyl pyridinoline typical of human bone

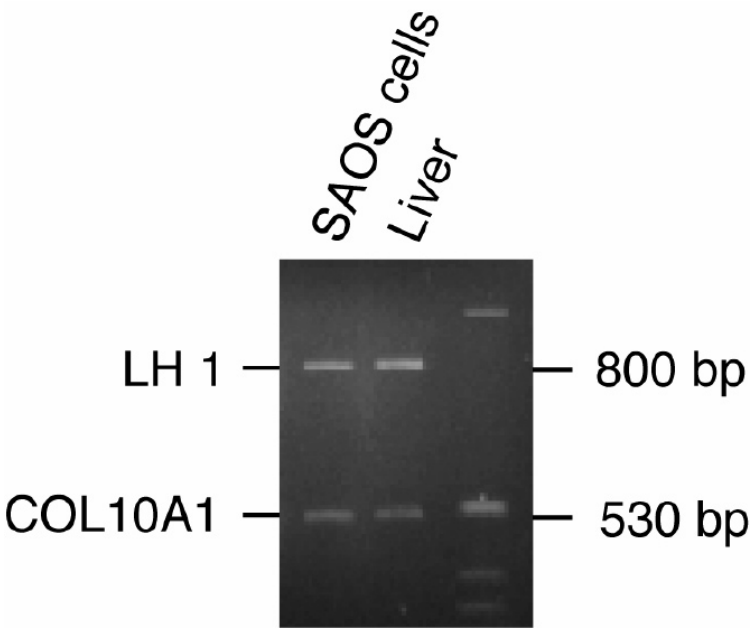

Figure 4: LH1 gene copy number in SAOS-2 cells and human liver cells.

collagen. This indicates that the lysine residues at the two helical cross-linking loci are fully hydroxylated. The isoform of lysyl hydroxylase, LH1, known to be required for full hydroxylation at these sites, was shown to be highly expressed by SAOS-2 cells. For comparison, a lack of LH1 activity caused by mutations that disrupt the LH1 gene, results in abnormally low HP/LP cross-link ratios in the tissues of patients with Ehlers-Danlos Syndrome type VIA. Our findings provide insight on the mechanism of post-translational overmodification of lysine residues in collagen made by osteosarcoma tumors, and may be relevant for understanding a similar overmodification observed in osteoporotic bone.

Recommended Reading

Eyre, D. R (1996) in Principles of Bone Biology

Lehmann et al., (1992) Biochem. J, 282:313

Shapiro and Eyre (1982) JNCI, 69:1009

Bailey et al., (1992) Biochem Biophy Res Commun,185:801

Glimcher et al., (1980) J. Bone Joint Surgery 62A: 964.

Valtavaara et al., (1997) J. Biol. Chem., 272:6831

Steinmann et al., (1995) Am. J. Hum. Gen., 57:1505

Supported by NIH grants AR 37318, AR 36794 and AR 52896

A manuscript incorporating this data is in press and will be published in the journal "Bone" in 2007. It can be accessed online at http://dx.doi.org/10.1016/j.bone.2007.01.011

Identification of Mimecan: A Small Leucine-Rich Proteoglycan in Bovine Epiphyseal Cartilage

Jiann-Jiu Wu, Ph.D., Mary Ann Weis, B.S., Bryan G. Carter, B.S., and David R. Eyre, Ph.D.

Collagens, proteoglycans and matrix proteins are the main components of cartilage. The collagenous framework of cartilage is based on a cross-linked heteropolymeric template formed from types II, IX and XI collagens. Small amounts of types III, VI, XII and XIV collagens are also present. Aggrecan is the most abundant proteoglycan but several other proteoglycans are present in cartilage, including perlecan, versican and a family of fibril-associated small leucine-rich proteoglycans (SLRPs, Table 1), fibromodulin, decorin, lumican, biglycan, chondroadherin and epiphycan . In purifying the precursor pool of type IX collagen, we have identified a novel SLRP, mimecan, as a prominent component of fetal bovine epiphyseal cartilage.

Materials and Methods

Matrix proteins extracted by 8M urea from fetal bovine epiphyseal cartilage were fractionated by associative density gradient centrifugation in 3.5M CsCl. Proteins recovered from the low density fraction were dialyzed against 0.05M TrisHCl, pH 7.5, containing 1M NaCl. Native collagen molecules were precipitated from the 1M NaCl soluble fraction by adding ammonium sulfate to 30% saturation. The precipitate was redissolved in 0.5M acetic acid. After reprecipitating type II collagen at 0.7M NaCl, native types XI and IX collagens were precipitated at 1.8M NaCl. Individual collagen chains were then resolved by C4 reverse-phase HPLC followed by SDS-PAGE. After Coomassie Blue staining on SDS-PAGE individual protein bands were digested in-gel by trypsin. The resulting peptides were subjected to microbore C8 column liquid chromatography (μLC) interfaced directly to a ThermoFinnnigan LCQ Deca XP mass spectrometer. For protein identification, peptide fragments were compared with the FBSC non-redundant protein database using SEQUEST, an automated database search algorithm designed for use with tandem mass spectrometry data.

Results and Discussion

Using the two dimensional HPLC/SDS-PAGE method, we are able to resolve all the collagen chain components as well as co-purified non-collagenous proteins. Western blot analysis using antibodies specific for collagens II, IX and XI showed that the 1.8M NaCl fraction contained mainly intact types IX and XI collagen chains. Various processing forms of the N-propeptide domains of type XI collagen were also identified (results not shown). Several non-collagenous matrix proteins coeluted with the pool of type IX collagen chains on HPLC (Figure 1). In-gel trypsin digestion and mass spectrometry with data base matching identified a prominent protein band at about 36-kDa in fractions 43-46 as mimecan (Figure 2). Tryptic peptide sequences distinguished mimecan from epiphycan (also known as PG-Lb), a closely related SLRP to mimecan in the SLRP class III subfamily. Epiphycan was previously identified in bovine epiphyseal cartilage. In addition to mimecan, several other non-collagenous matrix proteins were also identified by in-gel trypsin digestion and mass spectrometry in adjacent fractions in the same extract, including matrilin-1, matrilin-3, fibromodulin and proline-arginine rich end leucine-rich repeat protein (PRELP).

Mimecan, as a full-length translation product, is a 34-kDa glycoprotein. It is the same gene product as osteoglycin initially identified as a 12-kDa protein from bovine bone and the 25-kDa KSPG25 from cornea. Fibromodulin and PRELP are cartilage components that belong to the SLRP superfamily and both associate with collagen fibrils through their leucine-rich repeats. Matrilin-1/ matrilin-3 tetramers also bind to type IX collagen. Mimecan-null mice appear to develop normally, but they showed collagen fibril abnormalities with a pronounced increase in collagen fibril diameter in the skin similar to findings on mice that lack other SLRP members.

In summary, we have identified mimecan in extracts of fetal bovine epiphyseal cartilage. The function of mimecan in cartilage is unknown but the co-purification of mimecan with collagen IX suggests that mimecan is bound to cartilage collagen and may be involved in the assembly and interactions of fibrils.

	SLRP	Amino-terminal cysteine cluster	Gene and protein structure	
Class I	Asporin Biglycan Decorin	CX_3CXCX_6C	8 exons	10 LRR
Class II	Fibromodulin Lumican Keratocan PRELP Osteoadherin	CX_3CXCX_9C	3 exons	10 LRR
Class III	Epiphycan Mimecan Opticin	CX_2CXCX_6C	7 exons	6 LRR
Others	Chondroadherin Nyctalopin	CX_3CXCX_8C CX_3CXCX_6C	3 exons	11 LRR

Table 1: Classification of small leucine-rich proteoglycans.

Recommended Reading

Eyre DR, Wu JJ, Fernandes RJ, Pietka TA and Weis MA (2002) Recent developments in cartilage research: matrix biology of the collagen II/IX/XI heterofibril network. Biochem. Soc.

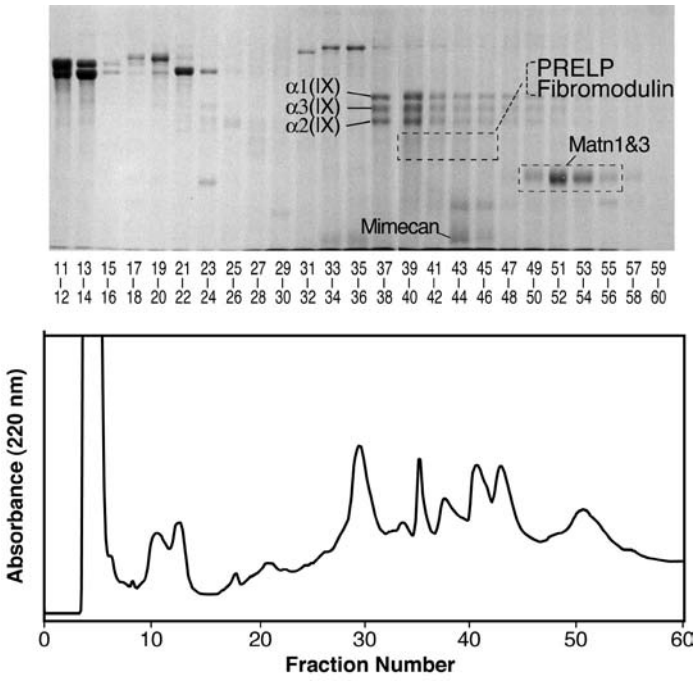

Figure 1: Reverse-phase HPLC and SDS-PAGE two dimensional resolution of type IX collagen chains and co-purified non-collagenous proteins extracted from fetal bovine epiphyseal cartilage and recovered in the 1.8M NaCl precipitate.

Residues	Mimecan/Osteoglycin Sequence	Mass[M+H]+
134-146	LTAKDFADIPNLR	1474.7
147-165	RLDFTGNLIEDIEDGTFSK	2171.4
182-195	LPVLPPKLTLFNAK	1551.9
265-271	DRIEEIR	931.0
272-281	LEGNPIVLGK	1040.2

Figure 2: Tryptic peptides identified by in-gel trypsin digestion and mass spectrometry.

Trans. 30, 894-899.

Ameye L and Young MF (2002) Mice deficient in small leucine-rich proteoglycans: novel in vivo models for osteoporosis, osteoarthritis, Ehlers-Danlos syndrome, muscular dystrophy, and corneal diseases. Glycobiology 12, 107R-116R.

Iozzo RV (1999) The biology of the small leucine-rich proteoglycans. Functional network of interactive proteins. J Biol Chem. 274, 18843-18846.

Wu JJ and Eyre DR (2003) Cartilage matrix assembly: Evidence for binding of matrilin-3 to collagens IX and XI. Trans. Orthop. Res. Soc. 28, 218.

Tasheva ES, Koester A, Paulsen AQ, Garrett AS, Boyle DL, Davidson HJ, Song M, Fox N and Conrad GW (2002) Mimecan/osteoglycin-deficient mice have collagen fibril abnormalities. Mol. Vision 8, 407-415.

Augmenting Bone Mass with Low Magnitude Loading

Sandra L. Poliachik, M.D., Sarah E. Warner, Ph.D., Dewayne Threet, B.S., Sundar Srinivasan, Ph.D., and Ted S. Gross, Ph.D.

The concept of enhancing skeletal morphology during growth to an extent that mitigates fracture risk posed by menopause and/or aging holds obvious appeal. However, demonstrations of 25 to 40% elevations in bone mass in humans have been confined to elite competitive athletes who initiated single handed racquet sports as children. Animal studies have demonstrated similar enhancements of bone mass following controlled mechanical loading, but these protocols typically induce hyperphysiologic bone strains. A further complication is that the osteogenic response of bone to a given stimulus substantially decays over time. We have recently observed that inserting 10 s rest intervals between each load cycle substantially elevates the induced new bone formation while greatly reducing the number of loading cycles required to achieve this response. We hypothesized that rest-inserted loading, when initiated during the later stages of skeletal growth, would significantly enhance bone morphology while requiring minimal integrated strain input.

Methods

We exposed the right tibia of 12 wk old C57Bl/6 female mice to a 3 d/wk loading protocol consisting of 50 cycles/d, with each cycle separated by a 10 s rest interval. The applied bending forces were calibrated to induce peak normal strains of either 1700 με (Group A, n=6) or 2100 με (Group B, n=6) at the tibia mid-shaft. The experimental intervention consisted of 3 wk of loading followed by 1 wk without exogenous loading followed by a second 3 wk bout of loading. On day 10 and 19 of each 3 wk period, fluorescent labels were injected IP (alizarin, calcein). Following sacrifice at 19 wk of age, the left and right tibia mid-shaft morphology was assessed by micro-CT imaging (10.5 μm voxel resolution) using standard software (Scanco Viva40). Following imaging, standard dynamic histomorphometry techniques were used to assess periosteal bone formation rates (p.BFR) at the mid-shaft of the contralateral left tibiae and externally loaded right tibiae. Comparisons were performed with 1-tailed t-Tests. Experimental procedures were approved by the University of Washington (IACUC).

Results

The 7 wk intervention altered the bone morphology by significantly increasing tibia cortical volume compared to contralateral tibiae for both Group A (6.8%, $p=0.03$) and Group B (13.0%, $p<0.001$, Fig.1). Increased cortical volume was primarily achieved by increased periosteal volume (6.9%, $p=0.03$ and 10.2%, $p<0.01$). Moments of inertia (Imax and Imin), which represent the resistance of a bone to bending, were both enhanced due to loading. In Group A, Imax was not significantly elevated, but Imin (19.9%, $p<0.01$) was significantly elevated compared to contralateral tibiae, while both Imax (14.0%, $p=0.05$) and Imin (34.1%, $p<0.001$) were significantly elevated in Group B (Figure 2). The enhanced bone morphology was achieved by elevated periosteal osteoblast activity, which was greatly enhanced after 3 wk of intervention. At the time of the first labeling (mouse age: 13.5 to 14.5 wk), mean (S.D.) p.BFR in the left tibiae was negligible (Group A: 0.06 ± 0.06; Group B: 0.04 ± 0.06 μm 3 /μm 2 /d) and did not differ between groups. During the first 3 wk protocol, p.BFR was greatly elevated both in group A (0.98 ± 0.33, $p<0.001$) and Group B (0.86 ± 0.49, $p<0.004$) but did not differ between groups. The p.BFR induced in the 2nd 3 wk loading regimen was similar to that induced in a previous study by our group when 16 wk mice were exposed to the same mechanical stimulus for the first time.

Discussion

We found that 150 cycles of rest-inserted mechanical loading per week at a physiologic magnitude was capable of substantially elevating cortical bone morphology within 7 wk, when initiated during the later stages of skeletal growth. In C57 mice, cortical bone morphology and surface osteoblast activity plateau by 16 wk of age, so the 12 wk old C57 mice used here can be considered to be in the later stages of growth (as confirmed by the p.BFR observed in the contralateral tibiae). At the end of 3 wk, p.BFR was significantly elevated in loaded mice, and the sustained osteoblast activity enhanced bone morphology by 7 wk. While other studies have noted minimal changes in Imax, with more dramatic changes occurring in Imin, we have produced significant increases in Imin and Imax with much lower

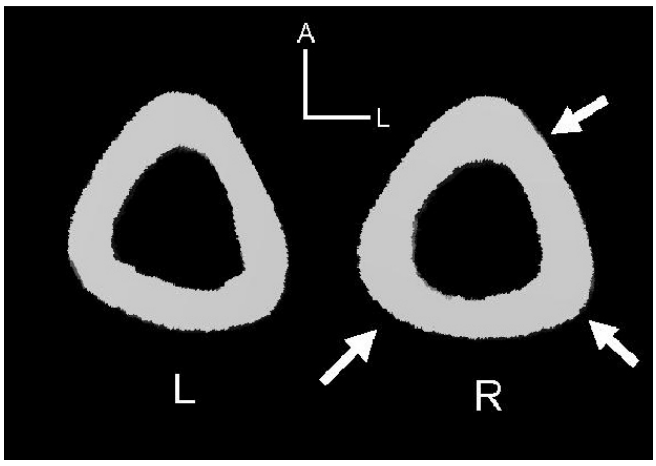

Figure 1: Micro-CT images from the tibia midshaft of contralateral tibia (L) and right tibia (R) exposed to rest-inserted loading. The regions of greatest bone accretion were the medial posterior, lateral anterior and lateral posterior cortices (arrows).

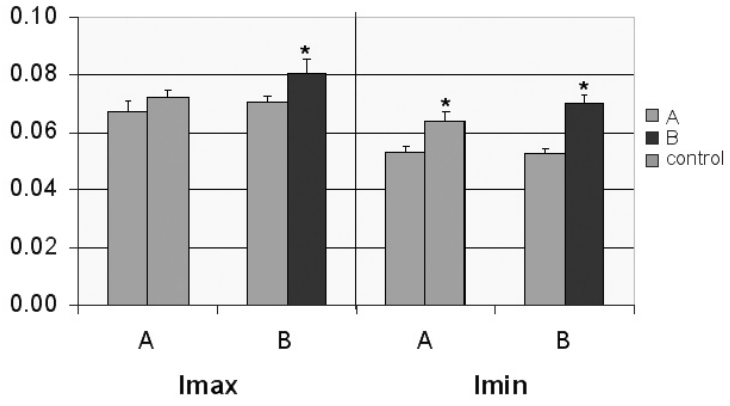

Figure 2: Moments of Inertia (Imax and Imin) for Group A and Group B (left bar is the contralateral tibia, right bar is the experimentally loaded tibia). Imin was significantly elevated in both groups, but Imax was enhanced only in the higher magnitude Group B.

strain input. The increased moment of inertia in the larger magnitude Group A would provide a 14 to 34% increase in bending resistance (depending on the orientation of the applied loads) based on beam theory estimates. These results suggest that rest intervals hold potential for positively stimulating bone formation for extended exercise periods. In our view, these data strongly support the efficacy of rest-inserted loading to augment bone mass and morphology when initiated during the later stages of skeletal growth, in direct support of our initial general hypothesis. Our estimates suggest that the increased bone strength generated during the 7 wk regimen would be sufficient to counteract nearly 50% of the degradation in bone strength observed in C57 mice by the age of 2 yr. A critical issue for future study is whether continued mechanical loading is required to retain augmented bone morphology.

Acknowledgements

This work was supported by NIH (AR48102) and the Sigvard T. Hansen, Jr. Endowed Chair for Orthopaedic Traumatology.

Recommended Reading

Parfitt, AM, The attainment of peak bone mass: what is the relationship between muscle growth and bone growth, Bone, 34:767-770, 2004.

Haapasalo H, Sievanen H, Kannus P, Heinonen A, Oja P, Vuori I., Dimensions and estimated mechanical characteristics of the humerus after long-term tennis loading, J Bone Min Res, 11:864-872, 1996.

Forwood MR, Bennett MB, Blowers AR, Nadorfi RL., Modification of the in vivo four-point loading model for studying mechanically induced bone adaptation, Bone. 23:307-10, 1998.

Schriefer JL, Warden SJ, Saxon LK, Robling AG, Turner CH., Cellular accommodation and the response of bone to mechanical loading, J Biomech, 28:1838-45, 2005.

Srinivasan S, Agans SC, King KA, Moy NY, Poliachik SL, Gross TS., Enabling bone formation in the aged skeleton via rest-inserted mechanical loading, Bone, 33:946-55, 2003.

Cadaveric Simulation of a Pes Cavus Foot

S. Bradley Daines, B.A., Eric S. Rohr, M.S., Andrew P. Pace, B.S.,
Michael J. Fassbind, M.S., Bruce J. Sangeorzan, M.D., and William R. Ledoux, Ph.D.

Pes cavus is an umbrella term encompassing several high arch conditions; it can affect primarily the hindfoot or the forefoot, or it can affect the foot more globally. There is not a universally accepted definition of pes cavus, but there are common trends mentioned in the literature, including inversion of the calcaneus and midfoot, adduction of the forefoot, plantar flexion of the first metatarsal and an increase in force on the lateral foot.

Several muscular imbalances stemming from neurologic disorders have been cited as underlying factors for pes cavus development. Mann describes a strong peroneus longus (PL) and tibialis posterior (TP) coupled with a weak peroneus brevis (PB) and tibialis anterior (TA) in Charcot-Marie-Tooth disease. Dehne notes spasticity of the TA, flexor hallucis longus (FHL) and flexor digitorum longus (FDL) after stroke resulting in equinovarus.

The goal of this study was to produce a cadaveric model of a pes cavus deformity in an otherwise normal foot by attenuating ligaments and generating muscle imbalances. Such a model would be useful in evaluating corrective surgical procedures.

Methods

In this IRB-approved study, we tested nine freshly frozen, unpreserved human cadaver feet (mean age of 77.1 ± 8.3, range 65-90 yrs) on a customized loading frame capable of loading the extrinsic muscles and tibia/fibula via eight pneumatic cylinders. The feet were screened for osseous deformity by X-ray and gross examination. Each foot was dissected above the level of the medial malleolus to expose the tendons of the TA, PL, PB, TP, FHL and FDL muscles as well as the Achilles tendon. A hole was drilled in the tibia and fibula to insert compressive rods. Tendons were attached to the loading frame with plastic clamps and nylon cords (Figure 1).

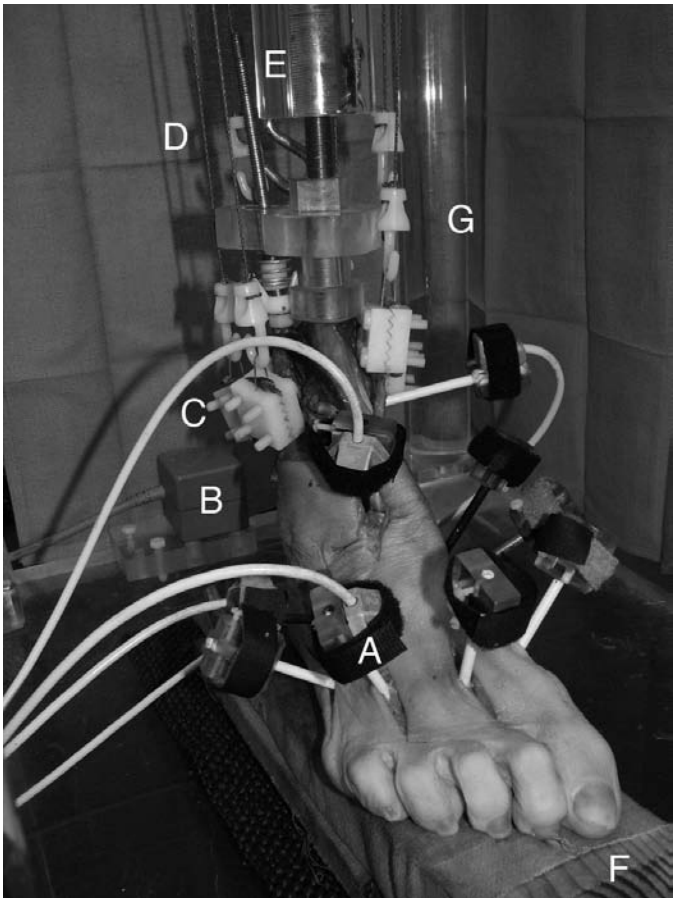

Figure 1: Anterolateral view of cadaver foot in testing apparatus. (A) Polhemous electromagnetic sensors in mounts on carbon fiber rods, (B) Polhemus transmitter, (C) plastic tendon clamps, (D) extrinsic muscle tensile nylon cords, (E) compressive rod, (F) wood block for 7° dorsiflexion, (G) acrylic loading frame.

We drilled holes in the tibia, talus, calcaneus, navicular, medial cuneiform, cuboid and first metatarsal to insert carbon fiber rods (diameter 4.78 mm) which were secured with super glue. Polhemus Fastrak™ electromagnetic sensors were attached to the rods using acrylic mounts, allowing us to track spatial orientation and rotations of the bones of interest. Force distribution was measured using a Novel Pedar® insole measurement system.

The dorsal tarsometatarsal and intercuneiform ligaments were weakened by making five incisions with a 15-blade scalpel parallel to fiber orientation. The foot was mounted in the loading frame at 7º dorsiflexion using a wooden ramp. Tendon forces were calculated using muscle cross-sectional areas, maximum specific tensions, cosines of pennation angles and EMG activities to simulate physiologic midstance (30% of the gait cycle). Following ligament weakening, the TA and TP were overpulled at 1 Hz for one hour (3600 cycles), with the other extrinsic muscles pulled at 1/4 physiologic force.

Overpulls were chosen from common muscle trends seen in pes cavus patients and from successful pilot studies. To maximize the effect of the overpulls, axial compression and muscle forces were set at 1/8 of body weight during data collection. Data for midstance and the following three non-physiologic conditions were collected: 1) overpull of Achilles, TA, TP, FHL, FDL, 2) overpull of Achilles, PL, TP, and

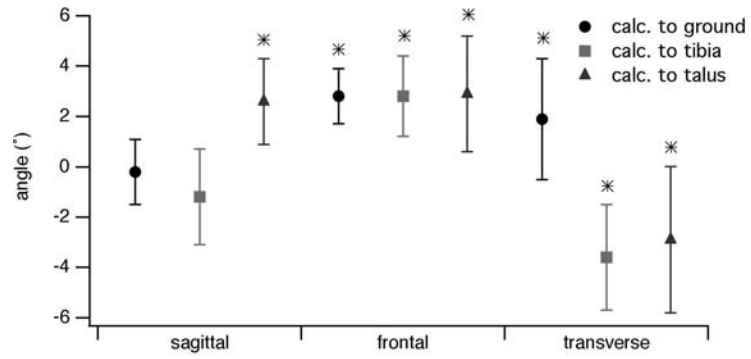

Figure 2: The angular change of the calcaneus (calc.) relative to the ground, tibia and talus. All data are normalized to the balanced condition. An asterisk signifies a significant difference from the balanced condition. sagittal positive = plantar flexion, sagittal negative = dorsiflexion; frontal positive = inversion, frontal negative = eversion; transverse positive = external rotation, transverse negative = internal rotation.

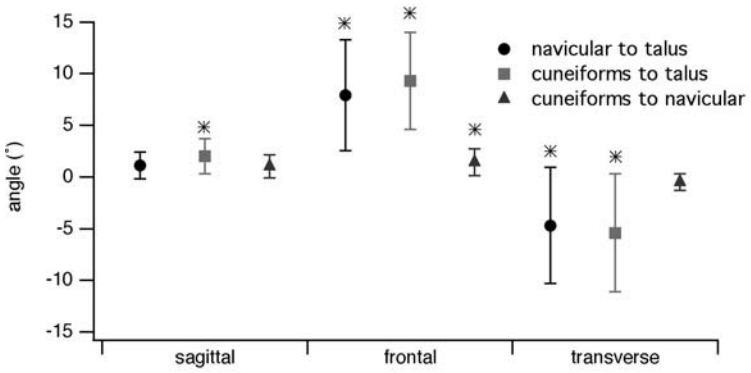

Figure 3: The angular change of the navicular to the talus, cuneiforms to talus and cuneiforms to navicular. All data are normalized to the balanced condition. An asterisk signifies a significant difference from the balanced condition. sagittal positive = plantar flexion, sagittal negative = dorsiflexion; frontal positive = inversion, frontal negative = eversion; transverse positive = external rotation, transverse negative = internal rotation.

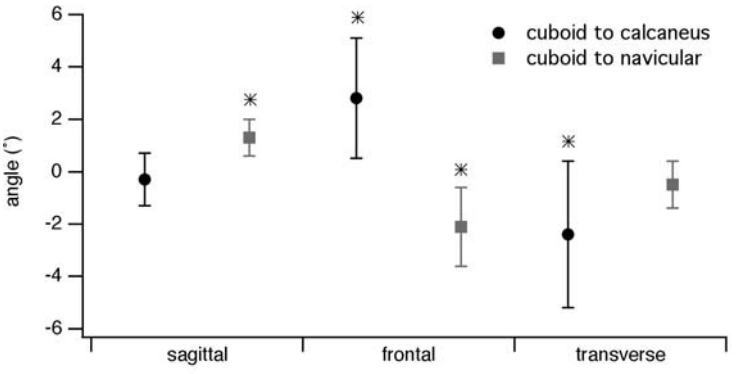

Figure 4: The angular change of the cuboid to calcaneus and cuboid to navicular. All data are normalized to the balanced condition. An asterisk signifies a significant difference from the balanced condition. sagittal positive = plantar flexion, sagittal negative = dorsiflexion; frontal positive = inversion, frontal negative = eversion; transverse positive = external rotation, transverse negative = internal rotation.

3) overpull of PL, TP with underpull of TA, PB. The testing order of these conditions was randomized during data collection. Overall differences from midstance and the overpull conditions were assessed using linear mixed effects models.

Results

Of the three muscle conditions that were implemented, only the first demonstrated a pronounced cavus foot with several significant changes of the hindfoot, midfoot and forefoot alignment consistent with the pes cavus deformity.

The motion of the hindfoot was, for the most part, as expected for a high arched foot (Figure 2). The calcaneus inverted relative to the ground, tibia and talus by 2.8º (1.1º), 2.8º (1.6º) and 2.9º (2.3º) respectively and externally rotated relative to the ground by 1.9º (2.4º). In the sagittal plane, the calcaneus plantar flexed relative to the talus 2.6º (1.7º), but given the relative lack of motion of the calcaneus relative to the ground and the tibia, this motion is better thought of as talar dorsiflexion. In a finding not typical of the pes cavus foot deformity, the calcaneus significantly internally rotated relative to the tibia by 3.6º (2.1º) and relative to the talus by 2.9º (2.9º).

Representing the movements of the medial midfoot, the navicular and medial cuneiform inverted relative to the talus by 7.9º (5.4º) and 9.3º (4.7º), respectively, and internally rotated by 4.7º (5.6º) and 5.4º (5.7º), respectively (Figure 3).

Describing motion of the lateral midfoot, the cuboid was measured relative to the hindfoot (i.e., calcaneus, Figure 4) and medial midfoot (i.e., navicular, Figure 4). The cuboid inverted relative to the calcaneus [2.8º (2.3º)], but everted relative to the navicular [2.1º (1.5º)].

Representing motion of the forefoot, the first metatarsal inverted relative to the talus by 7.5º (5.4º) and adducted relative to the talus by 5.0º (5.4º) (Figure 5). Though not significant, the first metatarsal showed a trend of plantar flexion relative to the talus of 3.0º (2.2º).

As expected with the pes cavus deformity, there was an increase in force in the lateral forefoot and midfoot of 9.9 N (5.2 N) and 8.0 N (7.5 N).

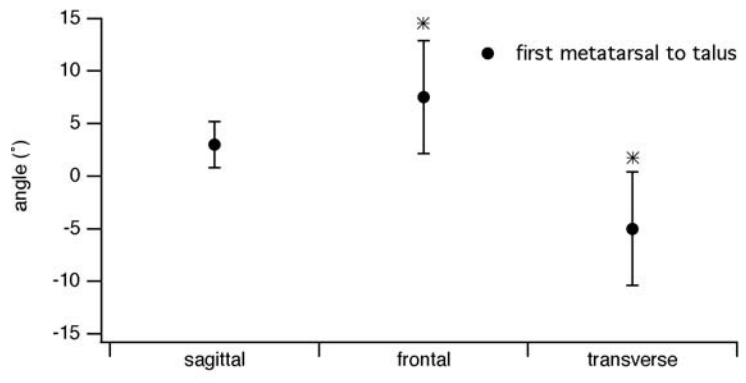

Figure 5: The angular change of the first metatarsal relative to talus. All data are normalized to the balanced condition. An asterisk signifies a significant difference from the balanced condition. sagittal positive = plantar flexion, sagittal negative = dorsiflexion; frontal positive = inversion, frontal negative = eversion; transverse positive = external rotation, transverse negative = internal rotation.

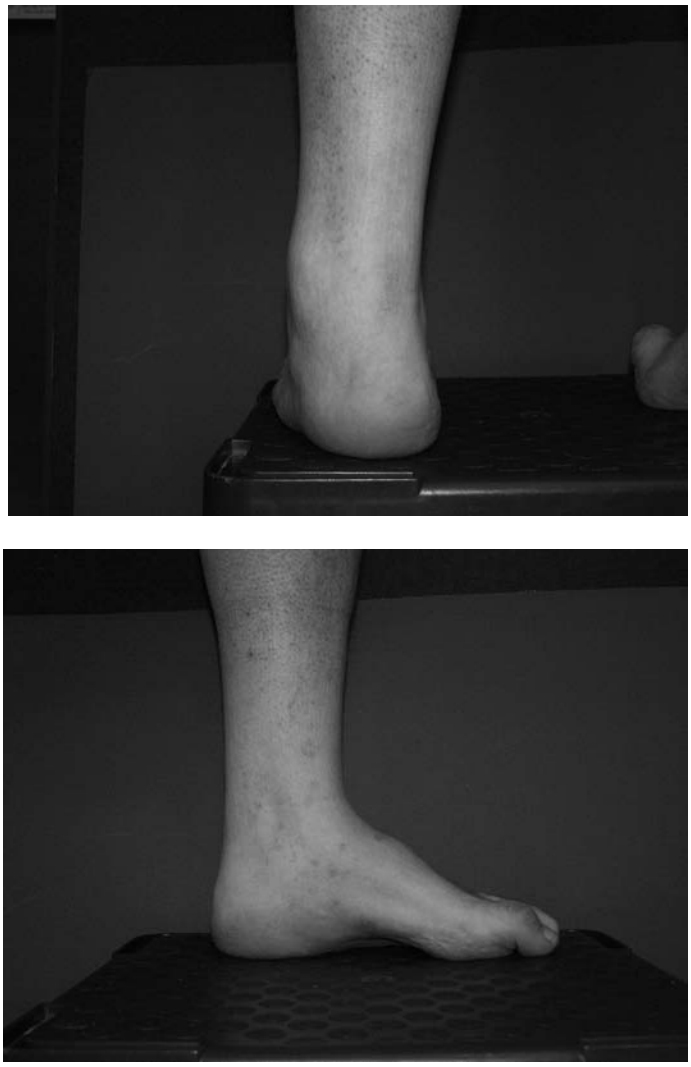

Figure 6: A pes cavus foot in the frontal and sagittal planes.

Discussion

Different combinations of overpulls of the Achilles, TA, TP, PL, FHL and FDL produced a model consistent with clinical measures of the pes cavus deformity. The hindfoot inverted and, consistent with an elevated medial longitudinal arch, the midfoot inverted. The increase in lateral force distribution reflects the weight-bearing changes of the pes cavus deformity. Adduction of the forefoot was also seen.

Though calcaneal internal rotation was seen, this measurement was relative to the tibia and talus; thus, it may in reality be a reflection of external tibial rotation. Potential limitations of the study include our inability to simulate long-term osseous changes, constriction of the plantar aponeurosis and/or dysfunction of the intrinsic foot musculature.

Further studies will focus on corrective procedures for pes cavus feet. For example, an osteotomy or tendon transfer could be performed on a cadaver foot after the pes cavus simulation. The foot could then be retested with the same protocol of this experiment. Corrective efficacy could be quantified by loading to the same parameters as the overpull that produced the pes cavus deformity in our study. An effective procedure should reduce the observed pes cavus characteristics.

Acknowledgement

This work was supported in part by the Medical Student Research and Training Program at the Univ. of Washington, and the Dept. of Veterans Affairs, Rehabilitation R&D Service grant number A2661C. Jane B. Shofer, MS, conducted the statistical analyses.

Recommended Reading

Brewerton OA, et al., BMJ. 2:659-661, 1963.

Burns J, et al., Foot Ankle Int. 26(7):540-544, 2005.

Dehne, R, Congenital and acquired neurologic disorders. In Mann RA, Coughlin MJ (eds): Surgery of the Foot and Ankle. St. Louis, Mosby, 1999, pp 525-557.

Mann RA and Missirian J, Clin. Orthop. 221-228, 1988.

Intramedullary Reaming for Press-Fit Fixation of a Humeral Component Removes Cortical Bone Asymmetrically

Michael Lee, M.D., Caroline Chebli, M.D., Doug Mounce, M.S., Alexander Bertelsen, P.A.-C, Michael Richardson, M.D., and Frederick A. Matsen III, M.D.

Shoulder arthroplasty is commonly used to manage glenohumeral arthritis and posttraumatic conditions. The humeral component is often press fit to avoid the use of cement. This technique requires sufficiently robust fixation to avoid implant loosening. Since humeral prostheses are generally cylindrical, reaming the endosteal diaphyseal cortex to achieve a cylindrical shape enhances the fit and fixation of the prosthetic stem. The endosteal cortex has been noted to be elliptical in cross section, with varying orientation of the elliptical major axis. Because the cross sections of the medullary canal are not symmetrically aligned, the path taken by the cylindrical reamer is determined by the shape and density of the endosteal bone at each segment all along its length. As a result, cylindrical reaming is likely to remove bone asymmetrically from the diaphyseal endosteal surface. Asymmetric cortical bone removal is a recognized risk factor for humeral periprosthetic fracture both at surgery or with trauma thereafter.

Periprosthetic fractures account for 20% of all complications associated with shoulder arthroplasty and the incidence has been reported between 1-2.3%. Such fractures are serious, often requiring more extensive and repeat surgery as well as compromising the rehabilitation program. Risk factors for fracture include osteopenia, osteoporosis, rheumatoid arthritis, inadequate operative exposure resulting in excessive manipulation, and overzealous reaming or impaction. Boyd et al noted that in their seven reported cases the fracture pattern involved the humeral shaft at the distal tip of the prosthesis where the amount of bone removed by the cylindrical reaming would be greatest (Figure 1).

Figure 1: Radiograph of the left shoulder of a 62 year-old man with periprosthetic fracture after a fall.

The effect of humeral reaming on cortical bone thickness has not been previously studied. This study tested the hypothesis that cylindrical intramedullary reaming removes substantial diaphyseal cortical bone in an asymmetrical manner. We hypothesize that the degree of cortical thinning would not be apparent to the surgeon on an anterior-posterior radiograph typically taken after shoulder arthroplasty.

Material and Methods

Ten unmatched human cadaveric humeri were used for this study (mean age 73 years). All humeri were free of fracture or evident bone disease. Soft tissues were stripped before testing. The humeri were cut at 16 centimeters distal to the proximal aspect of the greater tuberosity and the humeral head was excised at the anatomic neck.

The baseline cross sectional geometry of the humeral cortex was defined using the General Electric Lightspeed vCT scanner (General

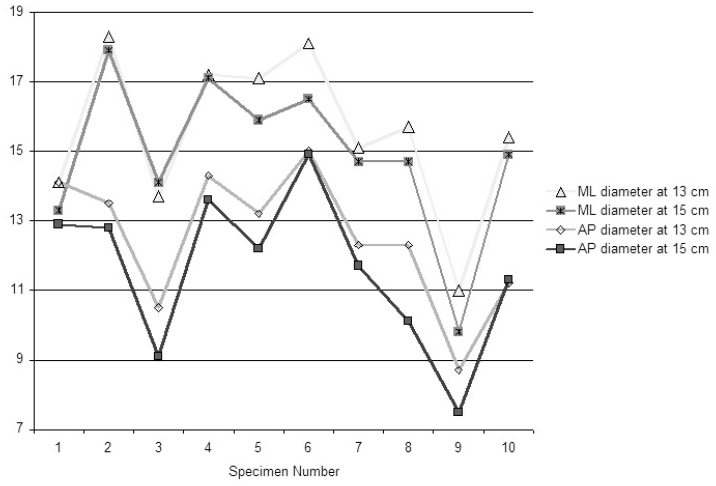

Figure 2: Medial-lateral(ML) and anterior-posterior(AP) diameters of the ten different humeri 13 and 15 cm distal to the proximal tuberosity.

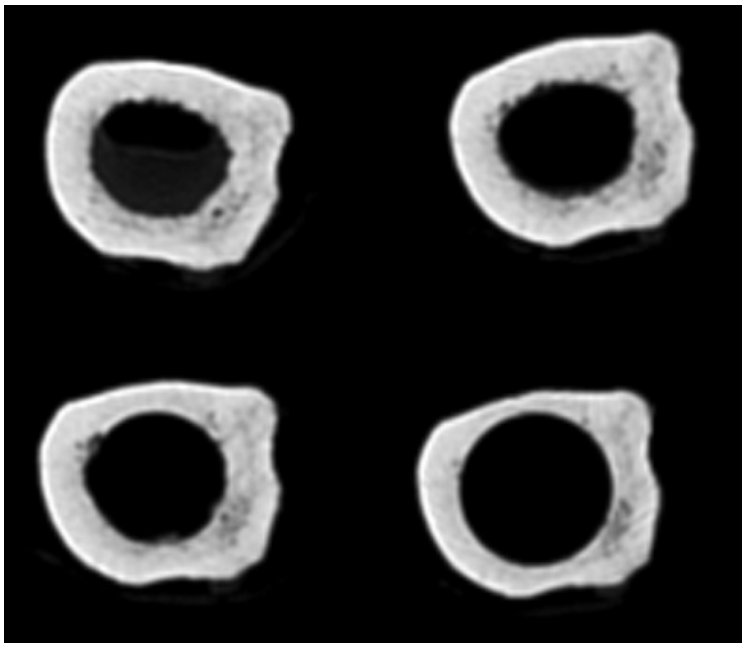

Figure 3: Preferential thinning of the anterior and posterior cortices with sequential reaming. Humerus #7 at 15cm distal to the proximal aspect of the greater tuberosity. Upper left, unreamed; upper right, reamed to 12mm, lower left, reamed to 14mm; lower right, reamed to 16mm.

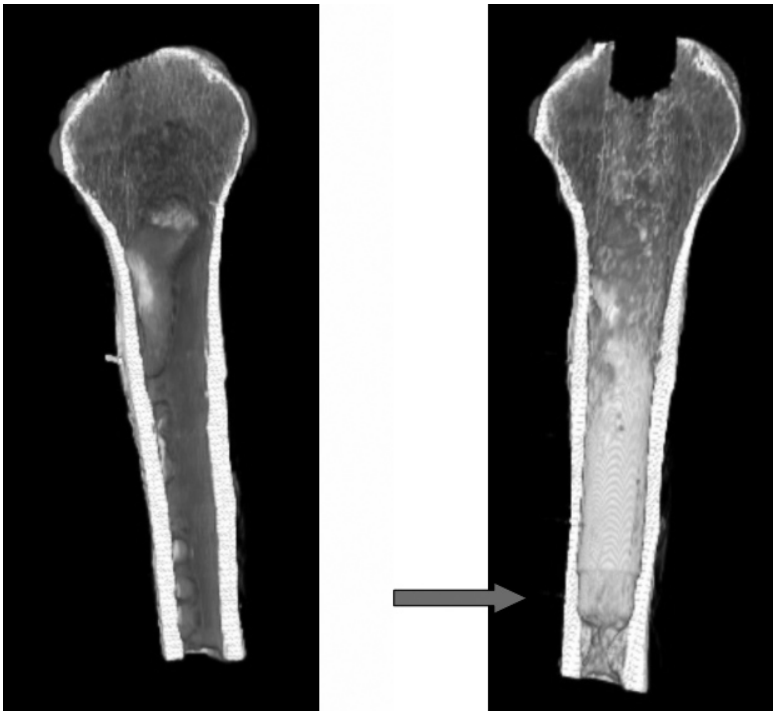

Figure 4: Anterior posterior endosteal notching caused by reaming as seen on the lateral projection in a three-dimensional reconstruction of humerus #7. Left, unreamed; right, reamed.

Electric, Fairfield, CT) at 0.62 mm intervals. Particular attention was directed to the cross sectional anatomy at 13 and 15 cm distal to the proximal tip of the greater tuberosity where fixation of the distal tip of a humeral component is characteristically achieved.

The humeri were then reamed by hand as performed in surgical practice. While no "standard" technique for reaming has been established, it is evident that fixation of the prosthetic stem requires that the diaphysis as the prosthetic tip be shaped to fit the prosthetic stem. In our protocol, reamers were inserted to 15 cm, the depth necessary to accommodate a humeral prothesis. Starting with the smallest reamer, reamers of progressively larger diameter were inserted until endocortical contact was first achieved. Since this first bite would provide fixation for only the distal tip of the prosthesis, reaming was repeated with reamers of a diameter two and then four millimeter greater than the one to first achieve a bite on the endosteal surface. CT scans were obtained after each reaming.

Data analysis of the cortical anatomy was conducted using the OsiriX medical imaging software program (http://homepage.mac.com/rossetantoine/osirix/). The anterior-posterior and medial-lateral endocortical diameters were measured 13 and 15 cm distal to the tuberosity before and after reaming. The significance of the difference in the anterior-posterior and medial-lateral diameters at each level was determined using the two-tailed student's t-test for paired samples. The amount of thinning of each of the anterior, posterior, medial, and lateral cortices at the point 13 cm distal to the tuberosity was determined by subtracting the cortical thickness in each of these directions before and after reaming.

Results

The average medial-lateral diamteter (15.6 $\pm$ 2.3 mm) was significantly greater that the anterior-posterior diameter (12.5 $\pm$ 1.9 mm) at 13cm distal to the tuberosity ($p<0.00005$) (Figure 2). Similarly, the average medial-lateral diameter (14.9 $\pm$ 2.3) was significantly greater than the anterior-posterior diameter (11.6 $\pm$ 2.2 mm) at 15cm distal to the tuberosity ($p<0.0001$). This result indicates that that endocortical contact in the medial-lateral direction cannot be achieved without removal of substantial anterior-posterior cortical bone.

When the diaphysis was reamed to a diameter 4 mm greater than that of

the reamer to obtain first cortical bite, the greatest amount of bone removed was from the anterior and posterior endocortical surfaces and least from the medial cortex. This loss of bone from the anterior and posterior cortices would not be apparent on standard anterior-posterior radiographs (Figure 3).

Discussion

In preparation for shoulder arthroplasty surgeons often use the anterior-posterior radiograph to template the size of the humeral prosthetic stem that would fit the humerus without substantial cortical reaming. This study demonstrates that this traditional method of templating may cause the surgeon to overestimate the size of the ideal humeral stem. The medullary canal diameter seen in the plane of the anterior-posterior radiograph at 13 cm and 15 cm distal to the proximal aspect of the greater tuberosity was 3.1 mm and 3.3 mm greater than that which would be seen in the lateral radiograph at these locations.

The results of our study confirm that the endocortical morphology of the humerus is variable as pointed out by Robertson et al. Intramedullary reaming with a rigid cylindrical reamer preferentially removed cortical bone from the anterior and posterior surfaces of the diaphyseal cortex. This creates a notching of the endosteal cortex that may not be recognized on the conventional anterior-posterior radiograph (Figure 4). Asymmetrical thinning may increase the risk of periprosthetic fracture, especially when combined with the abrupt change in material properties that would occur at the point of transition from notched cortex with a prosthesis to the unreamed cortex just below it.

Recommended Reading

Boyd, A. D., Jr.; Thornhill, T. S.; and et al.: Fractures adjacent to humeral prostheses. J. Bone Joint Surg. Am., 74(10): 1498-504, 1992.

Cameron, B., and Iannotti, J. P.: Periprosthetic fractures of the humerus and scapula: management and prevention. Orthop. Clin. North Am., 30(2): 305-18, 1999.

Choo, A. M.; Hawkins, R. J.; and et al.: The effect of shoulder arthroplasty on humeral strength: an in vitro biomechanical investigation. Clin. Biomech., 20(10): 1064-71, 2005.

McDonough, E. B., and Crosby, L. A.: Periprosthetic fractures of the humerus. Am. J. Orthop., 34(12): 586-91, 2005.

Robertson, D. D.; Yuan, J.; and et al.: Three-dimensional analysis of the proximal part of the humerus: relevance to arthroplasty. J. Bone Joint Surg. Am., 82(11): 1594-602, 2000.

The Effect of Associated Injuries on the Functional Outcome of Distal Humeral Fractures

James L. Howard, M.D., M.Sc., F.R.C.S.C., Chad P. Coles, M.D., F.R.C.S.C., Julie Agel, M.A., A.T.C., and David P. Barei, M.D., F.R.C.S.C.

Open reduction internal fixation (ORIF) is the preferred treatment for displaced intraarticular distal humeral fractures. Previous studies have evaluated the functional outcomes following surgical management of these fractures, but none have critically evaluated the effect of associated injuries. The purpose of this study was to evaluate outcomes of patients with supracondylar-intercondylar (AO/OTA type 13C) distal humerus fractures managed with ORIF. We hypothesized that patients with associated injuries would have worse outcomes compared to those with isolated injuries.

Methods

Between January 1998 and December 2003 inclusive, all patients presenting to our institution with a supracondylar-intercondylar distal humeral fracture were retrospectively identified. One hundred and forty-one fractures in 141 skeletally mature patients were eligible for review. Fractures treated with immediate amputation (n=5), nonoperatively (n=5), primary elbow arthroplasty (n=5), or allograft joint replacement (n=2) were excluded. Ballistic injuries (n=11) and those with other ipsilateral periarticular elbow fractures (n=8) were also excluded. One hundred and five fractures in 105 patients were available for review. Thirteen patients were lost to follow-up, five were deceased, and two declined to participate. Of these available 85 patients, 58 (68.2%) fully completed the Musculoskeletal Functional Assessment (MFA) and Disabilities of the Arm, Shoulder and Hand (DASH). Patients' charts were reviewed to determine age, gender, injury mechanisms, other injuries, treatment, and complications.

There were 30 male and 28 female patients with an average age of 43.5 years (range, 14 to 86). The mechanisms of injury included falls from a height (22 patients), motor vehicle or motorcycle collisions (17 patients), recreational activities (7 patients), falls from standing (6

Figure 1: Injury anteroposterior (A) and lateral (B) radiographs of a 32 year-old male involved in a high-speed motor vehicle collision. After stabilization of his other injuries, management consisted of open reduction with medial and lateral column internal fixation using a posterior exposure and olecranon osteotomy. Immediate post-operative anteroposterior (C) and lateral (D) radiographs demonstrate satisfactory restoration of articular and extra-articular osseous anatomy.

		Isolated Distal Humeral Fracture	Distal Humeral Fracture with Associated Injuries	p Value
Number of Patients		32	26	
Male:Female Ratio		19:13	11:15	0.30
Fracture Classification	C1	5	2	0.40
	C2	12	14	
	C3	15	10	
Open Fractures		14	17	0.17
Smokers/Tobacco Users		7	9	0.43
Time to OR (hours)*		59.4	95.2	0.08
Approach	Osteotomy	20	16	0.57
	Paratricipital	6	7	
	Triceps Split	1	0	
	Triceps Turndown	3	3	
	Triceps Sparing	2	0	
Mean Clinic Follow Up (months)		15.6	17.2	0.69
Mean Outcome Score Follow Up (months)		36.4	38.6	0.69

Table 1: Comparison of patients with isolated fractures to those with associated injuries
* - with exclusion of one outlier in the isolated group (432 hours to OR), there is a significant difference between the groups (Isolated: 47.4 hours, Associated injuries: 95.2 hours, p = 0.006)

patients), and car-pedestrian or car-bicycle collisions (6 patients). Injury radiographs were reviewed by two fellowship-trained orthopaedic trauma surgeons and classified according to the OTA (AO/ASIF) classification system as 13C1 (n = 7), 13C2 (n = 26), 13C3 (n = 25). There were 27 closed fractures and 31 open fractures.

All patients were treated surgically with medial and lateral column plate fixations using a posterior surgical exposure. Depending on fracture pattern and surgeon preference, deep surgical exposure was completed as follows: olecranon osteotomy (n=36), paratricipital (n=13), triceps turndown (n=6), and Bryan-Morrey "triceps sparing" exposure (n=2), and triceps split (n=1) (Figure 1). ORIF was performed when patients were medically stable. The mean time to definitive ORIF was 75 hours (median 49 hours, range 7 to 432 hours).

The mean clinic follow-up was 16.3 months (range 3 to 72 months, 15 patients <6 months; 43 patients >6 months). A functional elbow motion arc was defined as 30°-130°. Patients that developed functionally limiting elbow stiffness were referred for surgical release. Radiographs were reviewed to determine fracture union.

MFA and DASH scores were prospectively obtained at a mean 37.4 months post injury (range, 6-74 months). All scores were obtained after patients had completed their course of management. The mean outcome score follow up time for patients who required subsequent surgery was 25.5 months following their final surgical procedure.

Statistical comparisons were completed using Student's t test, paired t tests, Fisher's exact test and Chi square tests. Differences were considered statistically significant with a p value less than 0.05.

Results

Fifty-eight patients with 58 fractures were included in the study. Thirty-two had isolated fractures; 26 sustained associated injuries (Tables 1 and 2). Overall, the mean MFA was 33.7 and the mean postoperative arc of motion was 93°. The mean maximum extension was 24°; the mean maximum flexion was 117°.

Patient outcomes according to the presence or absence of associated injuries are given in Table 3. Two of 32 patients (6%) with isolated distal humeral fractures required subsequent surgical release. Ten of 26 patients (38%) with distal humeral fractures and associated injuries required subsequent surgical release. Table 4 compares the pre- and post-release range of motion. The mean MFA score for patients who had a surgical release was significantly higher than the MFA score for patients that did not have a release (50.8 vs 29.3, p=0.006). Furthermore, patients who underwent surgical release had a significantly higher DASH score compared to the remainder of the study population (38.1 vs 23.0, p=0.02)

One patient in the isolated group (3%) and one patient in the associated injuries group (4%) developed a deep postoperative infection after their ORIF procedure. All infections were managed with operative debridement and intravenous antibiotics. There were two nonunions in the isolated group (6%) and one nonunion in the associated injuries group (1%).

Discussion

Previous literature has addressed outcomes in patients with isolated distal humerus fractures. In comparison with McKee et al., patients with isolated distal humeral fractures in this study demonstrated similar outcomes (mean postoperative motion arc: 108° (McKee) vs. 107° (current); DASH: 20 (McKee) vs. 23.7 (current)). There have been no studies however, evaluating the effect of associated injuries on outcomes.

Patients with associated injuries had significantly worse MFA scores compared to those with isolated injuries. Despite almost half of the MFA questionnaire items being related to the upper extremity, it is a global health measure and the differences in MFA scores between the groups may be secondary to the outcome of an associated injury rather than impairment related to the distal humerus fracture. To isolate the upper extremity outcome from the global outcome, the upper extremity-focused

Patient	Associated Injuries
2	Closed head injury with subarachnoid hemorrhage, pulmonary contusion, rib fractures, acetabular fracture, femoral head impaction fracture, hip dislocation
3	Pneumothorax, rib fractures
4	Subarachnoid Hemorrhage, Ipsilateral AC separation, Great toe distal phalynx fracture, upper extremity lacerations
9	Acetabular fracture
10	Ipsilateral monteggia, medial malleolar fracture
12	Tibial plateau fracture, T12 compression fracture
14	Closed head injury, ipsilateral ulna fracture, contralateral radius/ulna fracture, acetabular fracture, femoral head fracture, hip dislocation, facial lacerations, mandible fracture, hematuria
17	Tib/fib fracture
19	Ipsilateral distal radius fracture
20	Ipsilateral segmental ulna, ipsilateral distal radius fracture, bilateral acetabular fractures, toe fractures, orbital wall fracture
25	Lateral malleolar fracture
26	Pneumothorax, rib fractures, liver laceration, ipsilateral clavicle fracture, ipsilateral segmental ulna, ipsilateral radius diaphyseal fracture, ipsilateraldistal radius fracture, pelvic fracture, open tibial fracture orbital floor fracture
29	Closed head injury, pulmonary contusion, contralateral C5-T1 neuropathy (brachial plexopathy), pelvic ring injury, hip dislocation, lisfranc/midfoot injury, L2 fracture, mandible injury
30	Ipsilateral radius/ulna fracture
32	Contralateral scaphoid/capitate/triquetrum fractures, contralateral radial head fracture dislocation
33	Pulmonary contusions, rib fractures, splenic laceration, bilateral clavicle fractures, ipsilateral humeral shaft fracture, pelvic fracture, femur fracture, T12 fracture, paraplegia
35	Ipsilateral proximal humeral fracture
36	Closed head injury, facial fractures, ipsilateral tip of olecranon fracture, ipsilateral triceps injury, tibial plafond fracture, lateral malleolus fractures, bilateral calcanei fractures, peroneal tendon dislocations, facial fractures (lefort III),open mandible fracture, lower limb lacerations
39	Closed Head injury, diaphragm rupture, mesenteric tears, ipsilateral radius/ulna fracture, ipsilateral proximal humerus fracture, distal femur fracture, metatarsal fractures
41	Contralateral humerus fracture, medial malleolus fracture
42	Ipsilateral distal radius fracture
43	Hemopneumothorax, pulmonary contusions, rib fractures, ipsilateral distal radius/ulna fracture, traumatic knee arthrotomy, T8/T9 fracture
48	Ipsilateral radial and ulnar nerve palsy, unstable pelvic ring injury
52	Bladder rupture, pelvic ring injury , T7 fracture, T12 fracture, L3/4 fracture

Table 2: The distribution of injuries of patients in the associated injuries group.

DASH questionnaire was used. This failed to demonstrate any significant differences between the isolated or associated injury groups (23.7 vs 29.1).

Range of motion is commonly used when assessing clinical outcomes after elbow fractures. Despite a significant difference in the mean postoperative motion between patients with isolated injuries (107°) compared to patients with associated injuries (75°), a similar difference was not identified when evaluating the DASH scores. Similarly, there was no difference between the two groups in the number of patients who achieved a functional arc of motion (30-130°). These results corroborate previous work demonstrating no significant correlation between the DASH score and elbow range of motion.

Functionally limiting postoperative stiffness was more common in patients with associated injuries. Ten patients in the associated injuries group (38%) required subsequent surgical release compared to only 2 patients (6%) in the isolated group. The presence of a head injury was the most common associated injury identified in these patients. Of the 8 head injured patients in the study, 6 (75%) required subsequent surgical release for stiffness. All patients who required a surgical release had a significant improvement in motion following that procedure (mean arc of motion 26° pre-release, 99° post release, $p<0.001$). Despite this improved range of motion, outcome scores were still inferior to those patients who did not require a release.

The two groups of patients in this study had similar demographics. After eliminating a single time outlier in the isolated injury group, a significant difference in time to operative management was found (isolated, 47.4 hours; associated, 95.2 hours; $p = 0.006$). Intuitively, patients with associated injuries take longer to be medically stable for operative management. The difference in time to surgery between patients with isolated injuries and those with associated injuries may represent a confounding variable.

In conclusion, outcomes for isolated distal humeral fractures in this study were comparable to published literature. Patients sustaining associated injuries at the time of distal humeral fracture have more elbow stiffness and a worse global outcome score (MFA). However, similar outcomes for both groups were identified on a limb-specific outcome score (DASH). Elbow range of motion did not appear to impact DASH scores. Patients with head injuries had a very high incidence of postoperative stiffness. Although patients had improvements in motion following surgical release, functional outcome scores were still worse when compared to patients who did not require surgical release.

Recommended Reading

McKee, M. D., Wilson, T. L., Winston, L., Schemitsch, E. H., and Richards, R. R.: Functional outcome following surgical treatment of intra-articular distal humeral fractures through a posterior approach. J. Bone Joint Surg. Am. 82-A:1701-1707, 2000.

Gofton, W. T., Macdermid, J. C., Patterson, S. D., Faber, K. J., and King, G. J.: Functional outcome of AO type C distal humeral fractures. J. Hand Surg. [Am.]. 28:294-308, 2003.

McKee, M. D., Kim, J., Kebaish, K., Stephen, D. J., Kreder, H. J., and Schemitsch, E. H.: Functional outcome after open supracondylar fractures of the humerus. The effect of the surgical approach. J. Bone Joint Surg. Br. 82:646-651, 2000.

Morrey, B. F.: The posttraumatic stiff elbow. Clin. Orthop. Relat Res.26-35, 2005.

Bruno, R. J., Lee, M. L., Strauch, R. J., and Rosenwasser, M. P.: Posttraumatic

	Isolated Distal Humeral Fracture (n=32)	Distal Humeral Fracture with Associated Injuries (n=26)	p Value
MFA score	27.2	41.7	0.01
DASH score	23.7	29.1	0.69
Arc of Motion	107°	75°	0.006
Maximum Extension	19°	31°	0.04
Maximum Flexion	126°	107°	0.02
Patients with a Functional Arc of Motion Post ORIF	15 (47%)	9 (35%)	0.5
Surgical Release for Stiffness	2 (6%)	10 (38%)	0.003
Nonunion	2 (6%)	1 (4%)	1.0
Infection	1 (3%)	2 (8%)	0.58
Isolated Hardware Removal*	2 (6%)	0 (0%)	0.50

Table 3: Outcomes for patients with and without associated injuries.
* Patients undergoing surgical releases had hardware removal performed simultaneously.

	Pre-release	Post-release	p Value
Arc of Motion	26	99	<0.001
Maximum Extension	50°	27°	0.007
Maximum Flexion	76°	126°	<0.001

Table 4: Range of motion values for patients pre and post surgical release.

elbow stiffness: evaluation and management. J. Am. Acad. Orthop. Surg. 10:106-116, 2002.

Commercially-Funded and US-Based Research is More Likely to be Published; Good-Quality Negative Studies are Not

Joseph R. Lynch, M.D., Mary R.A. Cunningham, M.D., Winston J. Warme, M.D., Douglas C. Schaad, Ph.D., Fredric M. Wolf, Ph.D., and Seth S. Leopold, M.D.

The topics of positive-outcome bias and industry effects on research outcomes have been recognized for decades within the internal medicine literature as worthy of study, but have been relatively unexamined in orthopaedics and other surgical subspecialties. This is despite the increased emphasis orthopaedics is placing on evidence-based approaches like meta-analysis, cost-benefit modeling, and decision analysis, all of which depend entirely on the absence of systematic biases and influence from non-scientific factors in the review process.

Previous studies, including our own, have identified strong associations between commercial funding and positive research outcomes in the orthopaedic literature; in fact, all studies of which we are aware in orthopaedics have pointed toward a higher proportion of positive studies in print than negative or non-supportive ones. However, these studies used only published and presented work as the denominator evaluated, and so are not appropriately designed to answer questions about the presence or absence of actual bias. In order to assess whether peer review results in actual positive-outcome bias, all investigations submitted for peer review to a journal must be analyzed to see whether positive studies are more likely to be published, and relevant confounding variables (such as study quality and sample size) must be controlled for. Similarly, only by evaluating the denominator of manuscripts submitted for review by a journal could one conclude that the disproportion of published commercially-funded "positive outcome" papers in fact represents a bias.

With the cooperation of the Journal of Bone and Joint Surgery, we evaluated all hip and knee arthroplasty manuscripts submitted during a 17-month period in order to test the following hypotheses:

1) Non-scientific variables, including commercial funding, are associated with positive outcomes in research submitted for peer review.

2) Positive study outcomes and non-scientific variables are associated with acceptance for publication by the Journal of Bone and Joint Surgery.

Methods

All initial manuscript submissions consisting of original research on the subject of adult hip or knee reconstruction to the Journal of Bone and Joint Surgery (American) between January 2004 and June 2005 were reviewed. Two-hundred nine manuscripts met the inclusion criteria. Journal staff redacted the manuscripts and no individual identifiers were transmitted to the study investigators at any point during the process.

Using information provided in the blinded manuscripts, two orthopaedic reviewers used previously published definitions to categorize all manuscripts as either: (1) Positive/Favorable/Significant Difference Observed; or (2) Not Positive/Unfavorable/No Significant Difference Observed.

Two reviewers classified manuscripts by study type (therapeutic, prognostic, diagnostic, or exposure/risk/harm) in order to assess level of evidence as set forth by the submission requirements of the Journal. These same reviewers recorded sample size for each manuscript. Sackett's criteria for study quality were used to grade submissions, since these criteria form the standard evidence-based medicine approach adopted across all disciplines. These criteria also are relatively straightforward, and grading is reproducible; kappa statistics for inter-observer agreement was nearly perfect on our two independent analyses of study quality (all kappa values ≥ 0.94).

The Journal maintained a database that prospectively recorded each manuscript's funding source

	Study Outcome†			
Variable	Positive (n=148)	Negative (n=49)	Undecided (n=12)	p value
Funding Source*				
Industry (n=54)	74% (n=40)	22% (n=12)	4% (n=2)	0.668
Independent (n=143)	69% (n=99)	25% (n=35)	6% (n=9)	
Other (n=11)	82% (n=9)	9% (n=1)	9% (n=1)	
Country of Origin				
United States (n=95)	75% (n=71)	21% (n=20)	4% (n=4)	0.107
Foreign (n=101)	70% (n=71)	23% (n=23)	7% (n=7)	
United States & Foreign (n=13)	46%(n=6)	46% (n=6)	8% (n=1)	
Statistician				
Present (n=126)	70% (n=88)	25% (n=31)	5% (n=7)	0.637
Absent (n=83)	72% (n=60)	22% (n=18)	6% (n=5)	
Disposition				
Accepted (n=64)	70% (n=45)	28% (n=18)	2% (n=1)	0.41
Rejected (n=145)	71% (n=103)	21% (n=31)	8% (n=11)	
Study Quality (n=209)				
Mean Sackett Score (SD)	49% (0.19)	60% (0.21)	61% (0.17)	*0.003
Mean Level of Evidence (SD)	2.9 (1.06)	3.2 (1.22)	3.1 (1.24)	0.091
Study Size (n=209)	202 (579)	782 (3446)	2211 (5313)	*0.05

Table 1: The relationship between study outcome and variables of interest.
* One manuscript submission was rejected by the Journal prior to receiving the conflict of interest form from the submitting authors, and thus funding source was not available for analysis on this particular submission. †Percentages represent the proportion of the study variable of interest listed in the left hand column.

	Manuscript Disposition†		
Variable	Accepted (n=64)	Rejected (n=145)	p value
Funding Source*			
Industry (n=54)	41% (n=22)	59% (n=32)	*0.027
Independent (n=143)	25% (n=36)	75% (n=107)	
Other (n=11)	55% (n=6)	45% (n=5)	
Country of Origin			
United States (n=95)	39% (n=37)	61% (n=58)	*0.020
Foreign (n=101)	22% (n=22)	78% (n=79)	
United States & Foreign (n=13)	38% (n=5)	62% (n=8)	
Statistician			
Present (n=126)	29% (n=37)	71% (n=89)	0.627
Absent (n=83)	33% (n=27)	67% (n=56)	
Study Outcome			
Positive (n=148)	30% (n=45)	70% (n=103)	0.410
Negative (n=49)	37% (n=18)	63% (n=31)	
Study Quality (n=209)			
Mean Sackett Score (SD)	50% (0.21)	53% (0.21)	0.206
Mean Level of Evidence (SD)	3.2 (1.12)	3.1 (1.10)	0.910
Mean Study Size (SD) (n=209)	523 (2948)	438 (1740)	0.796

Table 2: The relationship between disposition and variables of interest. * One manuscript submission was rejected by the Journal prior to receiving the conflict of interest form from the submitting authors, and thus funding source was not available for analysis on this particular submission. †Percentages represent the proportion of the study variable of interest listed in the left hand column.

(commercial, philanthropic, or non-funded/other), geographic origin, and presence/absence of a coauthor with expertise in statistics or epidemiology. Information concerning funding source was taken directly from the authors' disclosure statements.

After a database of outcome, study quality, and sample size was created, the database from the Journal that contained the additional variables of interest was added, and comparisons were made according to the a priori study hypotheses. Statistical analyses were performed by the two study statisticians using SPSS (version 13.0, Chicago, IL); statistical significance was set at the $p \leq 0.05$ level.

Results

Two hundred nine manuscripts met the inclusion criteria and served as the cohort for the proposed analysis. Seventy-one percent (148 of 209) concluded with a positive outcome. Thirty-one percent (64 of 209) were accepted for publication by the Journal's peer-review process. Twenty-six percent (54 of 208) of studies were classified as commercially-funded, whereas 69 percent (143 of 208) reported receipt of no funding, commercial or otherwise. Funding source information was unavailable for one manuscript.

Seventy-four percent (40 of 54) of commercially-funded studies concluded with a positive outcome, compared with 69 percent of non-funded studies (99 of 143); this difference was not significant with the numbers available (p=0.67). Country of origin, likewise, was not associated with study outcome with the numbers available (p=0.107). Studies that included a biostatistician as a co-investigator or collaborator were not more likely to conclude with a positive outcome than those that did not employ a statistician (p=0.64, Table 1).

Of the studies that concluded with positive outcomes, 30 percent (45 of 148) were accepted for publication. By comparison, 37 percent (18 of 49) of the non-positive studies were accepted. This difference in publication rate was not significant (p=0.41). Twelve manuscripts (6 percent) were not analyzable according to the predetermined positive/non-positive outcome criteria. Although there was no difference in the proportion of non-positive studies that were accepted for publication compared with positive ones, non-positive studies demonstrated higher scores for study quality than did positive studies (Sackett score of 60% vs. 49%, p=0.003) and larger sample sizes compared to positive studies (mean of 782 vs. 202, p=0.05). The relationship between variables of interest and manuscript disposition is shown in Table 2.

Further analysis of studies that were eventually accepted for publication demonstrated that they were more likely to be commercially funded (p=0.027; OR=2.1, CI=1.08-4.08), and more likely to have been authored by U.S. investigators (p=0.02) than were manuscripts rejected by the peer-review process, despite the fact that commercially-funded studies and U.S.-based studies were no more likely to demonstrate greater study quality as assessed by objective measures of Sackett's criteria, levels of evidence, and sample size (p=0.24-0.79).

Discussion

To our knowledge, our study is the first of its kind to examine the universe of manuscripts submitted rather than simply examining the published literature. We found that non-scientific factors, including industry funding, were not associated with positive study outcomes, and that positive study outcome was not a predictor of success in peer review. These results suggest that if there is an industry influence on positive outcomes, it does not occur at the level of study submission, and if there is a positive-outcome bias, it does not appear to be a dominant force affecting peer review.

That said, non-positive studies appeared to be better-quality research than positive studies; non-positive studies demonstrated significantly higher study-quality scores as well as significantly larger sample sizes. If, in fact, non-positive studies are better but are not more likely to be published, as seemed to be the case here, this may represent an insidious or low-level form of publication bias against non-positive studies during peer review. And if indeed reviewers tend to give lower merit scores to non-positive research, this has implications for evidence-based orthopaedics, as it would lead meta-analyses and other forms of synthetic literature (such as economic analyses and decision

analyses) to overestimate the size of apparent treatment effects.

We identified that two non-scientific factors, commercial funding and origin of research within the United States, were associated with a greater likelihood of a manuscript being accepted for publication. This occurred despite the fact that U.S.-based and commercially-funded manuscripts were not significantly better (in terms of study quality or sample size) from non-U.S.-based and non-funded research. This finding cannot be taken to be sinister, however, as peer reviewers were blinded to funding source and country of origin throughout the manuscript evaluation process. These findings may have been the result of a familiarity effect, with a largely U.S.-based pool of adult reconstruction reviewers tending to be more accepting of more recognizable study formats (product testing), North American syntax and familiar verbiage. Perhaps equally likely is apparent relevance; adult reconstruction is both technology- and implant-intensive, and so U.S.-based commercial studies may be more likely than non-funded research be perceived as relevant.

It is worth noting that the analyses performed in this report were limited to only adult hip and knee reconstruction manuscripts submitted to one journal. We do not assume that these results apply more broadly to other subspecialties or journals; however, our prior work has suggested that if commercial funding might have an impact on outcomes, it would be most readily detectable in the specialty of adult reconstruction. Also, our analysis sought only to evaluate for the possibility of bias during peer review. There is evidence that non-scientific factors may exert effects prior to manuscript submission in terms of selection of biased study endpoints, premature study termination, and the decision of whether to submit research for publication.

It is encouraging that, at least for the denominator surveyed, the peer-review process itself does not appear to suffer from severe positive-outcome bias; also, the impact of commercial funding on research outcomes is less pronounced than was previously suspected. We did identify what may be subtle influences in both of these areas, but we observed nothing that could be described as pervasive or sinister.

Recommended Reading

Leopold, S. S.; Warme, W. J.; Fritz Braunlich, E.; and Shott, S.: Association between funding source and study outcome in orthopaedic research. Clin Orthop Relat Res, (415): 293-301, 2003.

Bhandari, M., et al.: Association between industry funding and statistically significant pro-industry findings in medical and surgical randomized trials. CMAJ, 170(4): 477-80, 2004.

Bhandari, M.; Richards, R. R.; Sprague, S.; and Schemitsch, E. H.: The quality of reporting of randomized trials in the Journal of Bone and Joint Surgery from 1988 through 2000. J Bone Joint Surg Am, 84-A(3): 388-96, 2002.

The Detailed Anatomy of the 1,2 Intercompartmental Supraretinacular Artery for Vacularized Bone Grafting of Scaphoid Nonunions

Thanapong Waitayawinyu, M.D., Cassandra Robertson, M.D., and Thomas E. Trumble, M.D.

When scaphoid nonunion presented with avascular necrosis of proximal pole, surgical treatment by open reduction and internal fixation combined with conventional bone grafting techniques may not provide successful result. The use of pedicled vascularized bone grafts can improve the union rate and time to union. The vascularized bone graft from the dorsoradial aspect of the distal radius, the 1,2 intercompartmental supraretinacular artery (1,2 ICSRA), relies on the superior retinacular branch of the radial artery. With many potential advantages, this vascularized graft has been widely used with very satisfactory results up to 100% union rate. This vessel is not always well visualized along its entire course from the radial artery. It is therefore useful to know the anatomic features of this artery including the perforating vessels with the relationship to surrounding bony landmarks for prospective use as vascularized bone grafts for the treatment of scaphoid nonunions.

Methods

Ten fresh-frozen adults unpaired cadaveric forearms, 5 males and 5 females, 5 right-sided and 5 left-sided with an average age of 81 years (range 62-100 years), and 3 preliminary specimens were dissected. After injection of 10 ml red latex to the proximal radial artery, under 3.5X loupe magnification, the anatomic location of 1,2 ICSRA related to radial styloid were evaluated. The configurations of the arterial take-off from the radial artery of the 1,2 ICSRA in relation to the dorsal scaphoid branch was studied. The pedicle lengths were measured. The configurations of the perforating vessels were studied. The average number and frequency of perforators for the graft length of 1 cm were identified. The graft was then dissected off the distal radius. Mobilization of wrist joint of 20 degree radial and 30 degree ulnar deviation was performed; the pedicle span of this vessel to the proximal scaphoid was then measured. The ability of graft mobilization to reach scaphoid and lunate was also identified.

Statistical Analysis

All distances and numbers were analyzed to determine the averages and frequencies of the 1,2 ICSRA pedicle and perforators. Multiple pared t tests were used to analyze the difference of number of perforators and pedicle spans with wrist motions. The level of significance was defined as a p value of less than .05.

Graft Location from the Articular Surface (mm)	Frequency of Perforators	Average Number of Perforators
5 – 15	2	3.0
6 – 16	3	3.1
7 – 17	3	2.9
8 – 18	4	3.1
9 – 19	3	2.9
10 – 20	3	2.6
11 – 21	1	2.6
12 – 22	1	2.7
13 – 23	1	2.3
14 - 24	3	2.3

Table 1: Demonstrations of frequency and average number of the perforators within the graft length of 1 cm.

Results

The 1,2 ICSRA

The 1,2 ICSRA was present in all specimens. The average distance of arterial take-off from the radial artery was at 1.9 mm from the tip of radial styloid, with a range of 6.3 mm proximal to 3.2 mm distal to radial styloid. The 1,2 ICSRA bifurcation from radial artery presented as a direct branch from the radial artery, a separate branch from the dorsal scaphoid branch, in 6 of 10 specimens and in 1 of the pilot specimens (Figure 1). In 3 specimens, the 1,2 ICSRA and the dorsal scaphoid branch arose from different locations and anastomosed before splitting to supply distal radius and scaphoid (Figure 2). The average distance between these 2 arteries was 9.3 mm (range 5.2-14.7 mm). 1 of 10 specimens and 2 of the pilot specimens were found a shared origin of these 2 arteries from the radial artery (Figure 3). The average pedicle length of 1,2 ICSRA was 22.5 mm (range 15-31 mm).

The Perforators

The average distance of perforating vessels of the 1,2 ICSRA from the articular surface was 12.1 mm (mode 14.7 mm, range 3.5-23.5 mm), the average number of perforating vessels was 5.5 (range 3-7). When the graft length of 1cm was evaluated, the availability of perforators was present

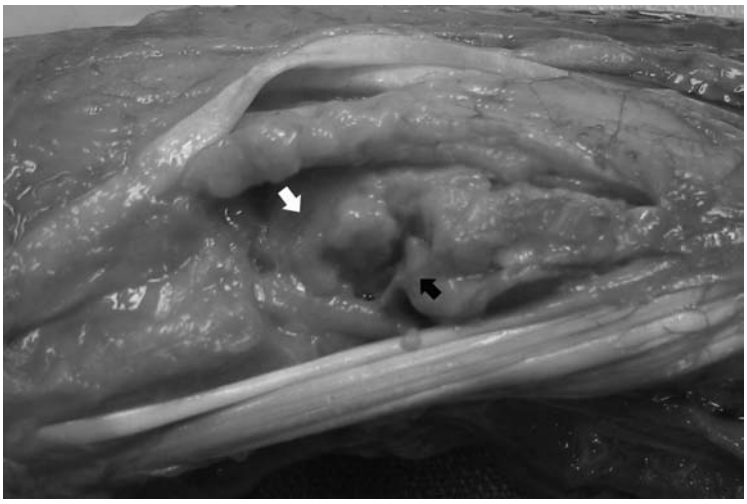

Figure 1: Demonstration of a direct branch of the 1,2 ICSRA bifurcates from radial artery (black arrow), separated from the dorsal scaphoid branch (white arrow).

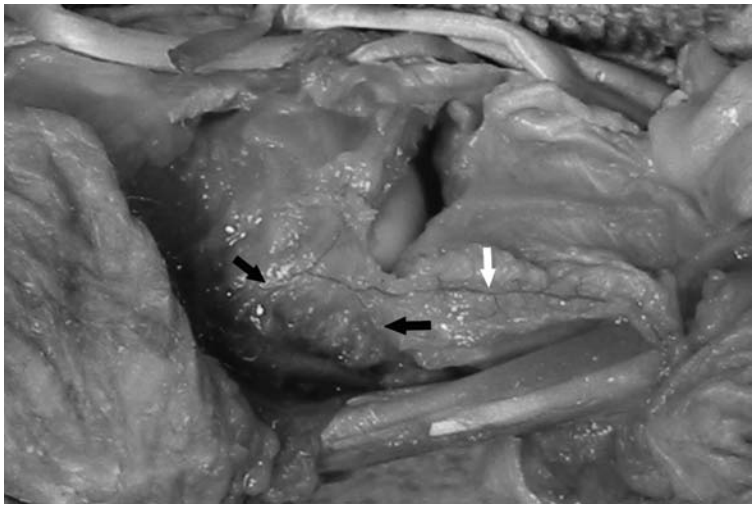

Figure 2: Anastomosis of the 1,2 ICSRA and the dorsal scaphoid branch (both black arrows) before splitting to supply distal radius and scaphoid is demonstrated. White arrow, 1,2 ICSRA.

as Table 1. The average number of perforators for a graft length of 1 cm was 2.75 (range 1-7). The graft location of 8-18 mm from the articular surface presented the maximal frequency of perforators. There was no statistically significant difference of the average number of perforators within the graft range of 5-15 mm to the range of 9-19 mm, and within the range of 10-20 mm to 14-24 mm, from the articular surface. When compared the average number for a graft length of 1 cm between these 2 groups, the graft length from 5-15 mm to 9-19 mm from the articular surface presented 3 perforators, whereas the graft length from 10-20 mm to 14-24 mm from the articular surface presented 2.5 perforators, with significant difference of p value = 0.01.

Availability for Scaphoid and Lunate Vascularized Bone Graft

The availability and sufficient length of graft for the placement of both dorsal and volar scaphoid was present in all specimens. The pedicle graft reached the lunate only 2 specimens, and the pedicles were taut in both specimens. The average pedicle span to the proximal scaphoid was altered from 16.2 to 14.3 mm, respectively, with radial and ulnar deviation of the wrist. These two averages were significant difference, with the p value of 0.03.

Discussion

From this study, we can categorize the relationship of 1,2 ICSRA and the dorsal scaphoid branch into 3 types (Figure 4); type I, separated type, the 1,2 ICSRA bifurcate directly from the radial artery, separated from the dorsal scaphoid branch, type II, combined type, the 1,2 ICSRA and the dorsal scaphoid branch bifurcate from the radial artery separately, anastomose, and then split to two branches, type III, shared type, the 1,2 ICSRA and the dorsal scaphoid branch shared the same bifurcation from the radial artery. Type II and type III present almost fifty percent of all specimens. Type III of the 1,2 ICSRA may be injured with the initial injuries or dissection of the pedicle intraoperatively. Thus, meticulous pedicle dissection must be performed.

The average distance of the 1,2 ICSRA and perforators from the articular surface may be helpful for dissection and indicating the site of harvesting the bone graft. The sufficient span for placement both dorsal and volar proximal scaphoid support the use of this vascularized bone graft for scaphoid nonunion, but not proper for avascular necrosis of lunate or Kienbock's disease. The span to reach the proximal scaphoid is changed significantly with wrist position. Radial deviation should be concerned during perioperative care and postoperative rehabilitation.

The detailed anatomy presented in this study may help increasing the reliability and success rate of dissection and harvesting the 1,2 intercompartmental supraretinacular artery graft for vascularized bone grafting of scaphoid nonunions by concerning many crucial steps and anatomical variations.

Recommended Reading

Steinmann SP, Bishop AT, Berger RA. Use of the 1,2 intercompartmental supraretinacular artery as a vascularized pedicle bone graft for difficult scaphoid nonunion. J Hand Surg 2002;27A:391-401.

Sunagawa T, Bishop AT, Muramatsu K. Role of conventional and vascularized bone grafts in scaphoid nonunion

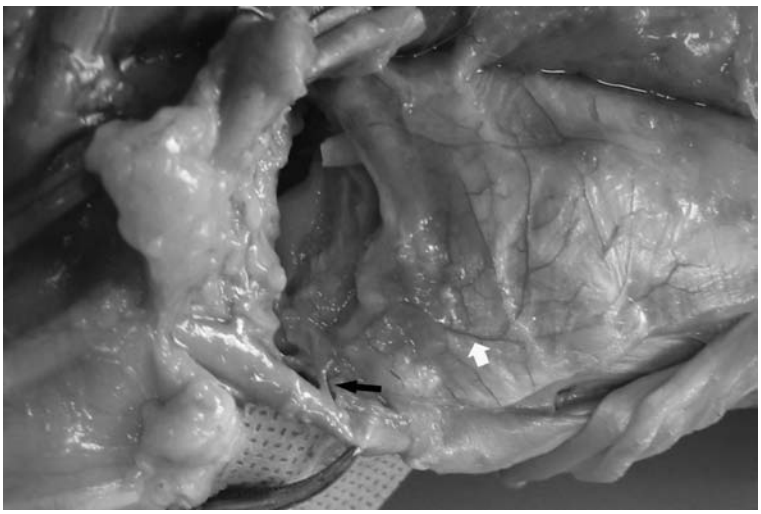

Figure 3: A shared origin (black arrow) of the 1,2 ICSRA (white arrow) and the dorsal scaphoid branch from the radial artery is demonstrated.

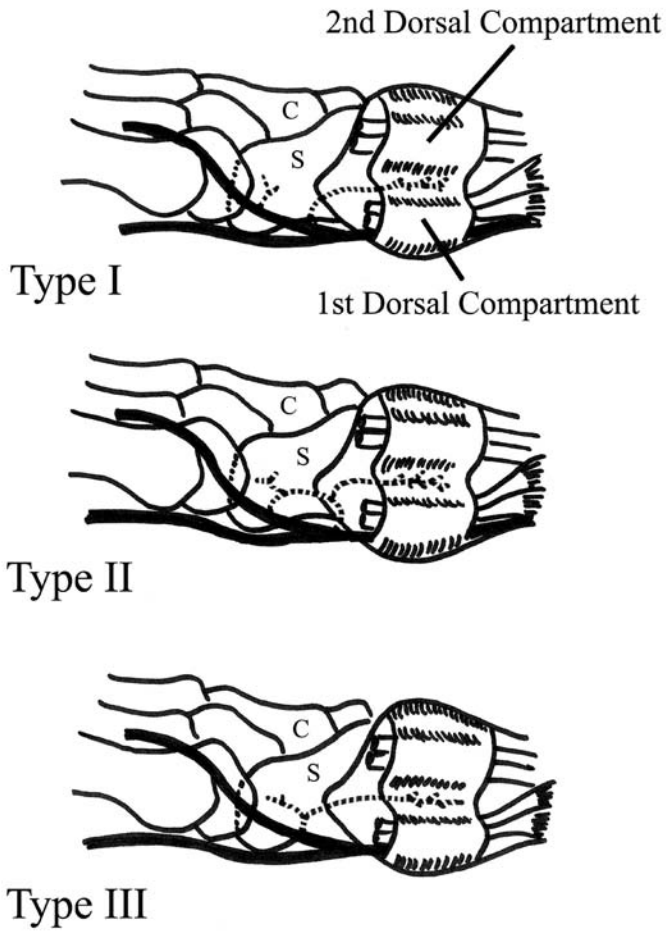

Figure 4: Illustration of 3 types of the 1,2 ICSRA related to the dorsal scaphoid branch. type I, separated type; type II, combined type; type III, shared type; S, Scaphoid; C, Capitate.

with avascular necrosis: A canine experimental study. J Hand Surg 2000;25A:849-859.

Shin AY, Bishop AT. Pedicled vascularized bone grafts for disorders of the carpus: scaphoid nonunion and Kienbock's disease. J Am Acad Orthop Surg 2002;10:210-216.

Zaidemberg C, Siebert JW, Angrigiani C. A new vascularized bone graft for scaphoid nonunion. J Hand Surg 1991;16A:474-478.

Sheetz KK, Bishop AT, Berger RA. The arterial blood supply of the distal radius and ulna and its potential use in vascularized pedicled bone grafts. J Hand Surg 1995;20A:902-914.

Hurlbut PT, Van Heest AE, Lee KH. A cadaveric anatomic study of radial artery pedicle grafts to the scaphoid and lunate. J Hand Surg 1997;22A:408-412.

Stabilization of the Posteromedial Fragment in Bicondylar Tibial Plateau Fractures: A Mechanical Comparison of Locking and Non-Locking Single and Dual Plating Methods

Brad Yoo, M.D., Daphne M. Beingessner, M.Sc., M.D., F.R.C.S.C., and David P. Barei, M.D., F.R.C.S.C.

A displaced posteromedial articular fragment is not an infrequent component of a bicondylar tibial plateau fracture. With displaced posteromedial fragments, posteromedial buttress plating may be necessary to maintain reduction and prevent late varus collapse. Solitary lateral locked plating, however, has become increasingly popular for bicondylar tibial plateau fractures. We sought to determine the ability of locked versus non-locked single and dual plating constructs to maintain the posteromedial fragment reduction in a bicondylar tibial plateau fracture model. We hypothesized the dual plating constructs would hold an anatomically reduced posteromedial fragment under higher loads than the lateral locked or non-locked constructs alone.

Methods

Thirty adult-sized third generation composite tibiae were used (Pacific Research Labs, Vashon, WA). The average dimensions of the posteromedial fragment have been previously investigated and were used in the present model. According to previously presented data, the posteromedial fragment was defined by four parameters: (1) Posterior cortical height (PCH) of 43 mm. (2) Sagittal fracture angle (SFA) of 83 degrees (range 33-112 deg). (3) Surface area of 23%, calculated as a percentage of the plateau's total area. (4) Axial fracture angle of 8.2 degrees, defined as the angle subtended from a line traversing the tibiae in its true coronal plane (Figure 1).

The lateral fracture pattern was based upon the fracture model previously described and investigated by Horwitz. One metaphyseal and three articular fragments (posteromedial, anteromedial and lateral) were created. This fracture pattern used maximized vertical instability. Specimens were identically recreated with the use of a custom manufactured jig.

Four lateral plate types were tested: (1) 8-hole 3.5 mm conventional proximal tibial plate (CP, Zimmer, Warsaw, IN), (2) 8-hole 3.5 mm Locked Compression Plate (LCP, Synthes, Paoli, PA), (3) 9-hole Less Invasive Stabilization System plate (LISS, Synthes, Paoli, PA), and (4) 8-hole 3.5 Proximal Tibial Locking Plate (PTLP, Zimmer, Warsaw, IN). The conventional plate was either tested alone, with 6-hole 1/3 tubular plate placed on the posteromedial surface, or with 6-hole contoured limited contact dynamic compression (LCDC, Synthes, Paoli, PA) plate placed on the posteromedial surface. The lateral locking plates were tested without

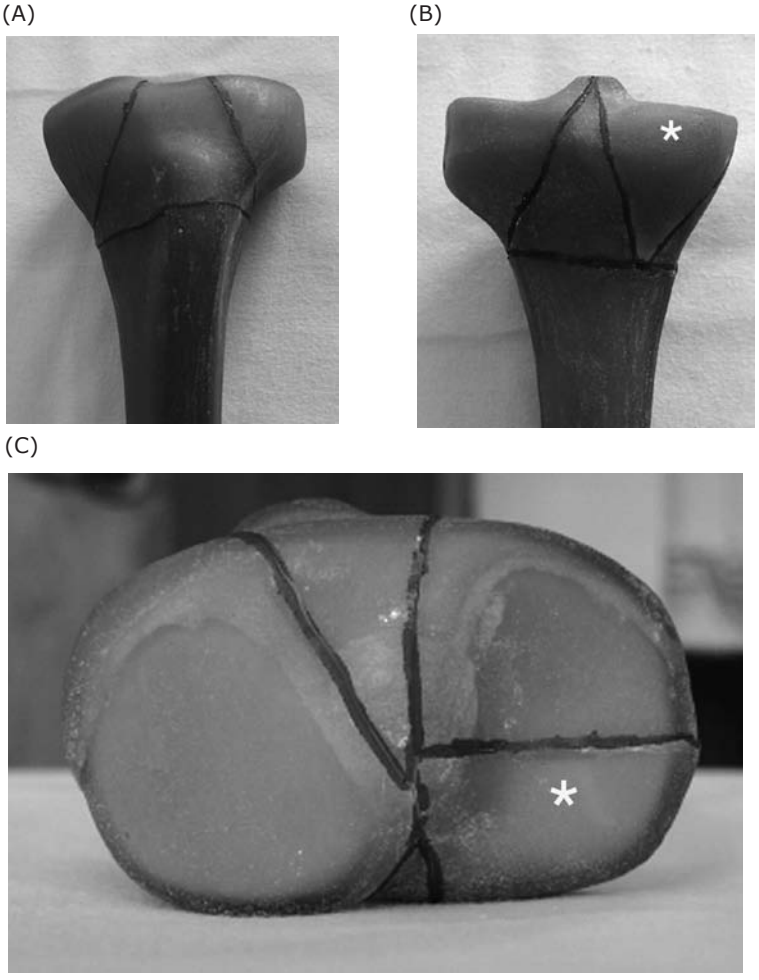

Figure 1: The anterior (A), posterior (B), and superior (C) views of a left composite tibia are demonstrated. The osteotomy sites involving the medial plateau, lateral plateau, and metadiphyseal portions are illustrated. The asterisk (*) denotes the posteromedial fragment.

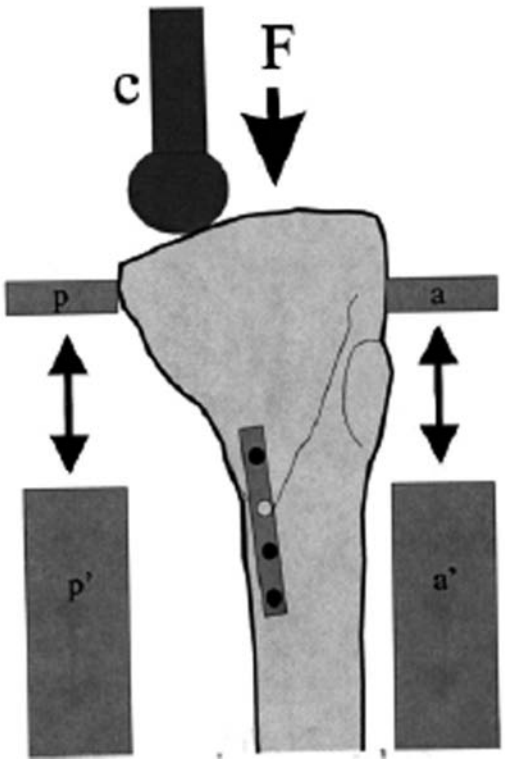

Figure 2: Schematic representation of specimen loading from a medial vantage point. Force (F) is applied to the center of the osseous medial tibial plateau via a 32mm hemispherical impactor (c). Changes in posteromedial fragment height (p and p') and anteromedial height (a and a') where identified with high-speed digital imaging.

posteromedial buttresses.

Fractures were anatomically reduced. Lateral plates were applied according to AO technique and in accordance with the manufacturer's guidelines. Along the transverse limb of the conventional plate, bicortical 3.5 mm fully threaded cortical screws were oriented perpendicular to the plate and in a divergent pattern. Therefore, the anteromedial and posteromedial fragments were each reproducibly secured with two symmetrically spaced bicortical screws. The 1/3 tubular and LCDC plates were positioned along the posteromedial corner of the tibia, manually contoured prior to application, and fixed with three bicortical 3.5 mm fully threaded cortical screws. The first screw was placed as an anti-glide screw adjacent to the apex of the posteromedial fragment and two further screws were placed at either end of the plate. Locked screws were bicortical for the PTLP and LCP systems. LISS screws were unicortical.

Each specimen was rigidly secured to the loading mount of a servohydraulic materials testing machine. Loading was performed by a 32 mm stainless steel hemispherical impactor applied to the osseous center of the medial plateau (Figure 2). The specimens were cyclically loaded at a given load range for 20 cycles at a rate of 1 Hz. The initial load range was from 0 N to 400 N. This load range was incrementally increased by 400 N to a final total of 4000 N. High-speed digital imaging recorded fragment behavior during cyclic loading. Digital analysis determined the precise load level at which fragment failure occurred. This was defined as either the initial appearance of plastic deformation or sudden catastrophic fixation failure,

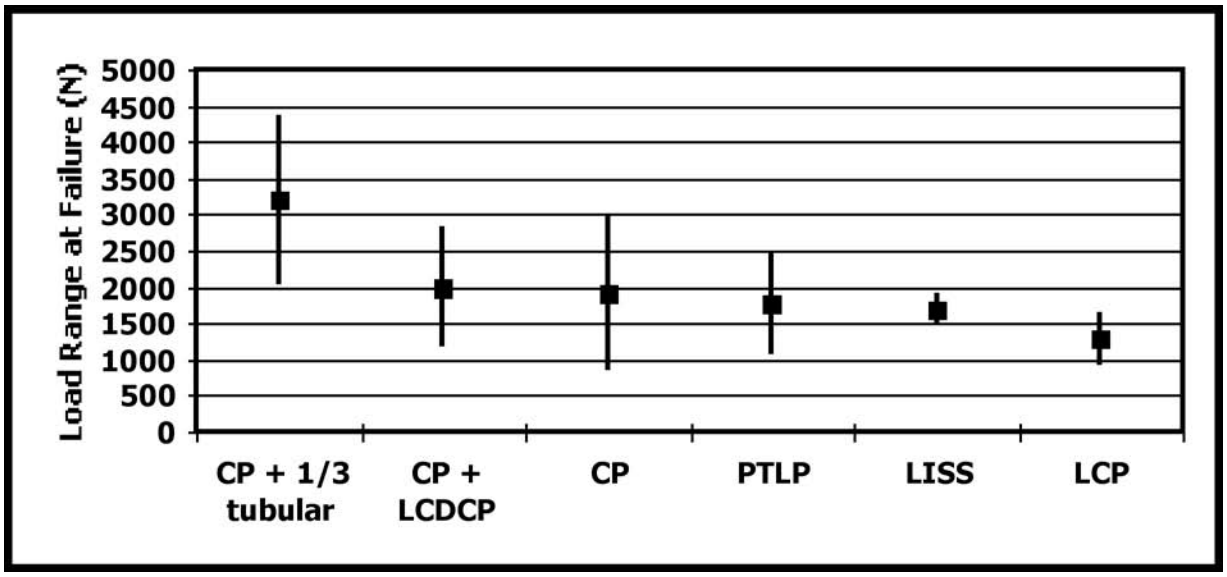

Figure 3: Load at failure. CP = Conventional plate, LCDC = Limited contact dynamic compression plate, PTLP = Proximal Tibial Locking Plate, LISS = Less Invasive Stabilization Plate, LCP = Locked Condylar Plate.

CP + 1/3 tubular	CP + LCDCP	CP	PTLP	LISS	LCP
3040 +/- 1131.4	2000 +/- 800.0	1920 +/- 1035.4	1760 +/- 669.3	1680 +/- 178.9	1280 +/- 334.6

Table 1: Load Range at Failure According to Plate Construct . CP = Conventional plate, LCDC = Limited contact dynamic compression plate, PTLP = Proximal Tibial Locking Plate, LISS = Less Invasive Stabilization Plate, LCP = Locked Condylar Plate.

whichever event occurred first. Analysis of variance was used to determine statistical significance.

Results

The quantitative results are illustrated in Figure 3. Fragment failure occurred at the posteromedial fragment first, either by plastic deformation or catastrophic fixation failure. The lateral or anteromedial fragments never failed during testing. The CP + 1/3 tubular posteromedial buttress design was found to have the highest average load at failure (Table 1). In two instances, the CP + 1/3 tubular construct did not fail under the highest loads applied (4000N). This dual plating construct demonstrated significantly higher load at failure compared with the LISS ($p = 0.048$) and the LCP ($p = 0.007$). Though the PTLP had a similar mean load at failure as the LISS or LCP, it did not differ statistically with the CP + 1/3 construct ($p = 0.068$). Both the CP + LCDCP and the CP constructs had similarly lower mean load at failure compared with the CP + 1/3 tubular construct. These differences were not statistically significant. The statistical analysis is summarized in Table 2. No statistical significance existed between the CP + LCDCP, CP, PTLP, LCP or LISS.

Qualitatively, the non-locked specimens with or without posteromedial buttresses never failed catastrophically. In contrast, in the locked specimens, the posteromedial fragment frequently failed catastrophically.

Discussion

The goal of open reduction and internal fixation of a displaced bicondylar tibial plateau fracture is to restore anatomic articular congruity and axial alignment with good initial strength to prevent displacement during healing. The results of this study suggest that the reduction of bicondylar tibial plateau fractures with an associated posteromedial fragment is best maintained with a laterally based implant and a posteromedial buttress.

Our data corroborates that dual plating constructs are more resistant to displacement and possess higher loads to failure than laterally based implants alone, whether locked or non-locked. A non-locked plate with a 1/3 tubular posteromedial buttress was the most durable construct in maintaining the reduction of the posteromedial fragment. Comparable values were found with a non-locked plate and the LCDCP posteromedial buttress. As expected, lateral locked implants alone were least able to maintain the posteromedial fragment reduction and had a qualitatively higher incidence of catastrophic failure of the posteromedial fragment. All constructs, however, were able to withstand minimum forces of 1000 N, well above the joint forces across the knee during non-weightbearing stance.

Interestingly, the CP alone had equal if not slightly higher mean loads to failure compared with the locked implants. Locked implants are axially and angularly stable devices, functioning as a single beam construct. We expected higher loads at failure for these locked constructs. Conventional plating may also function as single beam construct, but only in ideal situations, such as those with good bone quality and sufficient friction between the plate and bone. These ideal circumstances were probably met with our choice of specimen. The composite tibiae used in this study reportedly behave like young adult non-osteopenic bone with mechanical properties comparable to "good" or "very good" cadaveric bone. Because excellent screw purchase was always obtained with the non-locked implants, it is possible that the construct strength of the CP was similar to the locked plate. In the case of the CP, two screws were reproducibly directed into the posteromedial fragment. During plate application, we noticed that the LCP and LISS reliably had only one locked screw capturing the posteromedial fragment. The PTLP had one screw completely within the fragment, while another posteromedially directed screw would cross the fracture site. The disparity between the CP and the locked constructs' anticipated and observed load range at failure may be explained by both a) having similar construct strengths due to the high quality bone present in the synthetic model and b) having a difference in the number of fixation points with the locking models.

Limitations to the study must be addressed. The mechanism of

	CP + 1/3 tubular	CP + LCDCP	CP	PTLP	LISS	LCP
CP + 1/3 tubular		0.178	0.131	0.068	0.048	0.007
CP + LCDCP	0.178		1.000	0.996	0.985	0.684
CP	0.131	1.000		0.999	0.996	0.777
PTLP	0.068	0.996	0.999		1.000	0.919
LISS	0.048	0.985	0.996	1.000		0.961
LCP	0.007	0.684	0.777	0.919	0.961	

Table 2: Statistical Significances of Tested Constructs (p values). CP = Conventional plate, LCDC = Limited contact dynamic compression plate, PTLP = Proximal Tibial Locking Plate, LISS = Less Invasive Stabilization Plate, LCP = Locked Condylar Plate.

loading the proximal tibia does not precisely reflect forces encountered in vivo. Utilizing a femoral arthroplasty component as a load applicator would not necessarily ensure the load applied would be consistent between specimens. Finally, our model is an amalgamation of 170 patients with CT findings of a posteromedial fragment. As fragment sizes vary from our model, application of our findings to the clinical scenario may be limited.

Recommended Reading

Ali AM, Saleh M, Bolongaro S, Yang L. Experimental model of tibial plateau fracture for biomechanical testing. J Biomech 2006; 39(7):1355-60.

Barei DP, Nork SE, Mills WJ, Coles CP, Henley MB, Benirschke SK. Functional outcomes of severe bicondylar tibial plateau fractures treated with dual incisions and medial and lateral plates. JBJS 2006; 88 : 1713 - 1721.

Egol KA, Kubiak EN, Fulkerson E, Kummer FJ, Koval KJ. Biomechanics of Locked Plates and Screws. J Orthop Trauma. 2004; 18:488-493.

Georgiadis GM. Combined anterior and posterior approaches for complex tibial plateau fractures. J Bone Joint Surg Br. 1994; 76:285-289.

Gosling T, Schandelmaier P, Muller M, Hankemeier S, Wagner M, Krettek C. Single lateral locked screw plating of bicondylar tibial plateau fractures. Clin orthop. 2005; 439:207-214.

Heiner AD, Brown TD. Structural properties of a new design of composite replicate femurs and tibias. J Biomech 2001; 34(6):773-81.

Horwitz DS, Bachus KN, Craig MA, Peters CL. A biomechanical analysis of internal fixation of complex tibial plateau fractures. J Orthop Trauma 1999; 13: 545-549.

Barei DP, O'Mara TJ, Falicov A, Taitsman LA, Nork SE. The Tibial Less Invasive Stabilization System (LISS) and its Relationship to the Posteromedial Fragment in Bicondylar Tibial Plateau Fracture Patterns. OTA 21st Annual Meeting, Ottawa, Canada, October 2005.

Comparison of Minimally-Invasive and Traditional Medial-Parapatellar Surgical Approaches to Total Knee Arthroplasty: Evaluation of the Learning Curve and Early Post-Operative Recovery

Jason King, M.D., M.P.H., Daniel L. Stamper, P.A.-C, Douglas C. Schaad, Ph.D., and Seth S. Leopold, M.D.

Surgeons disagree whether so-called minimally-invasive total knee arthroplasty (MIS TKA) approaches indeed result in faster postoperative recuperation. In addition, concerns have been raised as to how best to disseminate such new surgical procedures in a way that clinical results are not compromised by issues pertaining to a surgeon's learning curve.

We tested the following hypotheses: First, the MIS approach results in a shortened recuperative period, as judged by length of hospital stay, need for inpatient rehabilitation, consumption of narcotic analgesics, and use of assistive ambulation devices. Second, operative time for MIS TKA is longer during a surgeon's learning curve than for traditional medial parapatellar arthrotomy TKA. Third, during the learning curve, implant alignment is compromised in patients having MIS TKA compared to those having traditional TKA.

Materials and Methods

Upon receiving IRB approval, an independent reviewer screened patients' electronic medical records, collecting demographics, surgical approaches, and clinical outcomes. The cohort was composed of the last 50 consecutive traditional TKAs done by the surgeon (SSL) before he began using the MIS approach, and his first 100 quadriceps-sparing MIS TKAs. During the initial part of the learning curve, the principal surgeon selected patients for the MIS approach who were height-weight proportional with mild to moderate knee deformities.

An independent investigator not involved in patients' care reviewed radiographs and recorded tibial component coronal and sagittal alignment, patellar tilt, patellar subluxation and patellar resection asymmetry. Measurements on all radiographs were from films obtained at six weeks postoperatively.

Patients in both the MIS and traditional TKA groups had the same cemented, modular, condylar-type prosthesis implanted (NexGen, Zimmer, Inc., Warsaw, IN). Patellae in both groups were resurfaced with a cemented, 3-pegged, all-polyethylene patellar component. All implants in the MIS group were posterior-cruciate-ligament substituting.

The principal differences between the MIS and the traditional TKA approach include: In the MIS group we did not evert the patella but rather lateral subluxated it during tibial and femoral preparation; we performed freehand resection of the patella with it tipped 90 degrees rather than everted; we made the tibial cuts in situ with an anteromedial cutting block without dislocating the tibiofemoral joint; we did not flex the knees >90 degrees until trial components were installed and final range of motion testing was done; we used a shorter anteromedial incision, rather than a longer direct-anterior incision.

Anesthesia and aftercare were similar in both groups: regional anesthesia was used unless contraindicated or refused by the patient, early range-of-motion protocols, early weight-bearing as tolerated, patient-controlled analgesia, pre/post-operative antibiotics, and thromboprophylaxis. The same physical therapy team managed all patients. No special emphasis was placed on shortening length of stay for the MIS

	MIS	Traditional	P-value
LOS*	2.8±0.9	3.7±1.3	<0.0001
% Home**	95	33.3	<0.001
Narcotic Use, % #			
2 weeks	77.5	89.2	0.001
6 weeks	21.1	27.0	0.01
No Assistive Device, %##			
2 weeks	21.0	11.6	0.025
6 weeks	92.3	83.7	0.2
ROM, 6 weeks ¥			
Flexion	118.6	117.8	0.65
Extension	1.7	1.3	0.24
Operative time, minutes	86.3	78.9	0.01
Patients 1 – 25	102.5	---	
Patients 26-50	84.6	---	
Patients 51-75	82.0	---	
Patients 76 - 100	76.0	---	<0.001§

Table 1: Clinical Outcomes. * Length of hospital stay, in days, presented as mean ± standard deviation. ** Percentage of patients discharged to home, rather than to inpatient rehabilitation. # Percentage of patients using narcotics at 2 and 6 weeks respectively. ## Percentage of patients not requiring assitive device to ambulate, i.e. cane or walker. ¥ Range of motion at six weeks. § P-value for overall trend between quartiles of MIS patients with regards to patellar resection.

	MIS	Traditional	P-value
Patellar Tilt, deg.	3.3°	3.0°	0.65
Patients 1 – 25	4.6°	---	
Patients 76 - 100	1.6°	---	0.006*
Patellar Subluxation, mm	1.8	1.8	0.78
Patellar Resection, mm	2.5	2.2	0.35
Patients 1 – 25	2.7	---	
Patients 76 - 100	1.4	---	<0.001¥
AP Tibial Alignment	89.8°	91.1°	<0.001
Lateral Tibial Alignment	84.1°	82.9°	0.003

Table 2: Radiographic Results. * P-value for overall trend between quartiles of MIS patients with regard to patellar tilt. ¥ P-value for overall trend between quartiles of MIS patients with regards to patellar resection.

patients. Criteria for discharge home or admission to inpatient rehabilitation were identical in both groups.

Results

Five patients in the traditional TKA group lived out of state and were excluded from the study. No patients in the MIS group were lost to follow-up. To date, there have been no clinical failures, radiographic loosening, infections, or revisions performed in either study group.

Patients 1 through 25 in the MIS TKA group represented 38.5 percent of all TKAs performed during that time period (e.g. 25 of 65 TKAs were performed using the MIS approach). MIS patients 26 through 50 and 51 through 75 represented 89.3 and 86.2 percent, respectively, of all TKAs in these time periods. Finally, 100 percent of all TKAs, representing patients 76 through 100, were performed using the MIS approach.

Clinical outcomes fairly consistently favored MIS over the traditional group as indicated in Table 1. The only non-significant variables tested between MIS and traditional TKAs included range of motion at six weeks and use of assistive devices for walking at six weeks after surgery. Overall, the MIS TKA approach took longer than the traditional approach, due to especially long operative times for the first 25 patients in the MIS TKA group. Subsequent quartiles showed no significant differences in the operative times between the MIS and traditional TKAs and the trend was significant.

Radiographic results presented in Table 2 showed no overall difference in patellar tilt, but the MIS group showed significant improvement over the learning curve. Mean patella subluxation was negligible in both groups. No significant difference in the frequency of radiographic outliers (subluxation greater than 2 mm) existed between the MIS and traditional TKA groups (p=0.76). Overall, patellar resection asymmetry was not significantly different between MIS and traditional TKAs. However, the MIS group demonstrated statistically significant improvement in resection accuracy over time. Mean values and the frequency of radiographic outliers for the tibial and femoral component alignment were not statistically different between the MIS and traditional TKA groups.

Discussion

We demonstrated that it took just over 25 cases before MIS operative times were comparable to those achieved using the traditional approach, and about 50 cases until patellar alignment was optimized with the MIS approach. Although patellar alignment in all quartiles of the MIS group was comparable to what has been published using traditional approaches, the MIS group clearly made improvements over time. This suggests that, at least

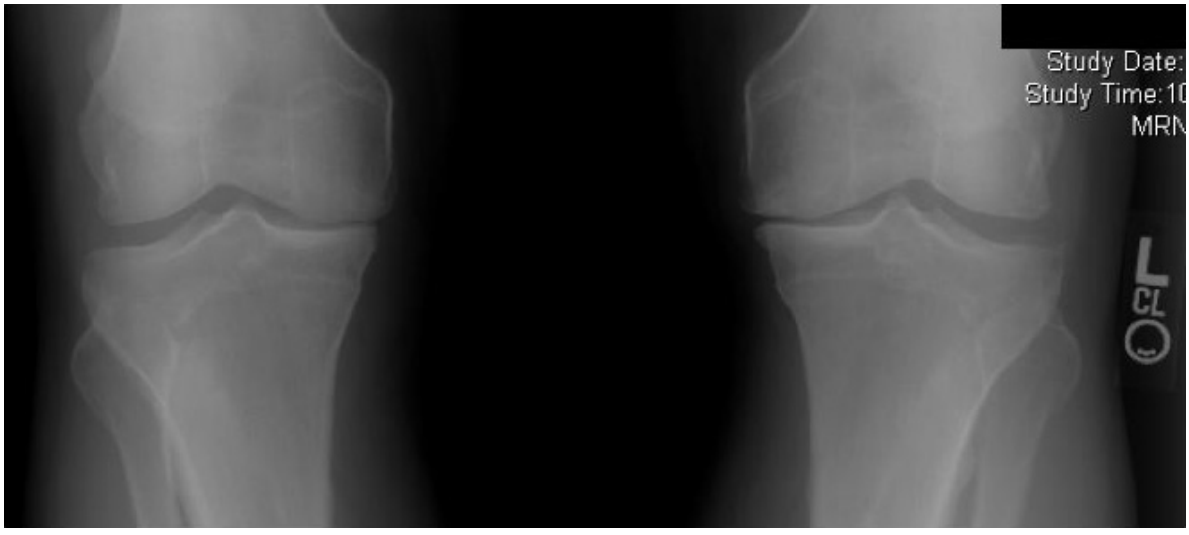

Figure 1: Radiograph showing frontal view of bilateral knee osteoarthritis and typical narrowing of the medial (inside) joint space, which is causing this patient to have significant discomfort.

Figure 2: Lateral (side) view of left knee showing osteoarthritis with joint space narrowing, bone-on-bone contact, and osteophyte formation (excess bone).

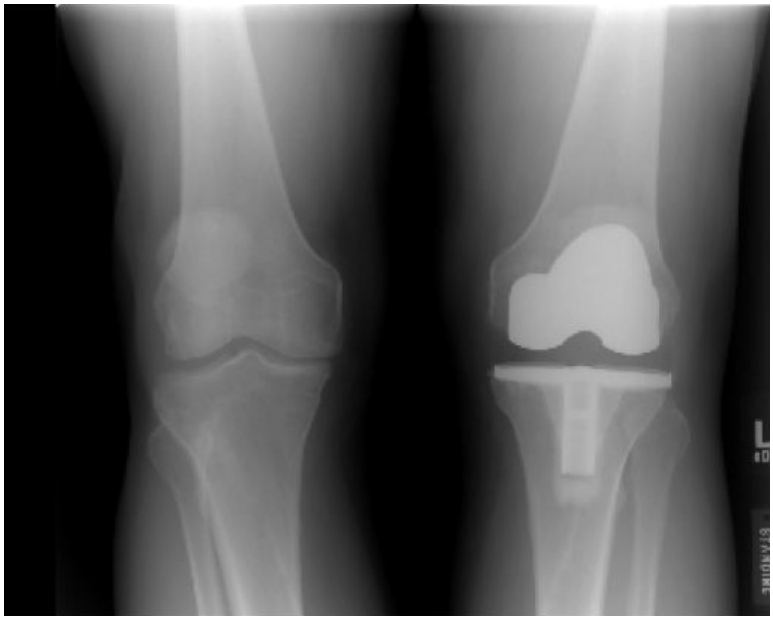

Figure 3: Frontal view of same patient after having minimally invasive total knee arthroplasty performed on the left knee with excellent component alignment.

potentially, there was some additional risk to being an MIS patient early in the learning curve. Clinical outcome data in this series tended to support the claims of MIS TKA proponents suggesting accelerated recovery.

Questions about implant alignment have been raised by critics of this procedure; tibial and femoral alignments in this series were found to be consistently excellent in both the MIS and traditional TKA groups. However, this study identified patellar malalignment issues early in the MIS learning curve, which appeared to be the result of underresection of the lateral facet. Surgeons adopting the MIS approach should verify that the "far side" of the patella is clearly visible prior to resection. This helps ensure a saw cut beneath the true chondral or osteophytic rim and that the patellar resection is symmetric.

This study has important methodological limitations and must be considered a best-case scenario for MIS TKA given the early selection bias toward easier cases from the practice of a high-volume arthroplasty subspecialist. Offsetting this somewhat, the control group of traditional TKAs represents an "all-comers" population that was assembled before the start of the MIS series. The strengths of the study include sample size, a control group, independent evaluators, and presentation of alignment and operative-time data as a function of case number (representing increasing surgical experience). Other points supporting the internal validity of this study are identical conventional condylar TKA implant design, physical therapy protocols, and criteria for inpatient rehabilitation.

Based on our results, we are cautiously optimistic about MIS TKA. It may have a role in the hands of high-volume arthroplasty surgeons who are willing to invest the time to learn and practice the procedure before performing it. Conversely, if our learning curve represents a typical experience, it appears not to be a worthwhile technique for a low-volume (5-10 cases/year) arthroplastic surgeon to attempt as the learning curve would stretch out over a period of years.

Figure 4: Lateral view of same patient's knee, demonstrating proper position of femoral and tibial components.

Recommended Reading

Alan R.K.; Tria, A.J.: Quadriceps-sparing total knee arthroplasty using the posterior stabilized TKA design. J Knee Surg, 19(1): 71–6, 2006.

Bonutti, P. M.; Mont, M. A.; McMahon, M.; Ragland, P. S.; and Kester, M.: Minimally invasive total knee arthroplasty. J Bone Joint Surg Am, 86-A Suppl 2: 26-32, 2004.

Scuderi, G.R.: Minimally-invasive total knee arthroplasty; surgical technique. Am J Orthop, 35(7 Suppl): 7–11, 2006.

Tenholder, M.; Clarke, H.D.; Scuderi, G.R.: Minimal-incision total knee arthroplasty: The early clinical experience. Clin Orthop Rel Res, 440: 67–76, 2005.

Scapholunate Interosseous Ligament Reconstruction: Results with a Modified Brunelli Technique Versus Four-Bone Weave

Annie C. Links, M.D., Simon H. Chin, M.D., Thanapong Waitayawinyu, M.D., and Thomas E. Trumble, M.D.

Scapholunate instability is caused by injury to the scapholunate ligament. The presentation is often chronic and insidious, with tenderness over the anatomical snuffbox and pain over the dorsal aspect of the scapholunate joint. The scaphoid shift maneuver will produce pain or a rotatory clunk. Radiography will indicate a scapholunate interval of 2mm or greater on the posteroanterior view and a dorsal intercalated segment instability (DISI) deformity on the lateral view. Finally, wrist arthroscopically is performed to definitively establish the diagnosis of scapholunate ligament injury.

Hand surgeons have introduced a number of interventions designed to treat chronic scapholunate instability. In 1991, Almquist and colleagues developed the four-bone ligamentous weave reconstruction which employed a strip of the extensor carpi radialis brevis (ECRB) tendon through carpus, and reinforced this with a wire loop through the scaphoid and lunate. However, persistence of the scapholunate gap on radiographs led to alternative proposals including Van den Abbeele and coworkers modification of the Brunelli tenchnique. The authors employ a strip of the flexor carpi radialis tendon and weave this through the scaphoid, anchor it to the lunate and then loop this around the radiolunotriquetral ligament as a pulley while tightening the repair.

We have modified the latter technique, combining this with the reduction and association of the scaphoid and lunate (RASL) technique described by Rossenwasser. This method was incorporated in a study comparing the results of the modified Brunelli + RASL repair versus the Almquist weave repair.

Methods

Twenty-one patients presented with chronic scapholunate dissociation and were treated with the modified Brunelli technique. Twenty-three were treated with the four-bone tendon weave technique as described by Almquist. All patients had preoperative stress-view radiographs demonstrating scapholunate ligament disruption, and all had positive MR arthrograms. Both groups were reviewed prospectively. Evaluation included radiographic changes, pain and DASH scores, grip strength and range of motion. The data set was analyzed using the student's t-test, two sample assuming unequal variances (p=0.05).

In the modified Brunelli + RASL technique, the third dorsal compartment is first released. The fourth dorsal compartment is released sharply off the capsule, creating a radially-based flap and an ulnarly-based flap. These flaps reinforce the ligament repair after the tendon weave is completed. The flexor carpi radialis (FCR) is harvested and passed through a bone tunnel drilled with a 3.5 mm cannulated drill bit. A guide wire helps to correct alignment of scaphoid rotation. Bone anchors are placed in the scaphoid and lunate. "Joysticks" (temporary K-wires inserted into bones) are used under fluoroscopic guidance to obtain anatomic rotation, and a cannulated drill is used to align the scaphoid and lunate. The bone anchors are used to repair the scapholunate interosseous ligament, with remnants from the lunate taken to the scaphoid anchor and vice versa. Next, the tendon of the FCR is tensioned and tied to the

	Modified Brunelli Technique	Four-Bone Tendon Weave
Patient demographics		
Mean age (years)	30.2	29
Male/female	15/6	17/6
Dominant hand injured	14	15
Mean follow-up (months)	28.9	29.4
Delay to treatment (months)	11.7	11.4
Deformity correction		
Mean Scapholunate angle decrease (degrees)	14.5	10
Pain/Functional Recovery		
Mean improvement in pain scores	4.8	3.2
Mean change in DASH score per item	+2.2	+0.9
Range of Motion		
Postoperative range of motion as percent of preoperative range of motion	86%	60%
Postoperative flexion versus contralateral flexion	62.8%	62.8%
Postoperative extension versus contralateral extension	63.8%	63.9%
Radial deviation versus contralateral	20.5%	20.6%
Ulnar deviation versus contralateral	27.9%	27.6%
Strength		
Postoperative versus preoperative grip strength	150.9%	119.7%
Grip strength postoperatively versus contralateral side	97.7%	84%

Table 1: Data, modified Brunelli and Four-bone tendon weave.

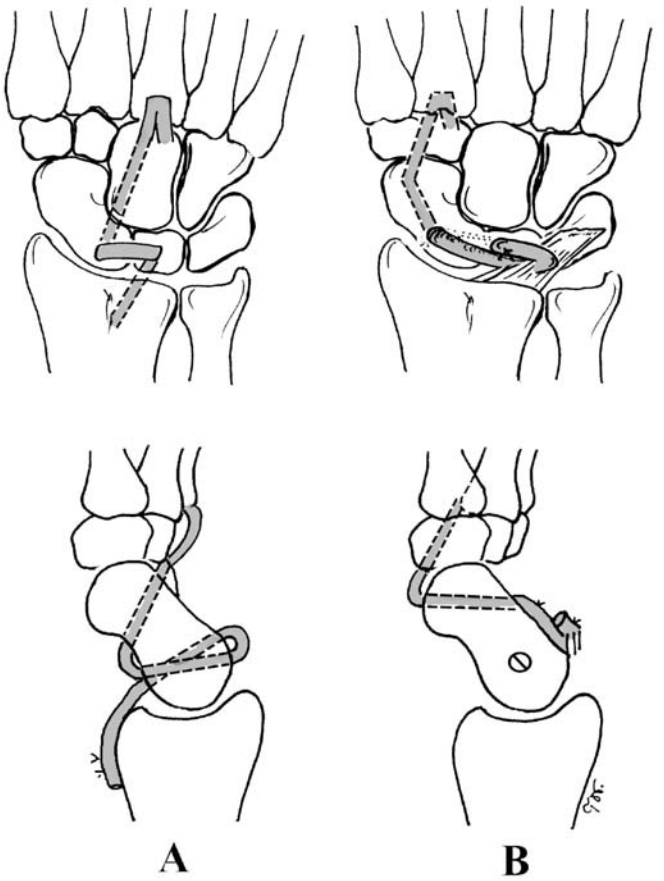

Figure 1: (A) Diagram illustrating the four-bone tendon weave technique as described by Almquist and (B) the modified Brunelli technique as described by Van Den Abbeele et al.

lunate anchor. The FCR tendon is then passed through the radiotriquetral ligament and folded back upon itself to reinforce the repair. Suture anchors from the scaphoid are then passed to the ulnar flap previously created, and suture anchors from the lunate are passed to the radial flap.

Next, a 5 cm incision is created along the radial aspect of the wrist from 2 cm proximal to the radial styloid distally to the ST joint. The 1st compartment is entered and the tendons as well as radial artery gently retracted. A radial styloidectomy is performed. A guidewire screw system such as the Herbert or Twin-fix system is then employed to creat a fibrous union between the scaphoid and the lunate after the cortical apposition surfaces have been gently denuded. This incision is then closed. Attention is then redirected to the dorsal flaps which are closed in a pants-over-vest fashion. The wounds are then closed over a drain and a thumb spica cast is applied for immobilization.

The four-bone tendon weave also involves a dorsal midline approach, releasing the extensor pollicis longus from its compartment. Likewise the fourth compartment is elevated off the dorsal capsule, and a longitudinal incision is made in the capsule over the scapholunate joint to provide dorsal exposure of the carpus. A second incision is made in the palm so that the tendon may be passed from dorsal to palmar. In the proximal forearm, one half of the extensor carpi radialis longus (ECRL) is harvested. Under fluoroscopic guidance, drill holes are made in the scaphoid, lunate, capitate and radius. The ECRL is passed from dorsal to palmar through the capitate, then palmar to dorsal through the lunate, dorsal to palmar through the scaphoid, and finally through the radius. The tendon is then anchored to the radius, either with a suture anchor, or with drill holes through the radius. The drill hole in the radius must be ulnar to the scaphoid drill hole so that the resultant force vector pulls the scaphoid ulnarly. The scaphoid is then sutured to the lunate or secured using a cerclage wire until healing occurs. Postoperatively the patient is casted for eight weeks, then started on gentle range of motion. Strengthening exercises begin twelve weeks after surgery.

Results

(See Table 1) Ages between the two groups of patients were comparable, as was follow-up time. The mean age in the modified Brunelli group was 30.2 years (range 19 to 44), and there were fifteen male patients. Thirteen of twenty-one were right-handed, and fourteen had their dominant hand injured. Follow up for the Brunelli group is 28.9 months, range 24 to 36 months, standard deviation 3.7, compared to 29.4 months for the four-bone tendon weave group, with a range of 23 to 39 months, standard deviation 5.5. The mean age in the four-bone tendon weave group was 29.0 years (range 24 to 40), and seventeen male patients. Fourteen of twenty-three were right handed, and fifteen had their dominant hand involved. The delay to treatment was very similar between the two groups with a mean delay of 11.7 months for the Brunelli group, (range three to 23 months, standard deviation 5.9 months) and 11.4 months for the four-bone tendon weave group (range also three to 23 months, standard deviation 5.7 months).

The scapholunate angle preoperatively and postoperatively decreased in both groups (mean 14.5 degree decrease for the Brunelli group, standard deviation 4.9 degrees, 10 degree decrease in the four-bone tendon weave group, standard deviation 3.9 degrees). Mean pain scores pre and postoperatively showed more improvement for the modified Brunelli group. Patients rated their pain from one to ten on a visual analogue scale.

Figure 2: Patient with scapholunate dissociation, preoperative radiograph AP and lateral.

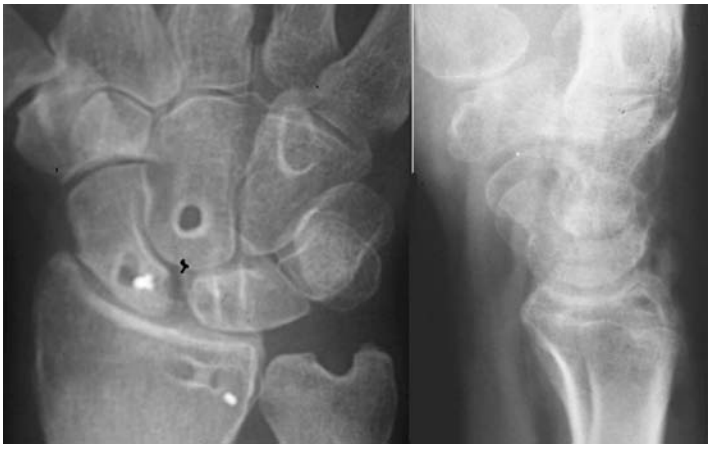

Figure 3: Postoperative radiographs of patient treated with four-bone tendon weave.

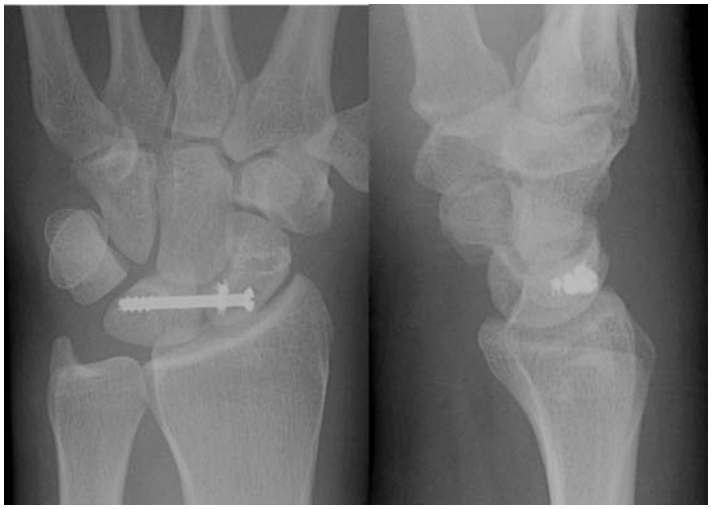

Figure 4: Postoperative radiographs of patient treated with modified Brunelli technique.

The mean difference in pain rating preoperatively and postoperatively for the Brunelli group was 4.8 points (range three to six, standard deviation one), and the mean difference in the four-bone weave was 3.2 points (range two to four, standard deviation 0.8), a 1.6 point discrepancy between the two groups of patients ($p<0.001$). The disabilities of the arm, shoulder and hand questionnaire, the DASH questionnaire, is another method of measuring self-rated upper extremity symptoms and disability. Scores are rated from zero, representing no disability, to one-hundred. Thirty different items are rated, and each item can be divided by thirty to get an average score. The difference between the mean itemized preoperative DASH and postoperative DASH were calculated. In this category, patients in the Brunelli group had an average itemized mean difference of 2.2 points versus 0.9 in the four-bone tendon weave group, with mean increase of 1.5 points, $p<0.001$).

Patients treated with the modified Brunelli technique had better range of motion overall. Postoperative range of motion as a percentage of preoperative range of motion increased more for the Brunelli group (mean 86%, standard deviation 7.2 versus 60%, standard deviation 11.6, $p<0.001$). Patients in the Brunelli group maintained more flexion than the four-bone tendon weave group (14 degrees, range negative five to 30, standard deviation 16, versus 33 degrees, range five to 65 degrees, with standard deviation of 14, $p<0.001$). Flexion postoperatively as a percentage of contralateral flexion was very similar between the two groups, with 62.8% for the Brunelli group, range 50 to 75%, standard deviation 8%, versus 62.8%, range 45 to 80%, standard deviation 9.3%, p0.99). Patients treated with the modified Brunelli technique also maintained more extension preoperatively to postoperatively, though the difference compared with contralateral extension was not significant (mean difference 6 degrees, range zero to twenty degrees, standard deviation 5.5, versus mean difference of 25 degrees, range five to forty degrees, standard deviation 11 degrees, $p<0.001$; percent of contralateral extension for the modified Brunelli group was 63.8 degrees, range 50 to 75 degrees, standard

deviation 6.7 degrees as compared with 63.9 degrees, range 55 to 80, standard deviation 7.83 degrees, p=0.96). The differences in radial deviation were not significant (for the modified Brunelli group, the difference preoperatively and postoperatively was 4.5 degrees, range 0-10, standard deviation 4.6, and percent contralateral radial deviation 20.5%, range 10 to 25, standard deviation 4.2%. For the modified four-bone tendon weave, the difference between preoperative and postoperative radial deviation was 4 degrees, range zero to 12, standard deviation 5.1 degrees, p=0.75, and percent contralateral radial deviation 20.6%, range ten to 27, standard deviation 4.6% p=0.92). Likewise, ulnar deviation differences were not significant. (For the modified Brunelli group, the preoperative to postoperative difference was 4 degrees, range zero to ten, standard deviation 4.3 degrees, percent contralateral 27.9% , range 25 to 35, standard deviation 3.4%. For the four-bone tendon weave group, the difference preoperatively to postoperatively was 4 degrees, range -5 to 12, standard deviation 4.4 degrees, p=0.95; percent contralateral ulnar deviation 27.6%, range 20 to 35, standard deviation 4.4%, p=0.82).

The Brunelli group had significantly better grip strength postoperatively. Differences in grip strength were greater in the Brunelli group (mean 2.2 kg versus 0.9 kg, increase of 1.2 kg, p<0.001), and the Brunelli group had a significantly higher grip strength post-operatively as a percentage of preoperative strength (mean 150.9%, range 100% to 211%, standard deviation 52.2%, versus mean 119.7%, range 79% to 210%, standard deviation 30.4%, p=0.02). Also, grip strength as a percentage of the contralateral side was higher in the Brunelli group (mean 97.7%, range 87.9% to 112%, standard deviation 6.4%, versus a mean of 84%, range 67.5% to 100%, standard deviation 12% for the four-bone tendon weave group, p<0.001).

Conclusions

The modified Brunelli technique and the four-bone tendon weave have comparable outcomes in terms of deformity correction and range of motion in patients undergoing scapholunate ligament reconstruction. In this study, the modified Brunelli technique has improved outcomes in pain relief, DASH scores, range of motion and grip strength.

There are many different operative treatment options for the difficult and relatively common problem of scapholunate instability. These include fusion, partial fusion, arthroscopic debridement and closed pinning of the scapholunate joint, bone-tissue-bone repairs, tenodesis or capsulodesis, scapholunate ligament reconstruction, and combinations of the above. Most hand surgeons have moved from fusion toward a more physiologic repair. There are no long-term studies establishing the ideal treatment method for any of these more physiologic methods. This study provides promising early results.

Recommended Reading

Gelberman RH, Cooney WP, Szabo RM (2001). Carpal Instability. Instructional Course Lectures, 50:123-124.

Almquist, EE, Bach AW, Sack JT, Fuhs SE, Newman DM. Four bone ligament reconstruction for treatment of chronic complete scapholunate separation. J Hand Surg [Am], 1991 Mar;16(2):322-7.

Brunelli GA, Brunelli GR (1955a) A new surgical technique for carpal instability with scapho-lunar dislocations (eleven cases). Annales de Chirugie de la Maine et du Membre Superieur, 14:207-213.

Brunelli GA, Brunelli GR (1955b). A new technique to correct carpal instability with scaphoid rotary subluxation: a preliminary report. J Hand Surg [Am], 20A:S82-S85.

Van Den Abbeele KL, Loh YC, Stanley JK, Trail IA (1998). Early results of a modified Brunelli procedure for scapholunate instability. J Hand Surg [Am],23B:258-261.

Component Position in Two-Incision Minimally Invasive Total Hip Arthroplasty Compared to Standard Total Hip Arthroplasty

Susan L. Williams, M.D., Casey Bachison, James Michelson, M.D., and Paul A. Manner, M.D., F.R.C.S.C.

Total hip arthroplasty (THA) is performed for degenerative joint disease and other arthritic conditions of the hip. There has been interest and popularization by the media of minimally invasive approaches to reduce morbidity of the procedure. There are three major categories of approaches: a standard approach, a single small incision minimally invasive approach, or a two-incision minimally invasive approach. Standard approaches utilize incisions that range from 15-30 cm, allowing direct visualization of both the proximal femur and the acetabulum. Single small incision approaches represent modifications of these, with special retractors and instrumentation to permit placement of components through incisions ranging from 6-10 cm. More recently, Mears developed a two incision minimally invasive surgery technique. In this technique, a 5 cm modified Smith-Petersen anterior incision is utilized for initial exposure and capsulotomy, femoral neck resection and removal of the femoral head, acetabular preparation and placement of the acetabular component. A second 2-3 cm posterior incision is made from inside out through the abductor/external rotator interval and is used for femoral preparation and stem placement. Lighted retractors and fluoroscopy are used as needed in conjunction with direct visualization to guide the cut of the femoral neck as well as to place acetabular and femoral components.

MIS techniques are controversial within the orthopaedic community. Detractors argue that components placed under full direct visualization are more reliably positioned that those placed "blindly" using 2 dimensional fluoroscopy through the MIS technique. Single incision MIS proponents report the ability to place components using a smaller incision and thus cause less soft tissue damage with earlier mobilization. Two incision MIS proponents argue that in addition to minimizing soft tissue damage with smaller incisions, components placed under fluoroscopic guidance are more accurately placed using immediate assessment of overall radiographic orientation in preference to relying solely on anatomic landmarks.

Early reports by the developers of the two-incision technique reported safe and rapid recovery of patients. More recent studies have been pessimistic with regard to both single incision and two incision minimally invasive surgery (MIS) approaches, reporting increased rates of complications, and no statistically significant difference of length of hospital stay, narcotic use, and rehabilitation. A single report comparing component position placed via a standard incision versus a single small incision showed no statistically significant difference. Another study compared component position of two incision MIS technique and single incision MIS, showing significant differences in component position. However, there are no studies to date comparing two incision MIS and standard THA.

Materials and Methods

Prior to collection of data, approval was obtained from the Institutional Review Board (IRB) of the Human Research Office. Between January and December 2004, 109 consecutive total hip arthroplasties were performed by a single surgeon utilizing either two incision (MIS) or a standard Hardinge surgical approach using a direct lateral incision of 10-15 cm (STHA). In that time period, 76 hip arthroplasties were placed with the two-incision MIS technique and 33 hip arthroplasties were placed with the standard technique. Satisfactory postoperative radiographs on 14 hips were not available, allowing data analysis on 95 total hip arthroplasties (67 MIS, 28 STHA). All procedures were performed with a fiber-metal backed titanium acetabular component (Trilogy, Zimmer), underreamed by 1-2 mm, a highly crosslinked polyethylene liner without an elevated rim (Longevity, Zimmer), and a titanium tapered proximally coated femoral stem (Versys, Zimmer).

Patients were selected for the MIS procedure if they had a BMI <35, Dorr index A or B femurs, adequate home support and motivation to permit rapid rehabilitation, and no other significant deformity. Accelerated rehabilitation consisted of bedside physiotherapy the morning of POD #1, with a second physiotherapy session which emphasized full weight-bearing, stair-climbing, and ambulation. Subsequent sessions were given as needed on postoperative day two. Criteria for discharge home included the ability to walk 150 feet and climb stairs unassisted, with comprehension of hip precautions and care. Patients with morbid obesity as determined by BMI >35, significant deformity, significant osteopenia, inadequate social support, motivation, or inability to comply with accelerated rehabilitation as noted above were encouraged to have a standard total hip arthroplasty. Standard rehabilitation consisted of bedside physiotherapy on postoperative day one, in-gym therapy on postoperative day two, emphasizing weightbearing and ambulation, and in-gym therapy on postoperative day three, emphasizing stair-climbing. Patients were allowed to progress as tolerated. All patients were placed on enoxaparin 30 mg SQ q12 for 14 days postoperatively, starting the morning of postoperative day one.

Radiographic measurements were taken from digitized radiographs obtained immediately post operatively or at the first post-operative clinic visit. Selected measurements included angle of inclination of the acetabular component, anteversion of the acetabular component, and femoral stem placement in the coronal plane. These measurements were performed in triplicate and averaged, using the marking elements of the

(A)

(B)

Figure 1 (A) & (B): Representative postoperative xrays; 52 yo female with no significant medical issues, with BMI of 32.

PACS system for direct determination of angulation of acetabular and femoral components. Anteversion was determined by measurement of the long and short axes of the ellipse formed by the projection of the face of the acetabular component. Statistical analysis (SPSS ver. 12.0, SPSS, Inc., Chicago, IL) was performed using the two tailed Student's t-test for the comparison of means and the ANOVA test (one way analysis of variance) for parametric data; for non-parametric data, methods included Mann-Whitney and Wilcoxon ranked sum tests. Radiographs were excluded if they were centered more than 2 cm away from the symphysis pubis, or if in-house digitized radiographs could not be obtained for insurance reasons.

Results

Patients undergoing the MIS 2-incision procedure demonstrated a mean age of 58.28 (SD 11.6) with a mean BMI of 26.2 (SD 4.06), while the patients undergoing standard total hip arthroplasty showed a mean age of 63.21 (SD 17.3) and a mean BMI of 28.9 (SD 6.39). Although mean age tended to be higher in the standard group, this was not significantly different (p=0.176); however, BMI was significantly higher in the standard group by approximately 2.5 kg/m2 (p = 0.041).

Acetabular inclination was acceptable in both groups, with mean values of 42.2º (SD=5.64, CI=40.8º – 43.5º) for two incision MIS and 38.7º (SD=5.44, CI=36.6º- 40.8º) for standard THA. This difference was statistically significant (p value <0.05); however, the difference of 3.5º was not clinically significant and both values are within the acceptable range of 35º-45º. In the MIS group, there were 4/67 (6%) outliers with acetabular inclination <30º or >50º and in the standard group there was 1/28 (4%) outlier, however, this was not statistically significant using the Fisher exact test (p value=0.67).

The mean acetabular anteversion was also acceptable in both groups, with values of 16.5º (SD = 5.78, 95% CI = 15.1 – 17.9º) for the two-incision MIS group, and 15.5º (SD = 5.51, 95% CI = 13.4 – 17.7º) for the standard THA group. The difference was not statistically significant. Outliers with unacceptable version were defined by version of <10 degrees or >25 degrees; 6/67 (10%) of the MIS group fell into this category, compared to 2/28 (10%) of the STHA group. No statistical difference was noted.

All femoral components were placed in less than 5º angulation in the femoral shaft with an overall average of 0.007º (SD = 1.31, 95% CI = 0.327º varus – 0.312º valgus) varus in the MIS group, and 0.411º varus (SD = 1.64, 95% CI = 1.047º varus – 0.226º valgus) in the standard groups. This difference is also not statistically significant. In the MIS group, 17 stems were placed in any amount of valgus, 21 stems in any amount of varus, and 29 stems in neutral. When acceptable

placement was defined as up to one degree of angulation in either direction, 44 stems were placed in neutral, 11 were in varus, and 12 were in valgus. In the standard group, 6 stems were placed in any amount of valgus, 15 stems in any amount of varus, and 7 stems in neutral. When acceptable angulation was similarly defined, 14 stems were neutral, 4 were in valgus, and 10 were in varus. Although the MIS group appeared to demonstrate a higher degree of accuracy in femoral stem placement, the difference was not statistically significant (p=0.072).

Discussion

Our results show that acetabular component positioning using the two-incision minimally invasive approach is at least equivalent to the standard direct lateral approach in the hands of the same surgeon after significant experience with both techniques. In addition, femoral component placement may be superior in the MIS group with respect to femoral angulation in the coronal plane. In essence, fluoroscopic guidance is equivalent to direct visualization when placing components. This study does not, nor was it designed to settle the overarching debate regarding the benefits of the two-incision minimally invasive approach versus a standard approach for total hip arthroplasty. However it does contribute one important piece of information: component positioning is not compromised by either approach and can be achieved in a reliable and reproducible fashion.

Recommended Reading

Berger RA, Duwelius PJ. The two-incision minimally invasive total hip arthroplasty: technique and results. Orthop Clin North Am. 2004 Apr; 35(2):163-72.

Berry DJ, Berger RA, Callaghan JJ, Dorr LD, Duwelius PJ, Hartzband MA, Liberman JR, and Mears DC. Symposium: Minimally Invasive Total Hip Arthroplasty- Development, Early results, and a Critical analysis. JBJS Am. 2003 Nov; 85A(11): 2235-2246.

Tanzer M. Two-incision Total Hip Arthroplasty: Techniques and Pitfalls. Clin Orthop Relat Res. 2005 Dec;441:71-9.

Pagnano MW, Leone J, Lewallen DG, Hanssen AD. Two-incision THA had modest outcomes and some substantial complications. Clin Orthop Relat Res. 2005 Dec;441:86-90.

Bal BS, Haltom D, Aleto T, Barrett M. Early complications of primary total hip replacement performed with a two incision minimally invasive technique. JBJS Am. 2005 Nov;87(11):2432-8.

de Beer J, Petruccelli D, Zalzal P, Winemaker MJ. Single-incision, minimally invasive total hip arthroplasty: length doesn't matter. J Arthroplasty. 2004 Dec;19(8):945-50.

Surgical Approach and Fixation of Unicondylar Medial Hoffa Fractures: A Technical Paper

Darius G. Viskontas, M.D., F.R.C.S.C., David Barei, M.D., F.R.C.S.C., Lisa A. Taitsman, M.D., Robert Dunbar, M.D., and Sean E. Nork, M.D.

A posterior femoral condylar fracture in the coronal plane is commonly referred to as a "Hoffa Fracture". While the approach and fixation methods of lateral Hoffa injuries have been well described, medial coronal fractures occur rarely and the optimal surgical approach has not been adequately described. The purpose of this paper is to describe the surgical approach and fixation methods in a case series of patients treated for displaced medial coronal fractures.

Surgical Technique

A number of surgical approaches are available for identifying, reducing, and stabilizing medial condylar fractures including posterior approaches, direct medial approaches, anterior approaches, and combinations thereof. However, because of the locations of the important medial soft tissue structures, visualization and/or fixation may be compromised with non-extensile exposures. By using an extensile medial subvastus exposure combined with knee flexion, the articular reduction and fixation can be optimized in these complex injuries.

Figure 1: Anteroposterior x-ray of the right knee with medial Hoffa fracture, lateral ligament injury and proximal fibula fracture.

The patient is placed supine on a radiolucent table; a tourniquet is placed around the ipsilateral thigh and inflated; and the knee is flexed over a knee holder or small cushioned bump. A medial subvastus approach is used through an extensile longitudinal anterior skin incision. A full thickness medial skin flap is created, allowing exposure and retraction of the vastus medialis muscle belly. The sartorius, gracilis and semitendinosis tendons are retracted posteriorly and a longitudinal capsulotomy is made just anterior to the MCL. The meniscus is inspected for injury and any loose osteochondral fragments in the knee joint are removed. Lateral retraction of the patella allows visualization of the medial femoral articular surface. The fractured fragment(s) can be mobilized and cleaned of fracture hematoma. For fractures that exit more posteriorly, increasing knee flexion (up to 120 degrees) allows increasing visualization. In the rare circumstance where a posterior condylar fracture exists (that is, a posterior capsular avulsion fracture), an additional arthrotomy posterior to the medial collateral ligament can be performed.

Reduction can be optimized with knee valgus which can be obtained manually or with a medial femoral distractor. The primary reduction read is at the articular surface since the medial collateral ligament and medial soft tissues tend to hide the remaining non-articular visual reduction reads. Reduction and compression are primarily obtained with a pointed reduction clamp placed from anterior to posterior. Temporary fixation of any intercalary osteochondral fragments, as well as the major condylar fragment can be obtained with Kirschner wires. The reduction can be confirmed with biplanar fluoroscopic imaging. Fixation is primarily obtained with multiple lag screws placed from anterior to posterior and/or from posterior to anterior. Countersinking is necessary for implants placed through the articular surface. Additional fixation can be obtained with small- or mini-fragment plates. If the plate is placed directly medial, it should be contoured approximately 25 degrees in the coronal plane to match the medial contour of the distal femur.

The capsule and retinaculum are closed with absorbable sutures. The sartorial fascia is allowed to resume its normal position and is sutured to the medial patellar retinaculum with absorbable sutures. Post-operatively, patients are restricted to non-weight bearing for 12 weeks. Full passive motion in a CPM and active assisted exercises are instituted immediately.

Case Series

The orthopaedic trauma database was used to identify patients over a 7 year period (January 2000 to December 2006) treated at Harborview Medical Center with a medial Hoffa fracture of the distal femur (OTA 33B3.2). Patients with associated supracondylar-intercondylar fractures or sagittal medial condylar fractures were excluded. Five patients were identified with an average age of 29 years (range was 15 to 38 years). The mechanism of injury was a motor

Figure 2: Lateral x-ray of the right knee with medial Hoffa fracture, lateral ligament injury and proximal fibula fracture.

Figure 3: Reconstructed sagittal CT image of the right knee with a medial Hoffa fracture.

vehicle collision in four and a soccer injury in one. One fracture was open. Four patients were polytraumatized with associated orthopaedic, chest, abdominal and head injuries. One patient had associated posterolateral and lateral collateral ligament injuries to the same knee (Figures 1 - 3). All patients were treated operatively with an average time to fixation of 1.2 days (range 0 to 4 days). In all cases, a medial subvastus deep surgical dissection was used for exposure and reduction. The skin incision was altered based on any associated soft tissue trauma and/or wounds.

Figure 4: Post-operative anteroposterior x-ray of the right knee with fixation of the medial Hoffa fracture and lateral ligament repair.

A midline anterior longitudinal skin incision was used in three patients. In the one patient with an open fracture, the medial traumatic wound was incorporated into the medial surgical approach. In the remaining patient, the incision was placed medially to allow incorporation of an extra-articular knee laceration. The fractures were reduced and fixed as discussed in the surgical technique and the most appropriate hardware for the fracture was used (Figures 4 and 5).

The surgical approach allowed an accurate intraoperative assessment of the reduction and allowed fixation in multiple planes. There were no intraoperative or postoperative complications. One patient underwent a planned hardware removal 6 months after the original fixation in order to remove multiple countersunk screws used to stabilize small osteochondral fractures in the weighbearing potion of the distal femoral condyle.

Discussion

The Hoffa fracture was originally described by Hoffa in 1904 and is a coronal fracture of the posterior femoral condyle. The postulated mechanism is a high energy blunt force applied to the flexed knee, producing a shearing force on the posterior condyles. The lateral condyle is more commonly affected than the medial condyle and bicondylar injuries are rare. Associated injuries are common and occur in the ipsilateral knee, lower extremity and more distant locations.

The radiographic diagnosis can be difficult and cross sectional CT imaging with sagittal reformats is becoming the gold standard for any intra-articular fracture of the distal femur. Non-operative management often leads to displacement and malunion of the fragment with poor results. Detailed pre-operative planning helps to determine the type of hardware required, its optimal position and screw trajectory needed for stable fixation.

The skin incision in this small series of patients varied depending on associated knee lacerations and one medial wound from an open medial Hoffa fracture. None of the locations of the skin incisions were detrimental to the deep approach or fixation of the fractured fragment. Ideally, an anterior midline longitudinal incision should be used to facilitate potential

Figure 5: Post-operative lateral x-ray of the right knee with fixation of the medial Hoffa fracture and lateral ligament repair.

future surgical procedures. Fixation techniques should complement the fracture characteristics. In this series the screw sizes varied but were predominately 2.4 mm, 2.7 mm and 3.5 mm cortical screws. Different plates can also be used in a neutralization or posterior antiglide fashion. Mini-fragment reconstruction plates are useful and are available on mandibular plating sets.

Limitations of this study include the small number of patients, lack of prospective clinical and radiographic follow-up and a short time interval to judge outcomes. The patients treated at this center often live long distances away and it is difficult to have them return for follow-up assessments. Although conclusions regarding the long term outcomes of these injuries cannot be drawn, the short term outcome of these high-energy intra-articular injuries using this surgical approach is favorable.

Recommended Reading

Hak DJ, Nguyen J, Curtiss S, Hazelwood S: Coronal fractures of the distal femoral condyle: a biomechanical evaluation of four internal fixation constructs. Injury 36:1103-1106, 2005.

Holmes SM, Bomback D, Baumgaertner MR: Coronal fractures of the femoral condyle: a brief report of five cases. J.Orthop.Trauma 18:316-319, 2004.

Isolated Locked Plating of Periprosthetic Femoral Fractures Associated with Stable Hip Arthroplasties

Ginger Bryant, M.D., David Barei, M.D., F.R.C.S.C., Lisa A. Taitsman, M.D., Daphne Beingessner, M.D., F.R.C.S.C., Sean E. Nork, M.D., and M. Bradford Henley, M.D., M.B.A.

The number of hip arthroplasties and associated ipsilateral periprosthetic femoral fractures is anticipated to rise as the average age, life-expectancy, and activity level, of the population increases. The optimal method of fixation for Vancouver B-1 (fractures below a well-fixed proximal femoral prosthesis) fractures continues to be controversial due to the proximity of the fracture to the tip of the stem. A number of surgical techniques have been recommended including allograft struts, cerclage cables and wires, and combinations thereof. The recommended treatment for Vancouver C (femoral fractures above a total knee arthroplasty) periprosthetic fractures has been fixation using conventional plating techniques. However, fixation strength of conventional implants may be limited in this patient population due to age-related osteopenia. Fixed-angle fixation using a long lateral locked-plate that spans the majority of the femur appears to be mechanically advantageous for patients with Vancouver B-1 and C periprosthetic fractures. A locked plate-screw construct offers improved stability in the setting of osteoporotic bone and a long plate affords protection of the osteopenic bone from future peri-implant fracture. While the use of allograft struts, and cerclage cables and wires requires extension of the soft tissue dissection onto the anterior cortex of the femur, a lateral locked-plate minimizes soft-tissue dissection and may promote fracture union by maintaining osseous viability.

The purpose of this study is to report the results of periprosthetic femoral fractures adjacent or distal to a stable femoral stem (Vancouver B-1 and C fractures) using a locked-plate as the sole method of fracture stabilization. We hypothesized that this method of fixation results in clinically sufficient stability to achieve fracture union while maintaining alignment.

Materials and Methods

Initial radiographic and chart review identified twenty-six consecutive patients. Five patients were excluded from the study due to the use of allograft struts, cerclage cables, or wires, in addition to plate fixation. These five patients had similar fracture patterns and were treated differently at the preference of the attending surgeon. One patient was excluded secondary to fixation with a non-locking plate. These alternative methods of fixation were used based on surgeon preference and were early in the collection period, during the time of transition from conventional plating techniques to locked plating systems.

Clinical data were reviewed to identify patient age, gender, injury mechanism, and pre-injury ambulatory ability. Radiographs were analyzed by a fellowship-trained orthopaedic traumatologist, not involved with the care of the patients to assess each plate-screw construct and to determine the quality of fracture reduction. Clinical union was defined as painless unrestricted weight-bearing.

Figure 1: Pre-operative radiographs of an acute Vancouver C periprosthetic femoral fracture (AO/OTA 32-C1) that a 69 year-old male sustained in a fall from 3 feet.

Figure 2: Post-operative radiographs at four weeks. An 18-hole locking condylar plate spans a majority of the femur and includes screw fixation into the lesser trochanter. A combination of locking and non-locking screws was used in the area of the femoral stem.

Radiographic union was defined by evidence of bridging callus at two or more cortices on standard anterior-posterior (AP) and lateral radiographs. Adequate post-operative follow-up was defined as a minimum of twelve weeks.

The study group included twenty patients with an average age of 75.4 years old (range 45 – 95 years). Four patients (20%) also had an ipsilateral total knee replacement leaving them with an inter-prosthetic femoral fracture. There were thirteen (65%) Vancouver B-1 and seven (35%) Vancouver C periprosthetic fractures. Three patients were referred to our outpatient clinic for treatment of a periprosthetic femoral fracture non-union.

Results

A direct lateral surgical approach was used and soft tissue dissection was limited to the lateral aspect of the femur. Direct reduction and plating techniques were used in sixteen patients (80%), nine of which were also stabilized with interfragmentary lag screws. Four patients were stabilized with bridge-plating technique, chosen due to their comminuted fracture pattern. Fracture fixation consisted of a lateral locked-plate that spanned the majority if not the entire femur. Fifteen condylar plates ended at or proximal to the lesser trochanter and two condylar plates ended within two centimeters distal to the lesser trochanter. Plates were positioned to allow proximal fixation posterior to the prosthesis and into the lesser trochanter. Anatomical reduction was obtained in all patients who received direct reduction and plating technique, and normal femoral alignment was obtained in those patients in which bridge-plating technique was used (Figures 1, 2, 3).

Fifteen patients (75%) had follow-up beyond twelve weeks. Fourteen had satisfied both clinical and radiographic definitions of fracture union at that time. One patient, at seventeen weeks follow-up, had progressed to unrestricted weight-bearing and was asymptomatic clinically, with limited evidence of radiographic union. The surgeon was satisfied with the clinical and radiographic findings and recommended no further surgical treatment. For analysis purposes, this fracture was determined to have achieved union at seventeen weeks based on clinical exam. For the fifteen patients included in our analysis, average follow-up was 34.5 weeks (range 12-93 weeks). At the time of fracture union, no patient had any change in their fracture alignment or hardware position.

Two patients (13.3%) had complications related to their fracture fixation. One patient (6.6%) developed both a seroma and an ileus, both of which resolved spontaneously. One patient (6.6%) developed arthrofibrosis of the ipsilateral knee (range of motion 5º-95º) and subsequently underwent quadricepsplasty and removal of hardware one year after fracture union. The patient regained functional range of motion (0º-125º) of his knee and had no further complications.

Six patients (40.0%) had post-operative complications unrelated to their fracture fixation. Two patients (13.3%) developed a deep venous thrombosis and one patient (6.6%) developed a pulmonary embolism while on prophylactic anti-coagulation therapy. There was one wound infection (6.6%). This occurred in the patient with a Type IIIA open femoral fracture and an associated open degloving injury below the knee. The infection was successfully treated with intravenous antibiotics.

Discussion

Treatment for periprosthetic femoral fractures is determined by fracture location, implant stability, quality of bone stock, and patient demographics. When fractures are adjacent to a stable femoral stem (Vancouver B-1 and C fractures), the femoral stem is typically retained and the fracture is treated with open reduction and internal fixation. Various surgical treatment options have been described for Vancouver B-1 fractures, many requiring extensive

Figure 3: Radiographs at sixteen months demonstrating maintenance of fracture alignment and hardware viability.

soft-tissue dissection to allow for the use of allograft struts, cerclage cables, and wires. Extensive femoral exposure may disrupt blood supply to the fracture area, and the allograft struts, while initially strong, become weaker at four to six months into the incorporation process. If fracture union is delayed beyond this time, the integrity of the allograft struts may be compromised prior to fracture union. Cable-plate fixation has also been a commonly utilized surgical technique. Ricci et al. reported successful outcomes for Vancouver B-1 periprosthetic fractures treated by indirect fracture reduction and fixation using a cable plate without allograft. Current treatment recommendations for Vancouver C periprosthetic fractures involve standard conventional plating techniques. The fracture is distal to the femoral stem, which allows the use of standard screws instead of cables or wires for plate stabilization. The osteopenia that is often seen in the hip arthroplasty patient, however, may not afford adequate screw-bone interface strength and may lead to construct failure. Future peri-implant fracture may also occur secondary to the osteopenia often seen in this patient population.

This present study supports the idea that minimal soft tissue dissection promotes fracture union. Even though a long lateral incision may be required for some patients, the underlying muscle and periosteal elevation was minimized. Whether fracture reduction was obtained directly or indirectly, by lag screw-neutralization plate technique or by bridge-plating, surgical dissection was limited to only the amount needed for fracture reduction and plate placement along the lateral femoral cortex. In this series, locked-plates maintained fracture alignment beyond the time to fracture union. The locked plate-screw construct provided enough strength to maintain plate position in the area of the femoral stem, negating the need for additional stability from cerclage cables or wires. This sole method of stabilization appears to sufficiently neutralize flexion-extension, varus-valgus, and torsional forces. The use of a long plate that spans a majority of the femur provides additional strength along the femur and helps decrease the risk of future peri-implant fracture that may occur secondary to the osteopenia often seen in this patient population.

In conclusion, periprosthetic femoral fractures adjacent or distal to a stable hip arthroplasty can be a treatment dilemma for orthopaedic surgeons. Open reduction internal fixation of Vancouver B-1 and C fractures using a lateral locked-plate that spans a majority of the femur is a successful treatment method that minimizes soft-tissue dissection and provides adequate fixation strength to maintain fracture alignment throughout fracture union.

Recommended Reading

Brady, OH; Garbuz, DS; Masri, BA et al.: The reliability and validity of the Vancouver classification of femoral fractures after hip replacement. J Arthroplasty, 15(1): 59-62, 2000.

Haddad, FS; Duncan, CP; Berry, DJ et al.: Periprosthetic femoral fractures around well-fixed implants: use of cortical onlay allografts with or without a plate. J Bone Joint Surg Am, 84-A(6): 945-50, 2002.

Lewallen, DG; and Berry, DJ: Periprosthetic fracture of the femur after total hip arthroplasty: treatment and results to date. Instr Course Lect, 47: 243-9, 1998.

Ricci, WM; Bolhofner, BR; Loftus, T et al.: Indirect reduction and plate fixation, without grafting, for periprosthetic femoral shaft fractures about a stable intramedullary implant. J Bone Joint Surg Am, 87(10): 2240-5, 2005.

Injuries in Youth vs. College Women's Soccer

John W. O'Kane, M.D. and Melissa A. Schiff, M.D., M.P.H.

Soccer is the most popular sport worldwide. Although a generation ago, soccer took a back seat to football, baseball, and basketball in the US, participation especially by youths has exploded in the past 20 years. In 2005, the Soccer Industry Council of America estimated that 17.7 million youth under age 18 participated in soccer. Soccer's popularity is due in part to the perception that it is a relatively safe sport for children and adolescents. Several recent studies though, have found that soccer is one of the more common sports resulting in injury among youth aged 10-19 years. Soccer participation has also increased disproportionally for girls, driven by cultural changes valuing female participation in sports and also by Title IX which has increased the availability of college scholarships for female athletes.

Despite large numbers of youth participants, there is little research evaluating the rate of injury and potential risk factors for injury in young female soccer players. Researchers at the University of Washington are attempting to answer some of these questions with an NIH funded pilot study of female soccer player ages 12-14 participating in premier and recreational soccer in the Seattle area. This report outlines preliminary findings from the pilot study and compares injuries sustained by the youth players to data from the NCAA Injury Surveillance System (ISS) regarding injuries in female collegiate players.

Results

In the pilot study, four high level (premier/select) teams and four recreational level teams with a total of 92 female players were followed from the start of the 2006 soccer season for any soccer injuries. Premier/select soccer is a program for the best soccer players in the age group. As they play year round and attend regional and national tournaments, their data were collected from spring 2006 through the end of 2006. Recreational teams are not selected (no "try-out") and play for 10 weeks in the fall season. The college data represent injuries sustained by NCAA female teams that participated in injury reporting for the 2004-5 season. Of the 915 teams that play NCAA soccer, 73 (8%) teams reported data.

The injury rates reflect the number of soccer injuries per 1000 hours of soccer exposure hours, either in practice or games. For the youth players, the soccer playing time is collected by the parents and reported to the study coordinator. For the college athletes, the time is reported by the certified athletic trainers (ATC) that report the data. The injuries for the youth players and the college players are evaluated and recorded by ATCs More significant injuries in the youth group are evaluated and reported by Dr. O'Kane. Additional data collected for the youth players included strength and jump biomechanical measurements evaluated at the beginning of the season, field conditions, other sports participation, psychological factors, and coaching factors . These variables will be assessed as potential risk factors for injury as this study moves to a larger scale.

Table 1 reports the game injury rates for the college, premier, and recreational players respectively. Also reported, are the percentage of injuries that occur in games as opposed to practices. Table 2 reports the percentage of injuries occurring to the most commonly injured body regions comparing college game, college practice, and the combined high level and recreational youth teams for games and practices (few youth injuries were sustained in practice). A total of 48 injuries were reported in the youth soccer players. For the college players, 421 game injuries and 468 practice injuries were reported. Comparing all NCAA sports for women, women's soccer had the highest game injury rate at 16.1 per 1000 athletic hours followed by gymnastics at 14 per 1000 athletic hours.

Discussion

Although these are preliminary pilot data in an ongoing study, a number of interesting findings emerge. Despite a perception that soccer is a safe sport, it has the highest game injury rate among NCAA women's sports. Female youth soccer players also have a high rate of injury. While injury rates for practice and games are roughly equivalent in college, 80% of the youth injuries occur in games. Although the reason for these differences is not known, it may be that the college players may compete more aggressively in practice compared to games, resulting in more injuries. Alternatively, youth players may have more lax officiating or coaching which may result in excessively rough or "foul play" in game situations. The youth players also may not have the

Player	Game injury rate (injuries /1000 athlete exposures)	% injuries in game vs. practice
College	16.1	47%
Premier	11.4	80%
Recreational	17.3	86%

Table 1: Game injury rate and proportion of injuries in games compared to Practices among female soccer players.

Player	Ankle	Knee	Thigh	Hip	Foot	Lower leg	Concussion
College game	18	22	6	5	5	8	14
College practice	16	18	17	10	8	9	4
Youth	12	10	6	4	4	7	2

Table 2: Proportion of total injuries by body region among female soccer players.

athletic ability to protect themselves. It certainly appears that game play should be the focus if the desire is to decrease injuries in youth soccer.

The type of injuries also reveals interesting comparisons. Although much is made of the epidemic of knee injuries in female athletes, particularly ACL tears which are much more prevalent in female than male soccer players, knee injuries are only 20% of the total injuries in college and 10% of injuries in the youth players. It is interesting that by college the knee injury rate doubles. There is evidence that the biomechanics that place women at higher risk for knee injury develop after maturation, possibly accounting for the difference observed in this study. For the youth players, the combination of ankle and lower leg injuries is double that of knee injuries, and we are attempting to identify risk factors for these injuries in ongoing research.

Another impressive difference in types of injuries is the proportion of concussions. Literature in European professional male soccer players had raised a concern that soccer, possibly through heading the ball, may result in concussion and long term deterioration of cognitive function. Subsequent research using both men and women NCAA soccer players suggests heading the ball does not result in concussions or cognitive decline. Concussions occur most frequently secondary to contact with the ground and other players and from these data, concussions are more common in college. This may be secondary to more aggressive play or more aggressive heading resulting in more head to head contact. Sport related concussion in pre-adolescents is less studied and considered cause for greater concern than concussion in adults because of problems related to second impact syndrome (brain swelling and death with a second head injury following concussion). It is encouraging to note that in these preliminary data, concussion does not seem to be as prevalent in the youth players.

In conclusion, this pilot study has provided some intriguing information regarding youth soccer and interesting comparisons to the women's college game. We are currently working on obtaining funding to continue this project on a larger scale over a number of years to obtain sufficient information to evaluate which factors significantly contribute to injuries in the youth players. The ultimate goal is to develop effective strategies to prevent soccer injuries among youth players.

Recommended Reading

NCAA injury surveillance system database at www1.ncaa.org/membership/ed_outreach/health-safety/iss/index.html.

Emery,C.A.; Meeuwisse,W.H.; Hartmann,S.E. Evaluation of risk factors for injury in adolescent soccer: implementation and validation of an injury surveillance system. AJSM 2005, 33(12): 1882-91.

Junge,A.; Chomiak,J.; Dvorak,J. Incidence of football injuries in youth players. Comparison of players from two European regions. AJSM 2000, 28(5 Suppl): S47-50.

Radiographic Quantification and Analysis of Dysmorphic Upper Sacral Osseous Anatomy and Iliosacral Screw Insertions

Joseph M. Conflitti, M.D., Matt L. Graves, M.D., and M.L. Chip Routt, Jr., M.D.

Iliosacral screw placement has become a common technique for fixation of unstable posterior pelvic ring injuries. Despite its widespread acceptance and use, errors in screw placement are still occurring and are due to a variety of causes. Few studies report screw placement errors such as screw intrusion of the sacral spinal canal, sacral neural tunnels, or alar cortical limits. In almost all iliosacral screw series, postoperative computed tomography scans are not used to assess screw placement accuracy and errors. In one series that did, the screw placement error rate was four percent. Some iliosacral screw errors are simply due to the variability of posterior pelvic ring osseous anatomy, and its unique radiographic differences. The posterior pelvic bony variability includes upper sacral segment dysmorphism. Iliosacral screw misplacements are likely to occur more commonly when upper sacral segment abnormalities are present because the sacral osseous pathways available for safe screw insertions are seemingly smaller and also more difficult to image reliably in the operating room. Sacral dysmorphism is not uncommon, occurring in thirty to forty percent of adult patients. As a result of the dysmorphic osseous anatomy and associated imaging problems, second sacral segment iliosacral screws have been suggested but no details of osseous pathway limits have been defined.

Materials and Methods

We evaluated 24 consecutive patients with sacral dysmorphism and unstable pelvic ring injuries who were treated using second sacral segment iliosacral screws as a component of their overall fixation construct. The second sacral segment was selected for screw insertion because the dysmorphic upper sacral segment was of insufficient size for safe screw insertion, or the posterior pelvic instability pattern mandated supplementary fixation. There were seventeen male and seven female adult patients with an average age of 41 years (range, 19-74 years), and all were injured in high energy accidents. The mean Injury Severity Score was 22 (range, 5-57). All 24 patients were resuscitated and underwent physical examinations including detailed peripheral neurological assessments, and then imaged using pelvic anteroposterior, inlet, and outlet plain radiographs and a standardized two-dimensional pelvic computed tomography (CT) scan. The upper sacral symmetrical dysmorphism was noted for each patient on the outlet pelvic plain film and further detailed on the pelvic CT scan images. The unstable pelvic ring injuries were classified according to the Orthopaedic Trauma Association scheme.

The pelvic CT scan included the entire pelvis from iliac crest through ischial tubersosities, and was standardized for each patient with 2.5mm sequential axial images. A PACS workstation using Centricity version 2.1 (GE Medical Systems, Waukeshau, WI.) served to analyze the pelvic CT scans with a routine bone algorithm. On the PACS, each axial image of the upper two sacral segments was measured with the electronic measuring tool after controlled magnification to improve distance accuracy for a zoom factor of 2.3. The distances between the anterior cortical sacral limit and the upper two sacral nerve root tunnels were measured to the nearest tenth of a millimeter and documented for the two sequential greatest distances per sacral segment. These two measurements for each level were recorded and averaged.

We used a standard technique of S2 screw insertion for each patient. The pelvic reductions were achieved using both closed and open techniques. After reduction of the posterior pelvic ring disruption, fluoroscopic imaging using pelvic inlet, outlet, and lateral sacral views guided S2 screw insertions according to the preoperative plan for location, orientation, and length.

All patients had postoperative routine pelvic plain radiographs and two-dimensional CT scans for evaluation of reduction quality and implant safety. From these postoperative CT scans, the S2 iliosacral screws were graded as intraosseous (completely contained within bone), juxtaforaminal (adjacent to, but not within, the sacral neural tunnel), or extruded (any portion of the implant within the sacral nerve root tunnel or beyond any cortical limits). Reductions were assessed as accurate (maximal residual displacement of 3mm or less) or inaccurate. Maximum possible screw lengths were also measured for the upper and second sacral segments as markers for balanced internal fixation. After surgery, the neurological examinations were documented and compared to the preoperative examinations.

Results

The upper sacral dysmorphic segment safe zone averaged 13.2 mm (range, 7.2 mm to 17.2 mm). The second sacral segment safe zone averaged 15.2 mm (range, 11.3 mm to 17.7 mm). The second sacral segment safe zone was larger than that for S1 in twenty of the twenty-four patients (80%). The difference was statistically significant ($p<.0005$) as determined by a paired t-test.

The maximum possible screw length in the upper sacral segment averaged 100.8 mm (range, 87.1 mm to 114.4 mm), while the maximum possible screw length in the second sacral segment averaged 151.9 mm (range, 120.7 mm to 178.4 mm). This difference was also statistically significant ($p<.0001$) as determined by a paired t-test.

The screw lengths and sacral alar widths were not the only differences between the two dysmorphic upper sacral screw potential pathways. The S1 safe screw pathway was obliquely oriented relative to the sagittal axis of the sacrum and therefore length limited by the anterior sacral body. The S2 screw pathway was perpendicular to the sagittal axis and consequently the S2 screws could traverse from one

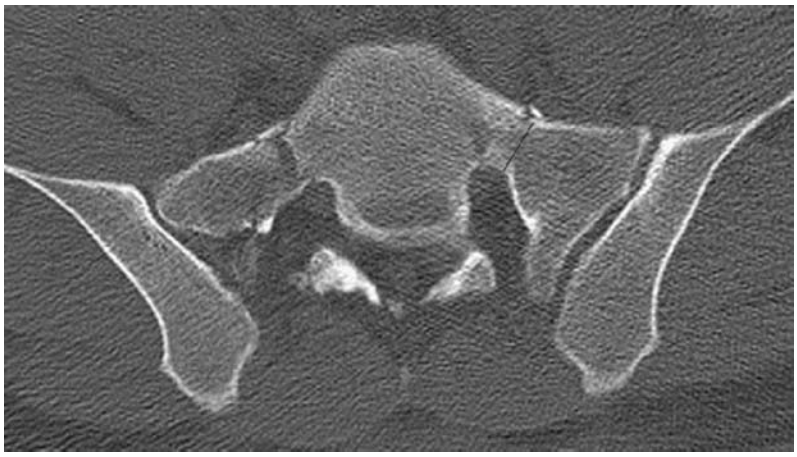

Figure 1A: This pelvic CT axial image allows the surgeon to quantify the narrowest alar zone for S1 iliosacral screw insertion as well as the oblique pathway and length for the upper sacral dysmorphic segment.

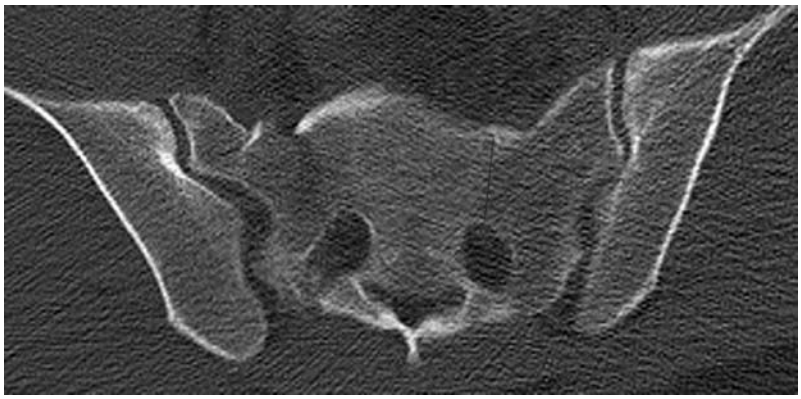

Figure 1B: This similar image at the second sacral dysmorphic segment reveals an increased alar width, the perpendicular orientation, and the greater length for S2 screw insertion.

posterior ilium to the contralateral posterior ilium.

Based on our screw location scale, twenty of the twenty-four patients (83%) had intraosseous S2 screws. The remaining four patients (17%) had juxtaforaminal locations, and there were no extruded screws. There was no correlation between the site of posterior pelvic injury and screw locations. All posterior pelvic reductions were accurate so that malreductions were not responsible for the juxtaforaminal screws locations. After surgery, there were no neurological changes related to S2 iliosacral screw placement. It is impossible to compare these results to other studies because S2 screw accuracy in patients with dysmorphic upper sacral segments has not been previously studied.

Discussion

Unstable pelvic ring disruptions are difficult to treat successfully for numerous reasons. Iliosacral screw fixation after accurate reduction has become a popular treatment method for unstable posterior pelvic injuries. Unfortunately, safe iliosacral screw insertion depends on consistent posterior pelvic osseous anatomy and its radiographic correlation. When the upper sacral anatomy and its resultant fluoroscopic markers are altered, reliably safe iliosacral screw insertion is compromised.

Sacral dysmorphism is an anatomical variant occurring in 30-40% of adult patients. The dysmorphic sacral upper segment is associated with alar osseous pathways that are narrowed and obliquely oriented, but these pathways for potential iliosacral screw insertion have not been well defined or quantified. Their altered alar anatomy complicates pelvic fracture management because imaging the dysmorphic upper sacral segment is more difficult intra-operatively. For these reasons, iliosacral screw use has been discouraged in patients with upper sacral dysmorphism and alternative fixation techniques have been advocated.

Based on our dysmorphic patients' pelvic plain radiographs and CT scans, symmetrical upper sacral dysmorphism was identified and quantified. In these patients, the upper sacral pathways for potential iliosacral screw insertion were greater in diameter at the second sacral segment when compared to the upper segment. This narrowing of the upper dysmorphic segment alar zone is important to be aware of. Once noted, the surgeon can either avoid it, or learn the radiographic markers for the upper sacral dysmorphic segment in order to insert safely contained intraosseus iliosacral screws. This alone should eradicate iatrogenic injuries due to wayward screw locations.

The upper S1 anatomical obliquity was in contrast to the perpendicular anatomy of the second sacral segment. The oblique upper sacral configuration limited potential iliosacral screw length and mandated a more posterior and caudally located lateral iliac cortical starting point for the upper sacral planned screw. The upper sacral oblique anatomy confines the iliosacral screw to within the vertebral body's anterior cortical limit. The second sacral potential screw pathway allows screw placement into the contralateral lateral iliac cortical bone if necessary. The length measurements obtained in our patients support this fact in that the second sacral screw lengths were significantly longer than those for the upper sacral segment. Screw length is especially important for patients with sacral fractures since short screw lengths may provide insufficient fixation strength when compared to longer and balanced screws. Based on our measurements and S2 screw insertions, the screws can be extended to the contralateral ilium when indicated. Extending the S2 screw between the posterior ilia does mean that the screw must pass safely through both alar zones. Our measurements were statistically significant between the upper and second sacral segments when considering both alar width available and total length for potential screw insertion.

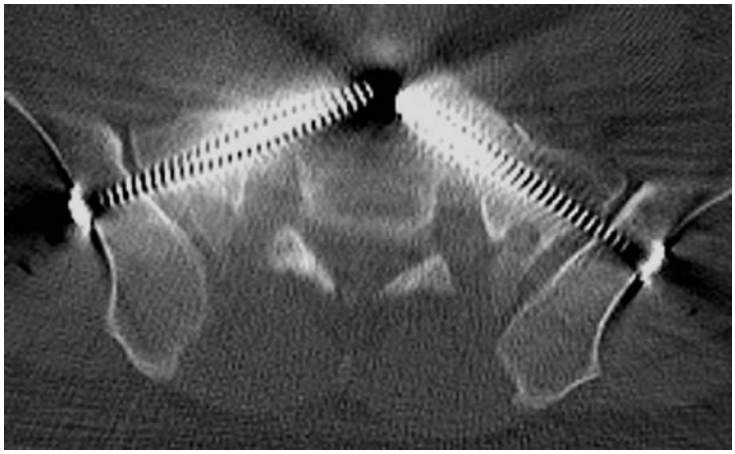

Figure 2A: The postoperative pelvic CT axial image at the dysmorphic upper sacral segment demonstrates the oblique, narrow, and shorter screw pathways bilaterally.

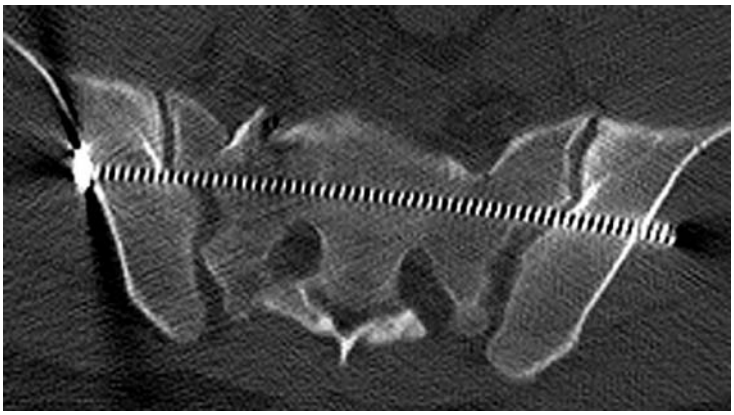

Figure 2B: This axial CT image of the second sacral segment reveals the horizontal screw orientation, as well as the longer screw length, and increased alar width for safe screw insertion.

Four patients had juxtaforaminal screw locations, all being adjacent to the second sacral nerve root tunnel but not violating its cortical integrity. There was no correlation with reduction quality or screw diameter for these four screws, each was simply located slightly caudal and posterior within the S2 osseous pathway.

In a recent publication regarding second sacral screw fixation of unstable posterior pelvic ring injuries and normal sacral osseous anatomy, Moed et al noted fixation failures and radiographic implant changes in patients with osteopenia. They used S2 screws that did not extend beyond the sacral osseous body. In our patients, we used S2 screw orientations that progressed from the lateral ilium on the unstable and injured side, crossed the ipsilateral SI joint, progressed through the sacral body and contralateral ala, and exited the contralateral iliac cortical bone. Perhaps such longer screws that obtain contralateral iliac fixation would have avoided such failures attributed to osteopenia.

Reduction of the posterior pelvic ring disruption correlates positively with iliosacral screw insertion accuracy and functional results. Malreductions, especially in sacral fractures, diminish the osseous pathway available for safe screw insertion. This fact was confirmed in our patient series as well. It is certain that posterior pelvic malreductions would have adversely affected our results of screw insertion accuracy.

We recognize that our investigation has certain limitations. The estimates of osseous pathway limits were based on standard two-dimensional computed tomography images that could vary in planar orientation. Volumetric measurements were not calculated for these patients. Although not geometrically ideal, our measurements were practical since preoperative planning is commonly based upon pelvic plain radiographs and two-dimensional CT scans alone.

Complex pelvic ring injuries continue to provide mechanical challenges for fixation constructs. The thirty plus percent incidence of dysmorphic upper sacral segments has previously limited options for improving stability. By recognizing the radiographic characteristics of dysmorphism, and understanding how these affect potential iliosacral screw placement at different sacral segment levels, posterior ring fixation is possible using such screws. Second sacral segment screws provide the surgeon with an additional tool to better treat unstable posterior ring injuries in patients with dysmorphic upper sacral segments.

Recommended Reading

Routt MLC, Kregor PJ, Simonian PT, et al. Early results of percutaneous iliosacral screws placed with the patient in the supine position. J Orthop Trauma. 1995;9: 207-14.

Moed BR, Geer BL. S2 iliosacral screw fixation for disruptions of the posterior pelvic ring: a report of 49 cases. J Ortho Trauma. 2006;20:378-83.

Carlson DA, Scheid DK, Maar DC, et al. Safe placement of S1 and S2 iliosacral screws: the "vestibule" concept. J Orthop Trauma. 2000;14:264-9.

Routt MLC, Simonian PT, Agnew SG, et al. Radiographic recognition of the sacral alar slope for optimal placement of iliosacral screws: a cadaveric and clinical study. J Orthop Trauma. 1996;10:171-7.

Kraemer W, Hearn T, Tile M, et al. The effect of thread length and location on extraction strengths of iliosacral lag screws. Injury. 1994;25:5-9.

Early Outcomes Following ACL Reconstruction Using Soft-Tissue Grafts Passed Across Open Physes

Gregory A. Schmale, M.D., Christopher Y. Kweon, M.D., and Roger V. Larson, M.D.

Anterior cruciate ligament disruptions in skeletally immature athletes are now common occurrences. Recognized alternatives for treatment include activity modification and surgery. Bracing without major activity modification has not been found to adequately stabilize the ACL deficient knee. Though many advocate reconstruction of all ACL deficient knees in youth because of the high risk of subsequent meniscal injury and/or early arthritis in unstable knees, others have shown that following an activity modification program while waiting until skeletal maturity prior to reconstruction may avoid the risk of a poor outcome from an unstable knee. The risks accompanying ACL reconstruction in the skeletally immature patient include possible abnormal growth and development of the limb, specifically leg length difference (operative leg long or short) and angular deformity, including valgus of the femur, and varus or recurvatum of the tibia.

Surgical procedures designed to decrease the risk of operative intervention in this population include extra-physeal reconstructions, trans-epiphyseal tunneling to avoiding crossing open physes, and trans-epiphyseal tibial tunnel placement with soft-tissue grafts placed in the over the top position of the distal femur. Though transphyseal procedures using soft tissue grafts across open physes have been shown to produce angular deformities in animal models, for many years we have used this procedure using hamstring autograft or soft-tissue allograft placed through central and more vertically placed tunnels without complication. We hypothesize:

1. Transphyseal ACL reconstructions in skeletally immature patients using soft tissue grafts will not affect leg lengths or angular alignment of the lower extremities.

2. The results of this procedure in skeletally immature patients will be comparable to results seen in adults.

Materials and Methods

We reviewed all ACL reconstructions performed on young adolescent and preadolescent patients between 1994 and 2003 at Children's Hospital and Regional Medical Center and the University of Washington Medical Center. 53 patients were identified who were likely skeletally immature at the time of ACL reconstruction and skeletally mature at the time of most recent follow-up, and at least two years from surgery. Thirty-one of fifty-three agreed to return for interviews, physical exams, basic skills tests, and radiographs.

All patients were initially treated surgically with ACL reconstruction using soft tissue grafts placed across open physes fixed on the femoral side with an endobutton and on the tibial side with a screw and washer, using the technique described previously by Simonian, Metcalf and Larson. The recommended post-operative rehabilitation was similar to that recommended for our adult patients, consisting of a nine month program of graduated return to sports.

Angular alignment of each leg was determined by measurement of anatomic axes estimated from the standing single shot bilateral anteroposterior knee radiograph;

	SI – Skeletally Immature*	SM – Skeletally Mature*	p-value (2-sample t-test)
Number of patients	13	18	--
Age at Reconstruction (yrs)	13.2 ± 0.8 (11.8 to 14.0)	14.9 ± 0.8 (13.7 to 16.3)	--
Tegner Pre-Injury Score	7.5 ± 0.9 (6 to 9)	7.8 ± 1.0 (6 to 9)	0.27
Tegner Post-injury/ Pre-surgery Score	2.7 ± 2.0 (1 to 7)	3.1 ± 1.7 (1 to 7)	0.75
Current Tegner Activity Score	6.6 ± 1.4 (3 to 9)	6.8 ± 1.4 (4 to 9)	0.83
Current Lysholm Score	92 ± 9 (66 to 100)	95 ± 9 (61 to 100)	0.46
IKDC Symptoms Score	3.2 ± 0.7 (2 to 4)	3.3 ± 1.0 (1 to 4)	0.71
IKDC Physical Exam	3.2 ± 0.7 (2 to 4)	2.9 ± 0.6 (2 to 4)	0.25
Post-op L/R Difference Femoral Valgus	1° ± 1° (-1 to +4°)	1° ± 2° (-2 to +4°)	0.76
Post-op L/R Difference Tibial Varus	-1° ± 1° (-3 to +1°)	0° ± 1° (-2 to +2°)	0.21
Post-op L/R Difference Sagittal Tibial Axis	0° ± 2° (-3 to +3°)	1° ± 2° (-1 to +4°)	0.20
Post-op Leg Length Difference	+3 ± 4mm (-4 to +9mm)	-2 ± 6mm (-15 to +8mm)	0.04
IKDC Radiologic Score	3.7 ± 0.6mm (2 to 4mm)	3.7 ± 0.5mm (3 to 4mm)	0.79

Table 1: Comparison of groups. *mean ± standard deviation (range)

Figure 1: Immediate post-op (a), and one (b) and two year follow-up radiographs (c) of a female patient 12 years of age at the time of surgery: she was noted to have a 5-degree flexion contracture and 1-2 degrees of excess valgus on the operative side at most recent follow-up, though the flexion contracture may have exaggerated the degree of valgus measured. Tibial hardware was removed and a cyclops lesion debrided at one–year post-reconstruction. She has since returned to her pre-injury level of activity, running track.

tibial recurvatum was determined by comparison of lateral radiographs of each knee. The contralateral unoperated limbs were used as controls for comparison. Pre-operative records were reviewed for each patient to determine height just prior to surgery, and surgical records were reviewed to confirm the surgical procedure performed. Patients with essentially closed physes at the time of surgery and less than 4 cm of subsequent height growth were placed into a skeletally mature group.

Results

Eighteen of the thirty-one patients returning for interview, exam, and radiographs were determined to be essentially skeletally mature at the time of reconstruction. This group of 18 was used as a comparison group as they were of nearly the same age as those found to be skeletally immature at the time of surgery. Thirteen patients remained who met all the inclusion criteria for a skeletally immature designation at the time of the original ACL reconstruction.

The results for the skeletally immature group suggest few symptoms, high function, and good satisfaction with early outcomes (Table 1, column 1). The mean Likert satisfaction score for overall outcome was 8.4 (range 3 – 10). One patient had pain and giving way with running and cutting sports, limiting her ability to pursue her activities of choice. Two patients had flexion contractures (3-5° and 6-10°), three patients had a pivot glide and one a frank pivot shift on exam. One patient lost 3 mm of medial joint space on radiographs without other evidence of arthritis.

The mean increase in height following surgery for the skeletally immature patients was 7.5 cm (range 4 to 26 cm). Mean leg length difference at skeletal maturity was 3 mm long (range 4 mm short to 9 mm long) on the operative side for those who were skeletally immature at surgery. This compares to a mean leg length difference of 2 mm short on the operative side for those who where skeletally mature at surgery ($p=0.04$). Although this comparison is statistically significant, the difference favors longer operative limbs in the skeletally

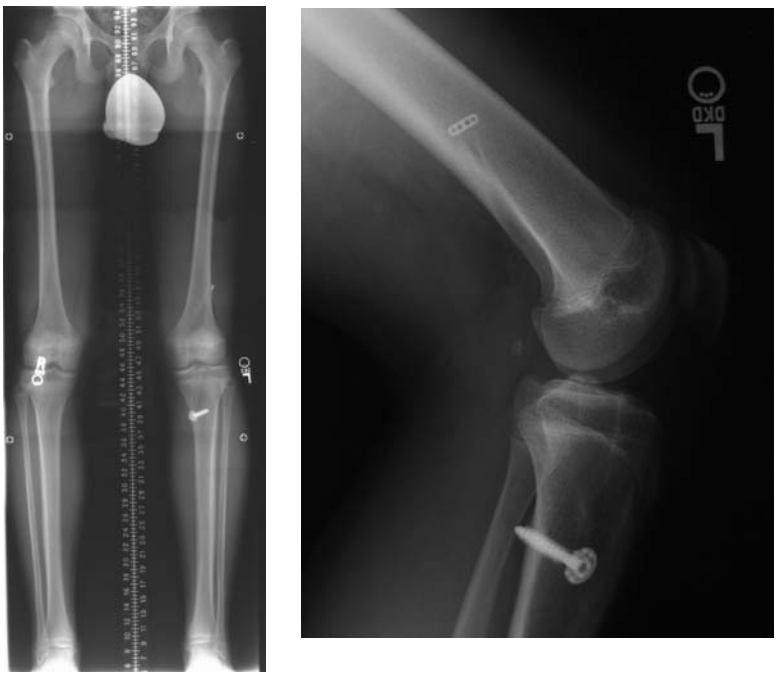

Figure 2: Male, 13 years of age at reconstruction with 4-year follow-up films: physes closed, 26 cm overall increase in height, no malalignments nor leg length differences apparent.

immature group, which clearly indicates that growth was not impaired in the skeletally immature patients.

There were no differences in the activity levels pre-injury, post-injury and pre-operatively, and at most recent follow-up when comparing those who were skeletally immature at the time of reconstruction to those who were skeletally mature (Table 1). There were no differences in the physical exam findings when comparing the two groups, nor were there differences in the radiographic analyses of the groups. There were no clinically evident angular malalignments in either group. When comparing operative to non-operative limbs, the greatest absolute differences in femoral valgus, tibal varus, and tibial recurvatum were comparable between groups.

In the skeletally immature group, there were 4 re-ruptures at a mean of 25 months (range 8 to 38 months); 3 patients sustained contralateral ACL ruptures at a mean of 27 months (range 6 to 50 months). In contrast, there was one re-rupture at 48 months and 6 contralateral ruptures at a mean of 32 months (range 12 - 58 months) in the group found to be skeletally mature at the time of surgery. Combining the two groups and comparing failures for allograft to autograft, three of six allografts failed as opposed to 2 of 24 autografts (odds ratio 11, 95% confidence intervals 0.7 to 688).

Discussion

In this small group of thirteen skeletally immature patients treated with ACL reconstruction using soft-tissues placed into tunnels drilled across open physes, no clinically significant leg length differences or angular malalignments were identified. These results suggest that this method of reconstruction for those with open physes and projected growth remaining of up to 8 cm is a reasonable treatment option.

Lysholm scores were comparable to those reported in studies of both children and adults. Our re-rupture rate was higher than that reported by others, and is generally higher than that seen in adult populations. Whether this is a function of the procedure performed, the age of the patients at the time of surgery, or the behavior and activity level(s) of these patients in the post-operative period cannot be determined from this retrospective review.

In conclusion, ACL reconstruction using soft-tissue grafts placed across open physes in skeletally immature patients is a reasonable treatment without undue risk for angular malalignment or leg length differences. Future work in this area should include prospective studies documenting skeletal age and limb length/alignment prior to reconstructive surgery.

Recommended Reading

Anderson, A. F.: Transepiphyseal replacement of the anterior cruciate ligament in skeletally immature patients. A preliminary report. J Bone Joint Surg Am, 85-A(7): 1255-63, 2003.

Graf, B. K.; Lange, R. H.; Fujisaki, C. K.; Landry, G. L.; and Saluja, R. K.: Anterior cruciate ligament tears in skeletally immature patients: meniscal pathology at presentation and after attempted conservative treatment. Arthroscopy, 8(2): 229-33, 1992.

Kocher, M. S.; Garg, S.; and Micheli, L. J.: Physeal sparing reconstruction of the anterior cruciate ligament in skeletally immature prepubescent children and adolescents. J Bone Joint Surg Am, 87(11): 2371-9, 2005.

Kocher, M. S.; Saxon, H. S.; Hovis, W. D.; and Hawkins, R. J.: Management and complications of anterior cruciate ligament injuries in skeletally immature patients: survey of the Herodicus Society and The ACL Study Group. J Pediatr Orthop, 22(4): 452-7, 2002.

Mizuta, H.; Kubota, K.; Shiraishi, M.; Otsuka, Y.; Nagamoto, N.; and Takagi, K.: The conservative treatment of complete tears of the anterior cruciate ligament in skeletally immature patients. J Bone Joint Surg Br, 77(6): 890-4, 1995.

Simonian, P. T.; Metcalf, M. H.; and Larson, R. V.: Anterior cruciate ligament injuries in the skeletally immature patient. Am J Orthop, 28(11): 624-8, 1999.

SRS Surgeon Members Risk for Thyroid Cancer: Is it Increased?

Theodore A. Wagner, M.D., Sue-Min Lai, Ph.D., M.S., M.B.A., and Marc A. Asher, M.D.

The Scoliosis Research Society (SRS) first met in 1966 with 35 members and has since grown to more than 938 (111 international and provisional) members. Over this period of time, the Society has lost 83 members. Three years ago, the SRS's 25th president died shortly after a diagnosis of thyroid cancer. In the following year, the 27th president of SRS was diagnosed with papillary carcinoma of the thyroid (with follicular variant). With this coincidence of disease, we have set out to survey all members for their health history concerning head and neck cancers.

Methods

The methodology included developing a survey with appropriate questions with Dr. Sue Min Lai, epidemiologist at the University of Kansas. Along with the staff of the SRS, the initial survey was sent out via email in January 2005, and then via hardcopy, followed by a second email. All of the non-responsive members were then contacted by phone and sent new surveys. As of 2004, 620 total responses have been collected out of a possible 670 active, inactive and deceased fellows.

Results

Five hundred and fifty-three of the five hundred ninety-six respondents (93%) provided enough information to be included in this report. The survey showed a total of 3 member surgeons who were diagnosed with thyroid cancers during a consecutive four-year period (2002 to 2005). Using the available average annual age-adjusted rate of thyroid cancer in the male population for the period of 2000 to 2003 published by the NCI SEER 9 registries, the expected number of thyroid cancers is 0.168 cases. This surveyed cohort, after adjusting for age, suggested a standardized mortality ratio (SMR) of about 18 (95% C.I. = 0.23 to 99.38) (Figure 2). A SMR of about 18 implied there was an 18-fold increased risk for thyroid cancer when comparing the surveyed group to the population served by the SEER 9 registries (Figure 2). However, the corresponding 95% confidence interval was very wide (due to a small sample size in our study cohort) and included one, suggesting the increased risk was not statistically significant at 0.05 level. Other forms of cancers reported by this cohort included prostate (n=16), melanoma (n=11), colon (n=4), and others (n=39). Some individuals have

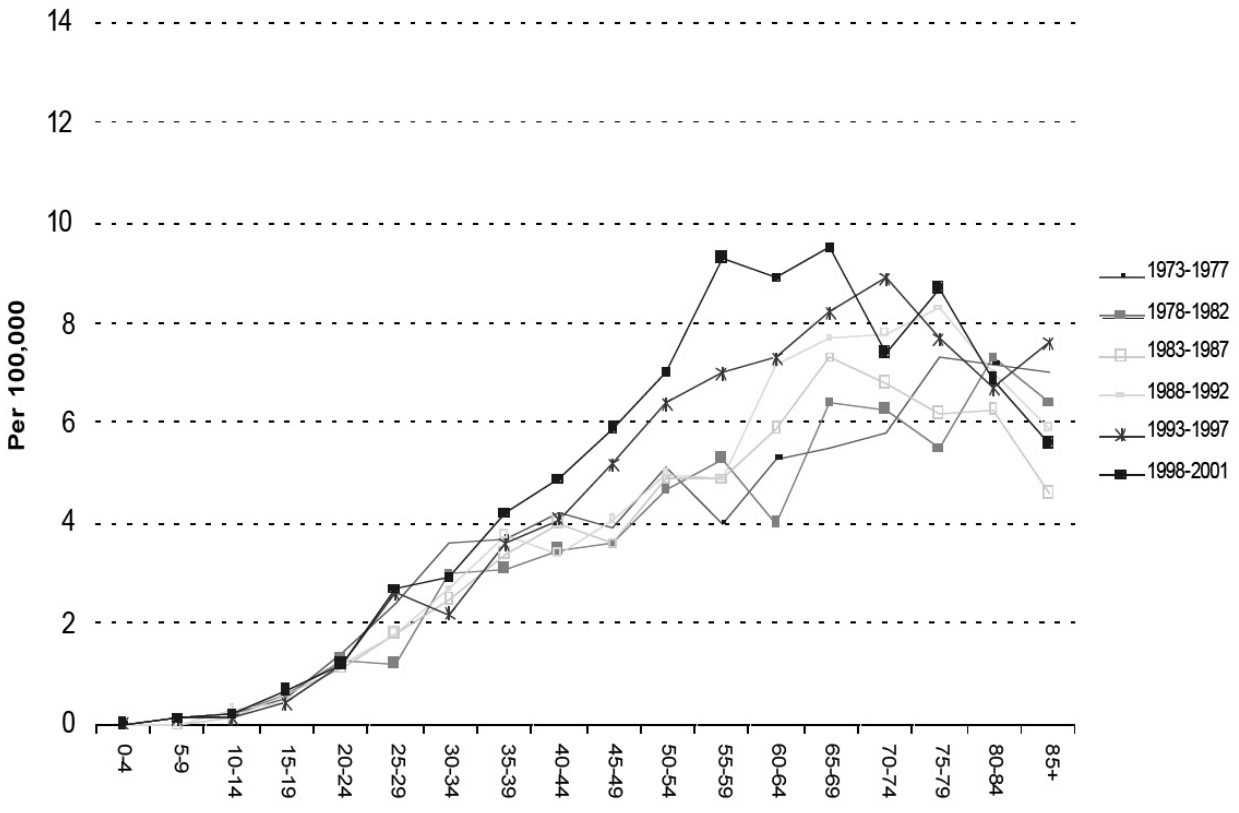

Figure 1: Thyroid cancer in males. Data from the National Cancer Institute's (NCI) Surveillance Epidemiology & End Results (SEER).

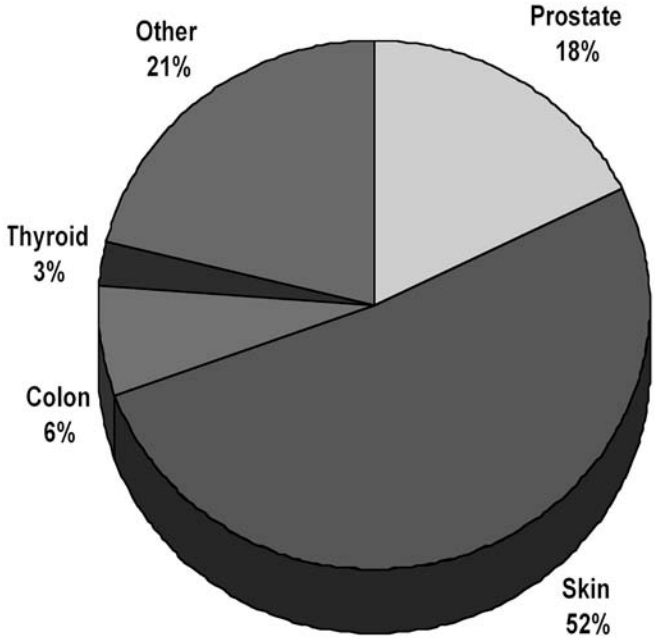

Figure 2: Cancer Statistics. Skin cancers: Basal Cell: 44%, Melanoma: 28%, Squamous Cell: 22%, Unidentified: 6%. (Other: Leukemia, Multiple myeloma, Pancreas, etc.)

been diagnosed with multiple cancers (Figure 1).

Discussion

In 2003, Dr. Sigurds, et al published the results of a large survey for cancer amongst 90,305 radiology technicians in the United States. Of the 70,859 response cohort, 77 were female. The relative risk (R.R.) estimate using cox proportional hazards regression with age as the time scale for all cancers in both genders was 1.04 and the risk of thyroid cancer was 1.54. The risk of thyroid cancer in males was 2.23. The incidence of melanoma in males was 1.39. The study was supported by finding similar data from a Canadian cohort of 191,000 who work around medical radiation and half of who were employed in dental or medical jobs.

In 1993, the European Journal of Cancer Prevention included two articles by Dr. Hallquist, et al who reviewed occupational exposures and thyroid cancer in Sweden. The case control study of thyroid cancer concerning 180 cases and 360 controls, age 20-70 years at diagnosis was performed. Sixty-three percent (63%) of all cases had papillary carcinoma, which yielded an odds ratio (OR) of 2.9 alone. The subset of this group included dentists and dental assistants only. The odds ratio for thyroid cancer in this group was 13.1.

Dr. Gordon Singer wrote a review article for the Journal of American Academy of Orthopedic Surgeons on occupational radiation exposure to surgeons. The average public is subjected to 360 millirems (mrem) per year of which 300 mrem was from background radiation and 60 mrem from diagnostic radiology. For reference, a chest x-ray exposes a patient to approximately 25 mrem, and a hip x-ray to 500 mrem. A regular C-arm exposes a patient to approximately 1,200 to 4,000 mrem per minute, depending on whether it is used in the extremity or in the truncal region. The recommended maximal annual units of occupational radiation are 5000 mrem to the total body, and specifically 15,000 mrem to the eye, 30,000 mrem to the thyroid gland, and 500 mrem for an embryo.

The estimated surgical time with the C-arm used for rodding and locking femoral fractures, with a mean average, is 4.6 minutes of fluoroscopy. During this procedure the surgeon would receive 15.3 mrem of exposure to the thyroid, and 27 mrem to his index finger. A significant decay of the risk occurs as one moves farther away from the beam generated, and there is very little exposure at six feet away from the general area.

Awareness of the risks of radiation is real and can be reduced by proper shielding. A 0.25 ml lead gown will reduce 90% of radiation to the torso. A thyroid shield 0.5 ml thick will reduce the radiation exposure to the thyroid gland by 90% (Figure 3). Leaded glasses will decrease radiation by 30-70%.

Conclusion

Our survey of the SRS membership suggests that we may have an increased risk of thyroid cancer particularly in the fifth and sixth decades of our life. The problem may be the result of an accumulation of exposure to ionized radiation, though this hypothesis remains to be tested with an inclusion of a control group in the study. While we are in the process of identifying a control group of age and geographically adjusted male physicians and/or surgeons who are not routinely using radiography, we would recommend an annual exam of the thyroid gland with each annual checkup after the age of 40. Since only 40% of 1.5 cm lesions can be palpated clinically, ultrasound would seem to be an important adjunct to that examination.

Recommended Reading

Sigurdson AJ, Doody MM, Rao RS, Freedman DM, Alexander BH, Hauptmann M, Mohan AK, Yoshinaga S, Hill DA, Tarone R, Mabuchi K, Ron E, Linet MS. Cancer incidence in the US radiologic technologists health study, 1983-1998. Cancer. 2003 Jun 15; 97(12):3080-9.

Wingren G, Halluist A, Hardell L. Diagnostic X-ray exposure and female papillary thyroid cancer: a pooled analysis of two Swedish studies. Eur J Cancer Prev. 1997 Dec; 6(6):550-6.

Hallquist A, Hardell L, Degerman A, Boquist L. Occupational exposures and thyroid cancer: results of a case-control study. Eur J Cancer Prev. 1993 Jul: 2(4):345-9.

Singer G. Occupational radiation exposure to the surgeon. J Am Acad Orthop Surg. 2005 Jan-Feb; 13(1):69-

Figure 3: Recommended Thyroid Shield.

76. Review.

Davies L, Welch HG. Increasing incidence of thyroid cancer in the United States, 1973-2002. JAMA. 2006 May 10; 295 (18):2164-7.

Ries LAG, Harkins D, et al. SEER Cancer Statistics Review, 1975-2003, National Cancer Institute. Bethesda, MD, http://seer.cancer.gov/csr/1975_2003/results_merged/sect_26_thyroid.pdf

Graduating Residents
Class of 2007

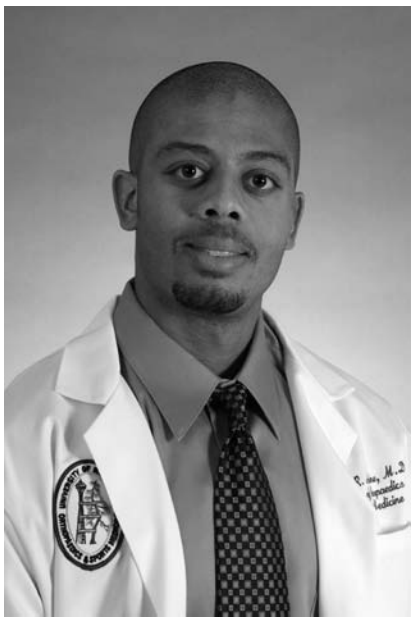

Jamie Antoine, M.D.

After residency, Jamie will complete a fellowship in Sports Medicine at the Palo Alto Medical Foundation next year. After his fellowship, he plans to do a sports or sports/general practice.

Mary Cunningham, M.D.

After residency, Mary will be completing a Spine Fellowship at New York University Hospital for Joint Diseases. She will complete her fellowship in 2008.

Joseph Lynch, M.D.

Joe will complete fellowship training in Shoulder and Elbow surgery here in 2008. He will then pursue an academic practice with the United States Navy. He and his family hope to return to the Pacific Northwest after completion of his military obligation.

Jeremiah Clinton, M.D.

He will be staying in Seattle to do a Shoulder and Elbow Fellowship. Afterwards, he plans to practice in a community setting in the mountains of the Northwest or back home in Montana.

Evan Ellis, M.D.

In the coming year, Evan will be going to St. Louis, MO for a Sports Fellowship at Washington University. Upon completion of his fellowship, he plans to practice in the Chicago area.

Allison MacLennan, M.D.

Allison will complete a hand and upper extremity fellowship at St. Luke's-Roosevelt Hospital in New York which includes rotations at Brigham and Women's Hospital in Boston and Scottish Rite in Dallas.

Incoming Residents

Aaron Chamberlain

Aaron is from Salt Lake City, UT. He received a bachelors degree from the University of Utah and received his medical degree from UCSF. He has a particular interest in sports, joints, and spine. He also enjoys spending time with family, skiing, soccer, football, and playing the violin.

Cory Lamblin

Cory was born and raised in Wyoming. He earned a degree in molecular biology at the University of Wyoming and his medical degree from the University of Washington. His orthopedic interests are in hand-upper extremity, sports, and trauma. His extracurricular interests are rockclimbing/mountaineering, snowboarding, cycling, and spending time with family and friends.

Brian Daines

Brian is from Boise, Idaho. He received a BS in biochemistry from Brigham Young University. He graduated from Columbia College of Physicians and Surgeons in 2006. His orthopaedic interests include trauma, sports, and hand. In his spare time, he enjoys spending time with with his wife Carly and son Cole. He also enjoys weight lifting, tennis, piano, eating out with friends and traveling.

Edward Moon

Edward is originally from Dayton, OH. He received a cellular and molecular biology degree from the University of Michigan and his medical degree from the University of Cincinnati College of Medicine. Currently, his orthopaedic interests include hand and upper extremity, sports medicine, and spine. He enjoys spending his free time snowboarding, playing guitar, and traveling.

Incoming Residents

Derek Rains

Derek is from Jacksonville, OR. He attended Oregon State University and received his medical degree from the University of Washington. His areas of interest in Orthopaedics are tumor and trauma. Outside of orthopedics, he enjoys spending much of his free time outdoors; fly fishing, backpacking and hiking throughout the Northwest.

Christian Sybrowsky

Christian is from Sandy, UT. He received his bachelor degree from the University of Utah and his medical degree from the University of Utah School of Medicine. His orthopaedic interests are trauma, sports, joints, bone modeling/remodeling, and osteoporosis. In his spare time he enjoys mountain biking, hiking, skiing, running, and spending time with his family.

Peter Scheffel

As the son of a gold miner, Pete Scheffel was raised in various rural communities in Nevada, and later attended the University of Nevada, Reno. He obtained his medical education at the University of Nevada School of Medicine prior to coming to Seattle for his orthopaedic surgery residency. His areas of interest in orthopaedics are sports, upper extremity, and trauma. In his free time he enjoys playing sports and hanging out with friends.

Brett Wiater

Brett is from Bloomfield Hills, MI. He received his B.S. from The University of Notre Dame and received his medical degree from Wayne State University School of Medicine. He is interested in Biomechanics and in his free time enjoys fishing, running, backpacking, traveling, cycling, snowboarding, boating, and hiking.

ACEs

Foot/Ankle

Arash Aminian, M.D.

Darcy S. Foral, M.D.

Angelique G. H. Witteveen, M.D.

Spine

Troy H. Caron, M.D.

Joshua C. Patt, M.D.

Trauma

Erik N. Kubiak, M.D.

Samir Mehta, M.D.

Amer J. Mirza, M.D.

Eric G. Puttler, M.D.

Hobie D. Summers, M.D.

Darius G. Viskontas, M.D.

ACEs

Hand

Shai Luria, M.D.

Oncology

Jennifer W. Lisle, M.D.

Shoulder/Elbow

Ryan T. Bicknell, M.D.

Fellows

Hand

Simon Chin, M.D.

Kevin Malone, M.D.

Jamie Pfaeffle, M.D.

Paul A. Martineau, M.D.

Research Grants

National Institutes of Health (NIH)

Changes in the Characteristics of Plantar Soft Tissue with Diabetes
Bruce J. Sangeorzan, M.D.

Collagens of Cartilage and the Intervertebral Disc
David R. Eyre, Ph.D.

Collagen Cross-Linking in Skeletal Aging and Diseases
David R. Eyre, Ph.D.

Collagen Type II/IX/XI Heteropolymer Assembly
Russell J. Fernandes, Ph.D.

Disuse Induced Osteocyte Hypoxia
Ted S. Gross, Ph.D.

Dysregulation of 3-prolyl- hydroxylation in Human Skeletal Dysplasia
David R. Eyre, Ph.D.

Imaging of Molecules by Oscillator-Coupled Resonance
John A. Sidles, Ph.D.

Organization of Mechanical Signals in Bone Cells via Membrane
Ted S. Gross, Ph.D.

Predicting Bone Formation Induced by Mechanical Loading Using Agent Based Models
Sunder Srinivasan, Ph.D.

Safety of Lumbar Fusion Surgery for Chronic Back Pain
Sohail K. Mirza, M.D.

Skeletal Dysplasias
David R. Eyre, Ph.D.

Veterans Affairs Rehabilitation Research and Development Service

Ankle Equinus and Plantar Pressure in Individuals with Diabetes
Bruce J. Sangeorzan, M.D.

Ewing's Sarcoma Fusion Proteins and mRNA Splicing Factors
Howard A. Chansky, M.D.

Dynamic Gait Simulation: Neutrally Aligned and Pathologic Feet
Bruce J. Sangeorzan, M.D.

Kinematic Models of Normal and Painful Osteoarthritic Feet
Bruce J. Sangeorzan, M.D.

The Epidemiology of Foot Structure and Ulceration in Diabetic Veterans
Bruce J. Sangeorzan, M.D.

Treatment Outcomes for Ankle Arthritis
Bruce J. Sangeorzan, M.D.

VA Center of Excellence in Amputation Prevention and Prosthetic Engineering
Bruce J. Sangeorzan, M.D.

Orthopaedic Research and Education Foundation (OREF)

Reduction of Total Knee Arthroplasty Risk in Morbidly Obese Patients Using Laparoscopic Bariatic Surgery: A Prospective, Controlled Trial
Seth S. Leopold, M.D.

The Effect of Obesity on Outcomes Among Trauma Patients with Lower Extremity Orthopaedic Injuries
Sean E. Nork, M.D.

A.O. North America

An Observational Study Assessment of Surgical Techniques for Treating Cervical Spondylotic Myelopathy (CSM)
Jens R. Chapman, M.D.

An Observational Study Comparing Surgical to Conservative Management in the Treatment of Type II Odontoid Fractures Among the Elderly
Jens R. Chapman, M.D.

AO Spine North America Fellowship
Carlos Bellabarba, M.D.

Stability After Pin Versus Dorsal Plate Fixation of Simulated Interarticular Distal Radius Fractures: A Biomechanical Investigation
Thomas E. Trumble, M.D.
Wren V. McCallister, M.D.

Amgen, Inc.

Contrasting the Ability of OPG and Alendronate to Inhibit Bone Loss
Ted S. Gross, Ph.D.

Inhibition of Muscle Paralysis Induced Bone Loss by OPG
Ted S. Gross, Ph.D.

Research Grants

Arthrex, Inc.

Mechanical Testing of Arthroscopic Soft Tissue Anchors
Allan F, Tencer, Ph.D.

BioAxone Therapeutique, Inc.

Cethrin Trial
Jens R. Chapman, M.D.

CeraPedics, LLC

An Assessment of P15 Bone Putty in Anterior Cervical Fusion with Instrumentation
Jens R. Chapman, M.D.

Christopher Reeve Paralysis Foundation

Using Muscle Stimulation to Mitigate Bone Loss due to Muscle Paralysis
Ted S. Gross, Ph.D.

Foundation for Orthopedic Trauma

The Role of Muscle Function in Fracture Healing
Sean E. Nork, M.D.

Integra Lifesciences Corporation

Comparison of Bioabsorable Tubes for Repair of Nerve Injury
Thomas E. Trumble, M.D.

Johnson & Johnson, Inc.

Clinical Spine Fellowship Grant
Theodore A. Wagner, M.D.

Depuy Mitek Fellowship Grant
Christopher J. Wahl, M.D.

Kythera Biopharmaceuticals, Inc.

Assessment of Collateral Nerve Sprouting Inhibitors Following Botox Induced Muscle Paralysis
Ted S. Gross, Ph.D.

National Science Foundation

University of Washington Engineered Biomaterials
Christopher H. Allan, M.D.
Frederick A. Matsen III, M.D.

Ostex International, Inc.

Molecular Markers of Connective Tissue Degradation
David R. Eyre, Ph.D.

Orthopaedic Trauma Association

The Effect of Obesity on Outcomes Among Trauma Patients with Lower Extremity Orthopaedic Injuries
Sean E. Nork, M.D.

Synthes Spine Co.

PRODISC-C Versus Anterior Cervical Discectomy and Fusion (ACDF)
Jens R. Chapman, M.D.

Spine End-Results Research Fund
Frederick A. Matsen III, M.D.

The Boeing Company

Randomized Clinical Trial of Open versus Endoscopic Carpal Tunnel Release and Hand Therapy Comparing Patient Satisfaction. Functional Outcome and Cost Effectiveness
Thomas E. Trumble, M.D.

US Army Research Office

UW Team-Advance on Single Nuclear Detection and Atomic-Scale Imaging
John A. Sidles, Ph.D.

US Department of Education

Advancing Orthotic and Prosthetic Care Through Research, Standards of Practice and Outreach.
Douglas G. Smith, M.D.

Zymogenetics, Inc.

Recombinant Human Thrombin Trial
Sohail K. Mirza, M.D.

Department Publications 2006-2007

1. Allan, C. H., P. Fleckman, et al. (2006). "Tissue response and Msx1 expression after human fetal digit tip amputation in vitro." Wound Repair Regen 14(4): 398-404.

2. Barei DP, Nork SE, Bellabarba C, Sangeorzan BJ. Is the absence of an ipsilateral fibular fracture predictive of increased radiographic tibial pilon fracture severity? J Orthop Trauma. 2006 Jan;20(1):6-10.

3. Barei DP, Nork SE, Mills WJ, Coles CP, Henley MB, Benirschke SK. Functional outcomes of severe bicondylar tibial plateau fractures treated with dual incisions and medial and lateral plates. J Bone Joint Surg Am. 2006 Aug;88(8):1713-21.

4. Barnes AM, Chang W, Morello R, Cabral WA, Weis MA, Eyre DR, Leikin S, Makareeva E, Kuznetsova N, Uveges TE, Ashok A, Flor AW, Mulvihill JJ, Wilson PL, Sundaram UT, Lee B, Marini JC. Deficiency of cartilage-associated protein in recessive lethal osteogenesis imperfecta. N Engl J Med. 2006;355:2757-2764.

5. Beingessner, D. M., C. E. Dunning, et al. (2007). "The effect of coronoid fractures on elbow kinematics and stability." Clin Biomech (Bristol, Avon) 22(2): 183-90.

6. Bellabarba, C., S. K. Mirza, et al. (2006). "Diagnosis and treatment of craniocervical dislocation in a series of 17 consecutive survivors during an 8-year period." J Neurosurg Spine 4(6): 429-40.

7. Bellabarba C, Schildhauer Th, Vaccaro A, Chapman JR : Complications of lumbopelvic stabilization in high-grade sacral fracture dislocations with spin-pelvic instability. Spine 2006 15 (11 Suppl):S80-8; discussion S104.

8. Bellabarba C, Mirza SK, West GA, Mann FA, Dailey AT, Newell DW, Chapman JR: Diagnosis and treatment of craniocervical dislocation in a series of 17 consecutive survivors during an 8-year period. J Neurosurgery Spine 2006; 4:429-40.

9. Bjornson, K.F., Schmale, G. A., Adamczyk-Foster, A., and McLaughlin, J.F.: The Effect of Dynamic Ankle Foot Orthoses (DAFOs) on Function in Children with Cerebral Palsy. Journal of Pediatric Orthopaedics, 26(6):773-776, November/December 2006.

10. Boorman, R. S., T. Norman, et al. (2006). "Using a freeze substitution fixation technique and histological crimp analysis for characterizing regions of strain in ligaments loaded in situ." J Orthop Res 24(4): 793-9.

11. Bransford R, Bellabarba C, Thompson JH, Henley MB, Mirza, SK, Chapman JR: The safety of fluoroscopically-assisted thoracic pedicle screw instrumentation for spine trauma. J Trauma 2006, 60(5) 1047-1051.

12. Cabral WA, Chang W, Barnes AM, Weis M, Scott MA, Leikin S, Makareeva E, Kuznetsova NV, Rosenbaum KN, Tifft CJ, Bulas CO. Kozma C, Smith PA, Eyre DR, Marini JC. Proly 3-hydroxylase 1 deficiency causes a recessive metabolic bone disorder resembling lethal/severe osteogenesis imperfecta. Nat. Genet. 2007;39: 359-365.

13. Coles CP, Barei DP, Nork SE, Taitsman LA, Hanel DP, Bradford Henley M. The olecranon osteotomy: a six-year experience in the treatment of intraarticular fractures of the distal humerus. J Orthop Trauma. 2006 Mar;20(3):164-71.

14. Cunningham, M. R., W. J. Warme, et al. (2006). "Industry-funded Positive Studies Not Associated with Better Design or Larger Size." Clin Orthop Relat Res.

15. Donescu OS, Battié MC, Kaprio J, Levalahti E, Risteli J, Eyre D, Videman T. Genetic and environmental influences on bone turnover markers – a study of male twin pairs. Calcif. Tiss. Intl., 2007;80(2):81-88.

16. Donescu OS, Battié MC, Videman T, Risteli J, Eyre D. The predictive role of bone turnover markers for BMD in middle-aged men. Aging Male 2006:9(2):97-102.

17. DuBois B, Montgomery WH, Dunbar RP, Chapman JR: Simultaneous ipsilateral posterior knee and hip dislocations. Case report including a technique for closed reduction of the hip. J Orthop Trauma 2006; 20 (3): 216-219.

18. Escobedo EM, Richardson ML, Schulz YB, Hunter JC, Green JR 3rd,Messick KJ. Increased risk of posterior glenoid labrum tears in football players.Am J Roentgenol. 2007 Jan;188(1):193-7.

19. Fernandes RJ, Harkey MA, Weis MA, Askew JW, Eyre DR. The post-translational phenotype of collagen synthesized by SAOS-2 osteosarcoma cells. Bone, 2007, e-pub. In Press.

20. Eyre, D. R., M. A. Weis, et al. (2006). "Articular cartilage collagen: an irreplaceable framework?" Eur Cell Mater 12: 57-63.

21. Goto T, Matsui Y, Fernandes RJ, Hanson DA, Kubo T, Kiminori Y, Michigami T, Komori T, Fujita T, Yang L, Eyre DR, Yasui N. Sp1 family of transcription factors regulates the human alpha 2(XI) collagen gene (COL11A2) in Saos-2 osteoblastic cells. JBMR 2006;21:661-673.

22. Gourlay D, Hoffer E, Routt M, Bulger E.Pelvic angiography for recurrent traumatic pelvic arterial hemorrhage. J Trauma. 2005 Nov;59(5):1168-73.

23. Greisberg J, Sangeorzan B. Hindfoot arthrodesis. J Am Acad Orthop Surg. 2007 Jan;15(1):65-71.

24. Hanel, D. P., T. S. Lu, et al. (2006). "Bridge plating of distal radius fractures: the Harborview method." Clin Orthop Relat Res 445: 91-9.

25. Kadel, N. J. (2006). "Foot and ankle injuries in dance." Phys Med Rehabil Clin N Am 17(4): 813-26, vii.

26. Largacha, M., I. M. t. Parsons, et al. (2006). "Deficits in shoulder function and general health associated with sixteen common shoulder diagnoses: a study of 2674 patients." J Shoulder Elbow Surg 15(1): 30-9.

27. Lauder, A. J. and T. E. Trumble (2006). "Idiopathic avascular necrosis of the scaphoid: Preiser's disease." Hand Clin 22(4): 475-84; abstract vi.

28. Lee, M.B., Schmale, G.A., and Leopold, S. S.: Total Hip Arthroplasty in the Osteoporotic Patient. Advances in Osteoporotic Fracture Management, 4(3), 2006.

29. Lenters, T. R., F. M. Wolf, et al. (2007). "Arthroscopic compared with open repairs for recurrent anterior shoulder instability. A systematic review and meta-analysis of the literature." J Bone Joint Surg Am 89(2): 244-54.

30. Ledoux WR, Rohr ES, Ching RP, Sangeorzan BJ. Effect of foot shape on the three-dimensional position of foot bones.J Orthop Res. 2006 Dec;24(12):2176-86.

31. Lynch, J. R., M. V. Jenkins, et al. (2006). "Bilateral exercise-induced compartment syndrome of the thigh and leg associated with massive heterotopic ossification. A case report." J Bone Joint Surg Am 88(10): 2265-9.

32. Lynch, J. R., G. A. Schmale, et al. (2006). "Important demographic variables impact the musculoskeletal knowledge and confidence of academic primary care physicians." J Bone Joint Surg Am 88(7): 1589-95.

33. Matsen, F. A., 3rd, C. Chebli, et al. (2006). "Principles for the evaluation and management of shoulder instability." J Bone Joint Surg Am 88(3): 648-59.

34. Matsen, L. J., C. Hettrich, et al. (2006). "Direct injection of blood into the labrum enhances the stability provided by the glenoid labral socket." J Shoulder Elbow Surg 15(6): 651-8.

35. Mazzuca SA, Brandt KD, Eyre DR, Katz BP, Askew J, Lane KA. Urinary levels of type II collagen C-telopeptide crosslink are unrelated to joint space narrowing in patients with knee osteoarthritis. Ann. Rheum. Dis. 2006;65:1055-1059.

36. McCallister, W. V., H. C. Ambrose, et al. (2006). "Comparison of pullout button versus suture anchor for zone I flexor tendon repair." J Hand Surg [Am] 31(2): 246-51.

37. McHenry TP, Mirza SK, Wang JJ, Wade CE, O'Keefe GE, Dailey AT, Schreiber MA, Chapman JR: Risk Factors for respiratory failure following operative stabilization of thoracic and lumbar spine fractures. J Bone Joint Surg Am. 2006 88(5): 997-1005

38. Miller AD, Vigdorovich V, Strong RK, Fernandes RJ, Lerman MI. Hyal2, where are you? Epub. Sep 20, 2006 OsteoArthritis Research Society International. OsteoArth. Cart. Published by Elsevier Ltd.

39. Mkandawire C, Ledoux WR, Sangeorzan BJ, Ching RP.Foot and ankle ligament morphometry.

40. J Rehabil Res Dev. 2005 Nov-Dec;42(6):809-20.

41. Morello R, Bertin TK, Chen Y, Hicks J, Tonachini L, Monticone M, Castagnola P, Rauch F, Glorieux FH, Vranka J, Bächinger HP, Pace JM, Schwarze U, Byers PH, Weis MA, Fernandes RJ, Eyre DR, Yao Z, Boyce BF, Lee B. CRTAP is required for prolyl 3-hydroxylation and mutations cause recessive osteogenesis imperfecta. Cell 2006;127:291-304.

42. Morgan, H. D., A. M. Cizik, et al. (2006). "Survival of tumor megaprostheses replacements about the knee." Clin Orthop Relat Res 450: 39-45.

43. Nork, SE; Barei, DP; Schildhauer, TA; Agel, J; Holt, SK; Schrick, JL; Sangeorzan, BJ: Intramedullary Nailing of Proximal Quarter Tibial Fractures. J Orthop Trauma, 20(8): 523-528, 2006.

44. O'Kane, J. W., E. Hutchinson, et al. (2006). "Sport-related differences in biomarkers of bone resorption and cartilage degradation in endurance athletes." Osteoarthritis Cartilage 14(1): 71-6.

45. Orendurff, M. S., E. S. Rohr, et al. (2006). "An equinus deformity of the ankle accounts for only a small amount of the increased forefoot plantar pressure in patients with diabetes." J Bone Joint Surg Br 88(1): 65-8.

46. Routt ML Jr, Falicov A, Woodhouse E, Schildhauer TA.Circumferential pelvic antishock sheeting: a temporary resuscitation aid.J Orthop Trauma. 2006 Jan;20(1 Suppl):S3-6.

47. Schildhauer TA, Bellabarba C, Selznick HS, McRoberts D, Vedder NB, Chapman JR. Unstable pediatric sacral fracture with bone loss caused by a high-energy gunshot injury. J Trauma 2006;

48. Schildhauer TA, Bellabarba C, Nork SE, Barei DP, Routt ML Jr, Chapman JR. Decompression and lumbopelvic fixation for sacral fracture-dislocations with spino-pelvic dissociation. J Orthop Trauma. 2006 Jul;20(7):447-57.

49. Schildhauer TA, Chapman JR, Muhr G, Köller M: Cytokine release of mononuclear leukocytes (PBMC) after contact to a carbonated calcium phosphate bone cement. Accepted for publication by Journal of Biomedical Materials Research Part A. March 2006 .

50. Schildhauer TA, Bellabarba C, Chapman JR: Fractures and Fracture-dislocations t the lumbosacral junction. Part III: Nonoperative treatment and pitfalls of management. Contemporary Spine Surgery 2006; 7(5): 1-6.

51. Schildhauer TA, Bellabarba C, Chapman JR: Fractures and fracture – dislocations at the lumbosacral junction. Part II: Surgical Treatment. Contemporary Spine Surgery 2006; 7(4):1-10.

52. Schmale, G. A. (2007). "Journal of Pediatric Orthopaedics January-June 2006." Clin Orthop Relat Res.

53. Schmale, G. A., R. E. Eilert, et al. (2006). "High reoperation rates after early treatment of the subluxating hip in children with spastic cerebral palsy." J Pediatr Orthop 26(5): 617-

54. Schoots, IG; Simons, MP; Nork, SE; Chapman, JR; Henley, MB: Antegrade locked nailing of open humeral shaft fractures. Orthopaedics, 30(1): 49-54, 2007.

55. Shapiro F, Mulhern H, Weis MA, Eyre D. Rough endoplasmic reticulum abnormalities in a patient with spondyloepimetaphyseal dysplasia with scoliosis, joint laxity, and finger deformities. Ultrastructural Pathol 2006;30:393-400.

56. Smith, CS; Nork, SE; Sangeorzan, BJ: The extruded talus: results of reimplantation. J Bone Joint Surg Am, 88(11): 2418-2424, 2006.

57. Srinivasan, S., B. J. Ausk, et al. (2007). "Rest-Inserted Loading Rapidly Amplifies the Response of Bone to Small Increases in Strain and Load Cycles." J Appl Physiol.

58. Taitsman, L. A., J. B. Frank, et al. (2006). "Osteochondral fracture of the distal lateral femoral condyle: a report of two cases." J Orthop Trauma 20(5): 358-62.

59. Taitsman, L. A., S. E. Nork, et al. (2006). "Open clavicle fractures and associated injuries." J Orthop Trauma 20(6): 396-9.

60. Tencer, AF, R Kaufman, P Huber, C Mock, ML Routt, Reducing primary and secondary impact loads on the pelvis during side impact, Traffic Injury Prevention, 8:101-106, 2007.

61. Warner, S. E., D. A. Sanford, et al. (2006). "Botox induced muscle paralysis rapidly degrades bone." Bone 38(2): 257-64.

62. Wolf, J. C., W. M. Weil, et al. (2006). "A biomechanic comparison of an internal radiocarpal-spanning 2.4-mm locking plate and external fixation in a model of distal radius fractures." J Hand Surg [Am] 31(10): 1578-86.

63. Woodhouse, E., G. A. Schmale, et al. (2006). "Reproductive hormone effects on strength of the rat anterior cruciate ligament." Knee Surg Sports Traumatol Arthrosc.

Contributors to Departmental Research and Education

April 2006 Through March 2007

We express our appreciation to all who have contributed to the work of the Department of Orthopaedics and Sports Medicine over the past year. Your assistance makes possible special research activities, educational programs, and other projects that we could not offer without this extra support from our alumni, faculty, and friends in the community. We owe a special thanks to the University of Washington Resident Alumni who have made significant contributions to help further the education of our current residents. We have tried to include in this list all who contributed; if anyone was overlooked, please be sure to let us know!

Friends of Orthopaedics

John H. Aberle
Alaska Orthopaedic Specialist
Christopher H. Allan
Edward Eugene Almquist
Franklin G. Alvine
Sean M. Amann
Mary Jane B. Anderson
Marlene M. Angel
Jamie Antoine
AO North America
AO Spine North America
AO-Stiftung-ASIF Foundation
Craig Thomas Arntz
Michael S. Aronow
Martha J. Baker
Bank of America Foundation
Sandra Barefield
David P. Barei
Jeremy P. Bauer
Timothy C. Beals
Bearly, Inc.
Brian D. Bechtel
Daphne Beingessner
Barbara G. Belfie
Carlo Bellabarba
Stephen K. Benirschke
Gwendolyn J. Bevard
Stephen Grant Bowman
Lynn R. Boyd
Jonathan P. Braman
Richard Bransford
Thomas R. Bridges
Janet B. Brown
Loan Bui
Tony Buoncristiani
Susan R. Cero
Aaron M. Chamberlain
Jens R. Chapman
Hsiang-Song Ernest Chen
Aric A. Christal
Gary J. Clancey
Burnet Todd Clarke
Jeremiah M. Clinton
John M. Coletti, Jr.
Ernest U. Conrad III
Jay L. Crary
Alea C. Culpepper
Gary C. Culpepper
Mary Cunningham
Frederick J. Davis
Susan E. DeBartolo
David A. Deneka
Mary Ann Derr
Richard Allan Dimond
Oriente Ditano
Benjamin Dubois
Robert P. Dunbar
Brady A. Elliott
Evan Ellis
Mr. and Mrs. Leonard Ely
Gwendolyn B. Emerson
Donald P. Ericksen
Dr. and Mrs. Edward L. Farrar III
Drew M. Fehsenfeld
Thomas J. Fischer
Daniel Lloyd Flugstad
Harold J. Forney
Dr. and Mrs. Jonathan L. Franklin
Mark A. Freeborn
Park W. Gloyd
George M. Gradt
Thomas M. Green
Theodore K. Greenlee, Jr.
Douglas P. Hanel
Dr. and Mrs. Jeffrey N. Hansen
Sigvard Ted Hansen Jr.
Robert A. Hasegawa
Helena Orthopaedic Clinic
John M. Hendrickson
Michael Bradford Henley
Joel Richard Hoekema
William A. Hoglund
Dr. and Mrs. Scott E. Hormel
Christopher R. Howe
John P. Howlett
Frederick S. Huang
Michael D. Hwang
Dr. and Mrs. Larry Dale Hull
Thomas W. Hutchinson
Illinois Orthopaedic & Hand
JMS Hand Associates
David E. Karges
Aino Karm
Mr. and Mrs. Tom Karnezis
William G. Keehn
Dr. and Mrs. Carleton A. Keck, Jr.
Bernice Kent
Jason C. King
Richard Murray Kirby
Jonathan L. Knight
Peter J. Kolloen
George D. Kramer, Jr.
Harry H. Kretzler Jr.
Barbara J. Lally
Roger V. Larson
Michael B. Lee
Seth S. Leopold
David G. Levinsohn
Joseph Lynch
Calvin R. MacKay
Allison MacLennan
Rajshri Maheshwari
Martin G. Mankey
Frederick A. Matsen III
Gregory K. May
Michael K. McAdam
Timothy K. McGonagle
David A. McGuire
Joseph S. Mezistrano
Jean Michele
John D. Michelotti
Ralph W. Miller
Sohail K. Mirza
Peter W. Mitchell
Edward S. Moon
Marr P. Mullen
Mark E. Murphy
Andrea K. Myers
Cheryl M. Neufeld
John A. Neufeld
Gregg T. Nicandri
Sean E. Nork
Northwest Biomet, Inc.
Jill C. Obremskey
Mark C. Olson
Soren L. Olson
William L. Oppenheim
Orthopedic Surgeons
J. Lee Pace
Pacific Medical, Inc
Lawrence V. Page
Karen N. Perser
Albert E. Peterson
Pfizer, Inc.

Friends of Orthopaedics

Mary Pleger
Gregory A. Popich
Proliance Surgeons, Inc.
Gregory H. Rafijah
Timothy B. Rapp
Mark C. Remington
Robert Gregory Ripley
Mr. and Ms. Rodney Roberts
Milton Lee Routt Jr.
Dr. and Mrs. Michael J. Sailer
Bruce J. Sangeorzan
Kenichi Sato
Gregory A. Schmale
Guy R. Schmidt
William P. Schutz
The Seattle Foundation
Seattle Hand Surgery Group
Marilyn E. Sheldon
Silicon Valley Community Foundation
Simonian Sports Medicine Clinic
Dr. and Mrs. Peter T. Simonian
William F. Sims
Greg B. Sjothun
Douglas G. Smith
Jeffery M. Smith
Kit M. Song
Michael A. Sousa
Larry Southern
Patricia A. Spence
SpineVision, Inc.
Susan S. Stephens
David Wayne Stevens
Jeffrey L. Stickney
Edward A. Stokel
Addison T. Stone
Marc F. Swiontkowski
Synthes Spine
T&P, LLC
Lisa A. Taitsman
Carol C. Teitz
John L. Thayer
Dr. and Mrs. Steven C. Thomas
Jason Hoyt Thompson
Trimed, Inc.
Martin Shelton Tullus
John W. Underwood
Robert L. Van Citters
JE Vanderhooft
Nicholas B. Vedder
Robert G. Veith
Iris M. Vinje
Theodore A. Wagner
William F. Wagner Jr.
Michael D. Walsh
Jane C. Walton
Washington Orthopaedic Center
Washington State Orthopaedic Association
Edward Weinberger
Ms. Loryn P. Weinstein
Neil J. Wells
Colleen Dishy Wes
John D. West III
Jason J. Wilcox
Doris M. Wilkinson
Robert T. Williamson
Darlena M. Wilson
Robert A. Winquist
Jay A. Winzenried
Christopher F. Wolf
Emma S. Woodhouse-Graber
Wright Medical Technology
Hansjoerg Wyss
Liu Yang
Zimmer Holdings, Inc.
Vinko Zlomislic

Alumni

1952
Park W. Gloyd, M.D. ★

1954
Trygve Forland, M.D. ★

1955
Robert W. Florence, M.D.

1956
J. Michael Egglin, M.D. ★
John E. Goeckler, M.D.
Robert L. Romano, M.D.

1957
John H. Aberle, M.D. ★
John R. Beebe, M.D.

1958
Harry H. Kretzler, Jr., M.D. ★
James R. Friend, M.D. ★
Kenneth L. Martin, M.D. ★
Samuel L. Clifford, M.D.

1959
James W. Tupper, M.D.

1960
Irving Tobin, M.D. ★
William V. Smith, M.D. ★

1961
Robert C. Colburn, M.D.

1962
Arthur Ratcliffe, M.D.
Marr P. Mullen, M.D. ★

1963
Alfred I. Blue, M.D.
Robert A. Kraft, M.D.

1964
David E. Karges, M.D. ★★★★
Harold J. Forney, M.D. ★
Theodore K. Greenlee II, M.D. ★★★★★
Thomas E. Soderberg, M.D.

1966
F. Richard Convery, M.D. ★
Joseph S. Mezistrano, M.D. ★
William A. Reilly, Jr., M.D.

1967
Ivar W. Birkeland, M.D.
J. Conrad Clifford, M.D. ★
Robert F. Smith, M.D. ★★★★★

1968
Lynn T. Staheli, M.D. ★
Stewart M. Scham, M.D. ★
William T. Thieme, M.D. ★

1969
Edward E. Almquist, M.D. ★★
Edward L. Lester, M.D.
Hugh E. Toomey, M.D. ★★★
Sigvard T. Hansen, Jr., M.D. ★★★★

1970
John C. Brown, M.D. ★
John M. Coletti, Jr., M.D. ★
Malcolm B. Madenwald, M.D. ★
Michael T. Phillips, M.D. ★
Robert D Schrock, Jr., M.D.

1971
Bruce E. Bradley, Jr., M.D.
Franklin G. Alvine, M.D. ★★★★
Jerome H. Zechmann, M.D.
Louis A. Roser, M.D. ★
Nils Fauchald, Jr., M.D.

1972
David J. LaGasse, M.D.
David R. Nank, M.D. ★★
Donald D. Hubbard, M.D. ★
John A. Neufeld, M.D. ★
Thomas L. Gritzka, M.D. ★

1973
Frederick J. Davis, M.D. ★
Larry D. Hull, M.D. ★
Robert P. Watkins, Jr., M.D. ★
Theodore A. Wagner, M.D. ★★★★★

1974
Richard A. Dimond, M.D. ★★
Ronald B.H. Sandler, M.D. ★★★
Samuel R. Baker, M.D. ★★
Robert A. Winquist, M.D. ★★★★★

1975
Donald L. Plowman, M.D. ★★★
Frederick A. Matsen III, M.D. ★★★★★
Gunter Knittel, M.D.
Larry R. Pedegana, M.D. ★
Thomas M. Green, M.D. ★★★★★
William M. Backlund, M.D., P.S. ★

1976
Douglas K. Kehl, M.D.
Douglas T. Davidson III, M.D. ★
John F. Burns, M.D. ★
Peter Melcher, M.D.
Richard A. Zorn, M.D. ★

1977
Carl A. Andrews, M.D. ★
Geoffrey W. Sheridan, M.D. ★★
Larry D. Iversen, M.D. ★
Mark C. Olson, M.D. ★
Steven T. Bramwell, M.D.

1978
Arnold G. Peterson, M.D. ★★★★
Gary J. Clancey, M.D. ★★★
John W. Brantigan, M.D.
Richard S. Westbrook, M.D. ★★
Robert J. Strukel, M.D.
William Oppenheim, M.D. ★

1979
Allan W. Bach, M.D. ★★★★★
Gregory M. Engel, M.D. ★★
Jonathan L. Knight, M.D. ★★
Richard L. Semon, M.D. ★★★★

1980
Carol C. Teitz, M.D. ★★★
Douglas G. Norquist, M.D.
John M. Hendrickson, M.D. ★★
Michael A. Sousa, M.D. ★★
Stuart R. Hutchinson, M.D. ★

1981
Dennis J. Kvidera, M.D. ★
John M. Clark, Jr., M.D., Ph.D. ★★★
Martin S. Tullus, M.D. ★★★★★
Robert G. Veith, M.D. ★★★★★

1982
John L. Thayer, M.D. ★
Richard M. Kirby, M.D. ★★★★★
Steven S. Ratcliffe, M.D. ★★
William D. Burman, M.D.

1983
E. Anne O. Elliot, M.D. ★
Edward L. Farrar III, M.D. ★★★★★
Henry K. Yee, M.D.
Joseph D. Zuckerman, M.D. ★★★★
Keith A. Mayo, M.D. ★★★
Robert M. Berry, M.D.

1984
Jeffrey C. Parker, M.D. ★
Jeffrey W. Akeson, M.D. ★★★
Kevin P. Schoenfelder, M.D. ★
Marc F. Swiontkowski, M.D. ★★★★★
Thomas J. Fischer, M.D. ★★★★

1985
Daniel L. Flugstad, M.D. ★★★★★
Jeffrey N. Hansen, M.D. ★★★
Paul J. Abbott, M.D. ★★★★
Richard J. Barry, M.D. ★
William P. Barrett, M.D. ★★★★★

1986
Carleton A. Keck, Jr., M.D. ★★★
Gary Bergman, M.D. ★★★★★
Lawrence E. Holland, M.D. ★
Michael E. Morris, M.D. ★★★★

1987
Craig T. Arntz, M.D. ★★★
Herbert R. Clark, M.D. ★★
Michael K. Gannon, M.D. ★
Steven L. Reed, M.D. ★

1988
Jonathan L. Franklin, M.D. ★★★★★
Michael A. Thorpe, M.D. ★★★★★
Richard V. Williamson, M.D. ★

1989
James P. Crutcher, M.D. ★★★★
Lawrence V. Page, D.O. ★★
Martin G. Mankey, M.D. ★★★★
Nancy J. Ensley, M.D.
Steve C. Thomas, M.D. ★★★★

1990
David M. Kieras, M.D. ★
J. Roberto R. Carreon, M.D.
Jay A. Winzenried, M.D. ★★
Ken Fujii, M.D. ★
Walter F. Krengel III, M.D. ★★

1991
David H. Bishop, M.D. ★★
Kit M. Song, M.D.
Mark Remington, M.D. ★★★★
Mark E. Murphy, M.D., Ph.D. ★
Tim P. Lovell, M.D. ★★

1992
Curt Rodin, M.D.
Don Striplin, M.D. ★★
Eli Powell, M.D. ★
Jeff Stickney, M.D. ★
John D. West, M.D. ★
Michael Sailer, M.D. ★★★

1993
J. Eric Vanderhooft, M.D. ★★★★★
Lyle S. Sorensen, M.D. ★★★★★
Philip J. Kregor, M.D. ★★
Susan R. Cero, M.D. ★★★★★

1994
Brodie Wood, M.D. ★★
Eric Bowton, M.D. ★★
Jim Vahey, M.D. ★
Sohail K. Mirza, M.D. ★
William Obremskey, M.D. ★★★

1995
Ron Kristensen, M.D. ★
Scott Hormel, M.D. ★★
Timothy Beals, M.D. ★
Todd Clarke, M.D. ★★
William J. Mills III, M.D. ★

1996
David Deneka, M.D. ★
Peter Mitchell, M.D. ★★
Peter T. Simonian, M.D. ★★★
Vernon Cooley, M.D. ★
William Wagner, M.D. ★★★

1997
Daniel Stechschulte, Jr., M.D.
David Levinsohn, M.D. ★
L. Anthony Agtarap, M.D. ★
Mohammad Diab, M.D.
Randall W. Viola, M.D.

1998
Colin Poole, M.D. ★
David Belfie, M.D. ★
Don Ericksen, M.D. ★★★
Jay Crary, M.D. ★★
Oriente DiTano, M.D. ★

1999
Craig Boatright, M.D.
Jeffrey Garr, M.D.
John Michelotti, M.D. ★
Julie A. Switzer, M.D.
Thomas D. Chi, M.D. ★

2000
Brett Quigley, M.D. ★
Cara Beth Lee, M.D.
Daniel Jones, M.D. ★
Joel Hoekema, M.D. ★★
Patrick McNair, M.D.

2001
Eric Novack, M.D.
Frederick Huang, M.D. ★★
Matthew Camuso, M.D.
Michael Metcalf, M.D. ★★
Richard Bransford, M.D.

2002
Timothy DuMontier, M.D.
Scott Hacker, M.D. ★
Timothy Rapp, M.D. ★
William Sims, M.D. ★
Carla Smith, M.D. ★

2003
Ben DuBois, M.D. ★
Andy Howlett, M.D.
Guy Schmidt, M.D. ★
Brian Shafer, M.D. ★
Emma Woodhouse, M.D. ★

2004
Jon Braman, M.D. ★
Alexis Falicov, M.D. ★
Mike McAdam, M.D. ★
Jason Thompson, M.D. ★
Thea Khan-Farooqi, M.D.

2005
Tony Buoncristiani, M.D. ★
Waqqar Khan-Farooqi, M.D.
Wren McCallister, M.D.
Tim O'Mara, M.D.
David Stevens, M.D.

2006
Heidi Ambrose, M.D.
Stacey Donion, M.D.
Eric Klineberg, M.D.
Bill Montgomery, M.D.
Mel Wahl, M.D.
Burt Yaszay, M.D.

2007
Jamie Antoine, M.D. ★
Jeremiah Clinton, M.D. ★
Mary Cunningham, M.D. ★
Evan Ellis, M.D. ★
Joseph Lynch, M.D. ★
Allison MacLennan, M.D. ★

STARS INDICATE TOTAL DONATIONS IN SUPPORT OF THE RESIDENCY

★★★★★ = $10,000 and over
★★★★ = $7,500 - $9,999
★★★ = $5,000 - $7,499
★★ = $2,500 - $4,999
★ = $1 - $2,499

Endowments

We express our appreciation to all who have contributed to the endowments of the Department of Orthopaedics and Sports Medicine. Your assistance makes possible special research activities, educational programs, and other projects that we could not offer without this extra support from our alumni, faculty, and friends in the community. Additional Contributions to these and new endowments are most welcome! If you have any questions, please contact our Chair, Rick Matsen (matsen@u.washington.edu), or our Administrator, Ken Karbowski (kkarb@u.washington.edu).

Hansjoerg Wyss Endowed Chair

Ernest M. Burgess Endowed Chair for Orthopaedics Investigation

Sigvard T. Hansen Jr. Endowed Chair in Orthopaedic Traumatology

Jerome H. Debs Endowed Chair in Orthopaedic Traumatology

Endowed Chair for Women's Sports Medicine and Lifetime Fitness

Surgical Dynamics Endowed Chair for Spine Research

Douglas T. Harryman II/DePuy Endowed Chair for Shoulder Research

Synthes Spinal Surgery Outcomes Research Endowment

Zimmer Fracture Fixation Biology Endowed Professorship

Ostex Bone and Joint Research Endowment

Orthopaedic Traumatology Endowed Lectureship

John F. LeCocq Lectureship in Orthopaedic Surgery

Don and Carol James Research Fund in Sports Medicine and Fitness

Victor H. Frankel Award

Esther Whiting Award

Ed Laurnen Award

Spine Research Endowment

James G. Garrick Lectureship in Sports Medicine

Regenerative Spine Surgery Endowed Professorship

Endowed Chair for the Health of the Student Athlete